Natural Radioactivity Concentrations and Occurrence of Heavy Metals in Shore Sediments along the Coastline of the Erongo Region in Western Namibia

By

ONJEFU SYLVANUS AMEH

A thesis submitted for the Degree of Doctor of Philosophy

Department of Physics and Electronics

Faculty of Agriculture, Science and Technology at the Mafikeng Campus

North-West University, South Africa.

Supervisor: **Prof. S.H. Taole**

Co-supervisor: **Prof. N.A. Kgabi**

May 2016

DECLARATION

I declare that the work presented in this thesis represents my original work and is being submitted for the degree of Doctor of Philosophy in Physics in the North-West University, Mafikeng Campus, South Africa. The work has not been previously submitted to any other University or similar Institution for any degree.

Signature: 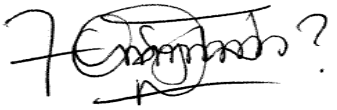

Date: 20th November 2016

ACKNOWLEGEMENTS

My profound gratitude goes to the Almighty God who in His infinite mercy has allowed me to share in His abundant love. “TO GOD BE THE GLORY”.

I am sincerely grateful to my supervisors Prof. S.H. Taole and Prof. N.A. Kgabi who in spite of their very tight schedule saw me through to earn my PhD. I owe a debt of gratitude to the Staff of the International Centre for Environmental and Nuclear Sciences, University of the West Indices, Mona Campus, Kingston, Jamaica for their assistance in analyzing the shore sediment for NORM. Also, not left out are the staff members of the Analytical Laboratory Windhoek, Namibia who assisted with the elemental analysis of the sediments for heavy metals.

I am deeply indebted to my wife Mary Onjefu and children Emmanuel and Nissi for their support and love throughout the duration of my programme. Posterity will judge me if I fail to acknowledge the wonderful support and encouragement from my parents, Sir Emmanuel Onjefu and Lady Veronica Onjefu.

Lastly, I offer my deep appreciation to Mr. Lawrence Olotu Bankole who supported me in sample collection.

ABSTRACT

Some human activities like uranium mining, sea port activities and improper wastes handling has been identified as potential sources of exposure to naturally occurring radioactivity materials (NORM) and heavy metals. However, some of these activities are not being effectively regulated for natural radioactivity and heavy metals in Namibia. Whilst some developed nations have identified these environmental challenges and have put measures in place to address it, very little attention is given in developing countries. However, most of the human activities that releases NORM and heavy metals are located in the developing nations that have paid little or no attention to address it. The Erongo region of Namibia is currently home to several active uranium mining companies, port harbor and other fish processing companies that are only a few kilometers from the shoreline. Namibia is an arid country with an average day temperature of 30^{o}C. This prevailing climate has necessitated the migration of both locals and international tourists to the beaches in the coastline. Most worrisome is the use of the shore sediment as building materials. These studies have been carried out to measure the natural radioactivity concentrations and occurrence of heavy metals in shore sediments along the coastline of the Erongo region.

A high purity germanium (HPGe) detector was used in radioactivity assessment. In evaluating the occupancy factor appropriate for the coastline, a questionnaire was administered to 2400 population that visit the beaches for different activities. Analysis of the shore sediment for heavy metals was done using inductively coupled-optical emission spectrometry (ICP-OES) Perkin Elmer Optima 7000 DV.

The mean activity concentration along the coastline of the Erongo region ranges from 142.79 to 199.76 Bq.kg $^{-1}$ for ^{238}U, 29.69 to 42.47 Bq.kg $^{-1}$ for ^{232}Th and 354.38 to 611.19 Bq.kg $^{-1}$ for ^{40}K. The results from the study were compared with world safe values of 50, 50, and 500 Bq.kg $^{-1}$, respectively (UNSCEAR, 2000). The modelled results showed outdoor occupancy factor of 0.48 and indoor occupancy factor of 0.52, which are 2.4 times higher than the UNSCEAR outdoor factor and 0.65 times less than the UNSCEAR indoor factor. The absorbed dose rate (ADR) in air at 1 meter above ground was estimated to be in the range 93.27 to 144.01 nGy.h $^{-1}$. The outdoor annual effective dose rate ranged from 121.01 to 176.61 µSv.y $^{-1}$ (UNSCEAR factor), 292.60 to 413.63 µSv.y $^{-1}$ (present modelled factor), with average values of 142.5 µSv.y $^{-1}$ and 339.36 µSv.y $^{-1}$, which are both above the world effective dose value of 70 µSv.y $^{-1}$. The mean values of Ra_{eq}, H_{ex}, H_{in} and ELCR obtained for all sediment samples showed that Ra_{eq} and H_{ex} are lower than the accepted world safe limit value of 370 Bq.kg $^{-1}$ and below the limit of unity. However, use of H_{in} and

ELCR values showed that the use of the shore sediment samples for building material poses internal radiation risk since the values are > 1 for H_{in} and above 0.29 x 10^{-3} for ELCR. Assessment on the contamination status of heavy metals in the shore sediment showed high enrichment for Cd in both seasons of summer and winter, moderate degree of contamination of As in summer in the beach of Walvis Bay. The geo-accumulation index revealed moderate pollution of Swakopmund beach with Cd in summer, unpolluted beach of Swakopmund and polluted to moderately polluted beach of Henties Bay with Cd in winter season. However, the evaluation of the results of pollution load index (PLI) from this present study indicated PLI < 1 which showed that all the beaches investigated in this present study are not polluted with metals.

TABLE OF CONTENTS

LIST OF ABBREVIATIONS

ADC	Analogue-to-digital Converter
AEDE	Annual Effective Dose Equivalent
ALARA	As Low As Reasonably Achievable
BDL	Below Detectable Limit
BEIR	Biological Effects of Ionizing Radiation
CF	Contamination Factor
DL	Duration of Life
EF	Enrichment Factor
ELCR	Excess Lifetime Cancer Risk
EPA	Environmental Protection Agency
ERC	Erongo Regional Council
GPS	Global Positioning System
H_{ex}	External Hazard Index
H_{in}	Internal Hazard Index
IAEA	International Atomic Energy Agency
ICP-OES	Inductively Coupled Plasma-Optical Emission Spectroscopy
ICRP	International Commission on Radiological Protection
IGEO	Index of Geo-accumulation
LET	Linear Energy Transfer
MCA	MultiChannel Analyzers
MET	Ministry of Environment and Tourism

MHSS	Ministry of Health and Social Services
NCRP	National Council on Radiological Protection
NORM	Natural Occurring Radioactive Materials
NPC	National Population Commission
NW	North West
PCA	Principal Component Analysis
PLI	Pollution Load Index
RF	Risk Factor
SEA	Strategic Environmental Assessment
SE	South East
SCA	Single Channel Analyzer
UNSCEAR	United Nation Scientific Committee on Effects of Atomic Radiation
UNEP	United Nation Environmental Programme
USEPA	United State Environmental Protection Agency
WHO	World Health Organization
WNA	World Nuclear Association
WSRA	World Surface Rock Average

LIST OF FIGURES

LIST OF TABLES

CHAPTER 1

INTRODUCTION

1.1 General background

Since radioactivity was discovered by Henri Becquerel's in the year 1896, it has been shown that ionizing radiation can impact human health significantly (UNSCEAR, 1998). Human exposure to Naturally Occurring Radioactive Materials (NORM) has been recognized as a scientific subject that stirs public curiosity (Jibiri *et al*., 1999; Farai, and Sanni, 1992; UNEP, 2012). There exist also artificial sources, which include anthropogenic radionuclides such as ^{137}Cs, ^{90}Sr etc., produced mostly from atomic bomb testing and nuclear explosions and accidents such as have been reported since the early 1960's up to recent times in some parts of the world (IAEA, 1987; Alenikov, 1989; Hu *et al*., 2010). Also, human activities such as uranium mining contribute to artificial sources of exposure to the human population (Cothern and Lappenbusch, 1986; Steinhausler and Lettner, 1992). Although, primordial radionuclides (^{238}U and ^{232}Th and their progenies, and ^{40}K) are present everywhere in the earth's crust (Jibiri *et al*., 1999; El- Dine *et al*., 2001), there exist several geological processes that lead to the accumulation of chemical elements up to concentrations many times higher than the crustal average, known as geochemical anomalies (Pereira and Neves, 2012).

The United Nation Scientific Committee on the Effects of Atomic Radiation (UNSCEAR, 2000) reported that the most significant radiation source to which human population is exposed is the ionising radiation which originates from radionuclides in the earth's surroundings and the interaction of cosmic rays in the earth's atmosphere. This exposure to naturally occurring radionuclides also accounts for up to 85 % of annual exposure dose received by inhabitant of the universe, as shown in Figure 1.1. The International Atomic Energy Agency (IAEA) reports that the exposure from natural radioactivity is, in most cases, of little or no concern to the public, except for individuals working with mineral ores and naturally occurring radioactive materials (NORM) (IAEA, 2005). Nevertheless, the World Nuclear Association (WNA) states that any dose of radiation carries its own degree of harm (WNA, 2011), even though the level of individual exposure to NORM is sometimes usually statistically insignificant on an individual basis from the perspective of a health physicist (BEIR, 2006). It is on this basis that the need to assess the risk from naturally occurring ionizing radiation in an environment arises with a view to

evaluate the biological effect on human population (UNSCEAR, 1993). To this end, this has become the focus of greater attention by the IAEA in recent years (IAEA, 2005).

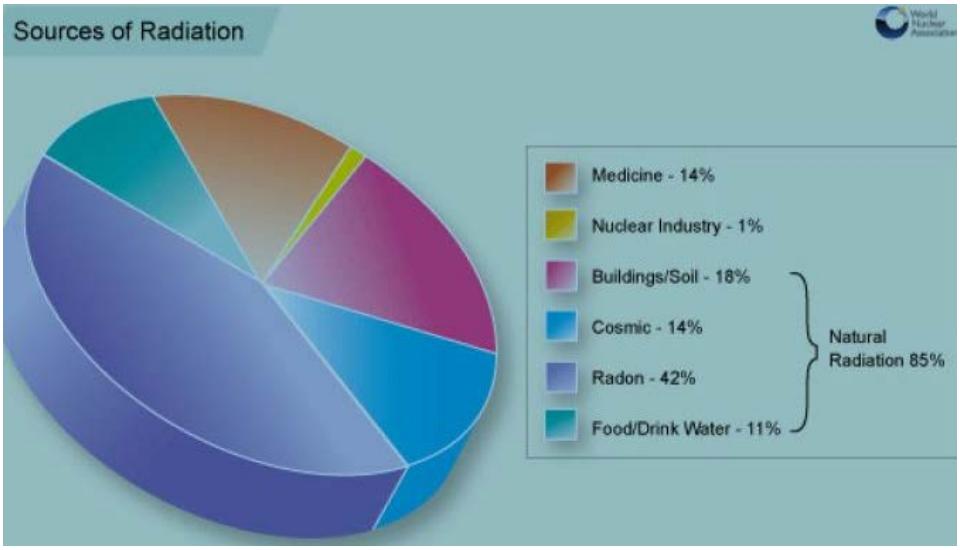

Figure 1.1: Average annual dose to the world population from different sources (WNA, 2011).

1.2 NORM overview

Humans are exposed to some background levels of ionizing radiation that stems from both natural and man-made sources. Naturally occurring radioactivity has been a constituent part of the earth since its creation (Scholten and Timmermans, 1996; NCRP, 1975). The radioactive sources are widely distributed in the earth's environment and they exist in various geological formations such as earth's crust, rocks, soils, plants, water, sediments and air (Wilson, 1994; Singh *et al*., 2005; Abusini, 2007). Naturally occurring radioactivity depends mainly on geological and geographical condition and appears at different levels in soils and sediments of each geological region (UNSCEAR, 2000). These radionuclides are referred to as Naturally Occurring Radioactive Materials (NORM) (Wilson, 1994). There exist several (NORM) in the environment. However, only the very long lived nuclides, with decay half-lives that are comparable to the age of the earth, and their progenies still exist in quantities of environmental significance (Abdi *et al*., 2008; UNSCEAR, 2000). There have been many studies concerning naturally occurring radioactive materials in soils and sediments which provide information on the nature of their distribution and levels of background radiation, and all the work on this topic agrees that most soils and sediments contain the radioactive nuclides of uranium and thorium series and ^{40}K (Chowdhury *et al*., 1999; Anjos *et al*., 2005). Findings have shown that these radionuclides are emitters of alpha, beta particles and gamma rays that give rise to internal and external exposures to

human population (Momont-Ciesla *et al*., 1982; UNSCEAR, 2000; Lorimore *et al*., 2003; Watson, *et al*., 2005;).

In recent, years, there has been growing concern regarding hazards from natural radioactivity (Nielson *et al*., 1996; El-Amri *et al*., 2003; Denagbe, 2000; El-Fawal, 2011 and Shams *et al*., 2013). In previous studies carried out in the Erongo region (Von Oertzen, 2010; Van Blerk *et al*., 2010; Steinhauster and Lettner, 1992; SEA, 2010) it was identified that parts of the region, also called the ''uranium province of Namibia'', have high levels of natural background radiation. Wackerle, (2009) examined the contribution arising from cosmic radiation to the contribution from natural occurring radioisotopes and detected exposure doses from cosmic radiation ranging from 0.3 mSv/yr at the coast to approximately 0.7 mSv/yr in the central highlands.

The levels at which terrestrial sources (soil and rock) contribute to the natural background radiation in the Erongo region was obtained from the study of airborne radiometric surveys with the dose rate from natural terrestrial gamma background ranging from close to zero up to 7.3 mSv/yr (Wackerle, 2009; Von Oertzen, 2010). Other forms of background radiation in the region emanate from radioactive dust, and from radon with its radioactive decay products. Dust is generated in copious amounts during mining processes. The Erongo regional average contribution of radioactive dust to the natural background radiation was recently undertaken as part of the Strategic Environmental Assessment (SEA), and was found to be ten times greater than the world average of 0.0058 mSv/yr (SEA, 2010). Van Blerk *et al*., (2010) noted that the baseline contribution of dust is due to natural background source of dust and those originating from the activities of the existing uranium mines. Oyedele *et al*., (2010) studied the radiological importance of naturally occurring radionuclides in soils around the Rossing Uranium Mine and its neighbouring town of Arandis. The average concentrations of ^{238}U, ^{232}Th and ^{40}K in the two areas surveyed were found to range from 45.9 ± 3.0 to 1752.1 ± 17.5 $Bq.kg^{-1}$ for ^{238}U, 70.4 ± 4.8 to 1865.5 ± 56.0 $Bq.kg^{-1}$ for ^{232}Th and 376.5 ± 18.1 to 1300.7 ± 50.7 $Bq.kg^{-1}$ for ^{40}K. These concentrations were used to calculate the absorbed dose rates and annual effective dose rates. The annual effective dose rates varied from 0.12 ± 0.01 to 1.60 ± 0.04 mSv/yr with a mean of 0.30 ± 0.21 mSv/yr. This indicates that the town of Arandis has safe levels of background radiation.

Studies of radiation from coastal sediments have been carried out in places such as the Indian subcontinent, Australia, South America, West and North Africa (Amekudzie *et al*., 2011; Shams, *et al*., 2013).

In the Indian subcontinent measurements of the natural radioactivity of river sediments and beach sand samples in Chittagong, Bangladesh were undertaken by Chowdhury *et al*., (1999). The results of the activity concentration of ^{238}U, ^{232}Th, and ^{40}K were found to be higher than the established world average values which are 35, 30 and 400

Bq.kg^{-1} respectively (UNSCEAR, 2000). Beach shore sediments were used for measuring the natural radioactivity levels of North East Coast in Tamilnadu, India by Ramasamy *et al*., (2009). The maximum activity concentrations observed were: ^{238}U (30.42 ± 7.90Bq.kg^{-1}), ^{232}Th (218.64 ± 8.02Bq.kg^{-1}) and ^{40}K (423.43 ± 26.52 Bq.kg^{-1}). In the same year, Ramasamy *et al*., (2009) evaluated the naturally occurring radioactivity content in sediments samples collected and evaluated the excess lifetime cancer risk due to gamma radiation from various sites of the Ponnaiyar River. The activity concentration ranges for ^{238}U, ^{232}Th and ^{40}K were below detectable limit (BDL) - 11.60 ± 6.13 Bq.kg^{-1} with an average of 7.31 ± 3.41 Bq.kg^{-1} for ^{238}U, BDL- 106.11 ± 6.13Bq.kg^{-1} with an average of 46.85 ± 5.25 Bq.kg^{-1} for ^{232}Th and 201.23 ± 19.90 - 467.71 ± 34.34 Bq.kg^{-1} with an average of 384.03 ± 26.82 Bq.kg^{-1} for ^{40}K.

In North Africa, El-Kameesy (2008) investigated the average activity of ^{226}Ra, ^{232}Th and ^{40}K in beach sand samples in the Tripoli Region of Libya and their results were 7.5 ± 2.5 Bq.kg^{-1}, 4.5 ± 1.3 Bq.kg^{-1} and 28 ± 6.7 Bq.kg^{-1}. Shams *et al*., (2013) determined the gamma radioactivity measurements in Nile River sediment samples in Egypt. The highest average concentrations of ^{226}Ra, ^{40}K and ^{232}Th were found to be 90.7 ± 4.5Bq.kg^{-1}, 383 ± 19Bq.kg^{-1} and 41.3 ± 2.4 Bq.kg^{-1} respectively.

In West Africa, Amekudzie *et al*., (2011) assessed the activity concentrations of natural radionuclides in shore sediment and also the annual effective dose rate to Ghanaians living along the coast of the greater Accra Region. The measurement showed specific activity concentration ranging from 8.60 Bq.kg^{-1} to 61.01 Bq.kg^{-1} with a mean of 29.78 Bq.kg^{-1} for ^{40}K, values of 0.62 Bq.kg^{-1} to 148.80 Bq.kg^{-1} with a mean of 22.04 Bq.kg^{-1} for ^{226}Ra and 0.17 Bq.kg^{-1}to 732.60 Bq.kg^{-1} with a mean of 108.60 Bq.kg^{-1} for ^{232}Th. Another study carried out in West Africa was the estimation of radiological hazard associated with the use of river sediment as building material (Oni *et al*., 2011). Samples collected from the Osun River in Nigeria were investigated by Oyebanjo *et al*., (2012). The results obtained showed that the mean concentration of ^{40}K, ^{238}U, and ^{232}Th in the sediments varied repectively, between 175.6 ± 6.1 Bq.kg^{-1} in the lower course of the river to 188.5 ± 7.2 Bq.kg^{-1} in the upper course, 28.4 ± 2.0 Bq.kg^{-1} in the upper course to 13.1 ± 1.4 Bq.kg^{-1} in the lower course and 11.4 ± 0.3 Bq.kg^{-1} in the upper course to 16.3 ± 0.4 Bq.kg^{-1} in middle course.

The use of sediment as an environmental indicator to trace contamination source and monitor contaminants is widely recognized (Taylor, 1990; USEPA, 1994; Benamar *et al*., 1997).

1.3 Heavy metals overview

The presence of heavy metals in soil has been identified as a useful indicator for contamination in surface soil and sediments (Ana and Zoran, 2010; Ubwa *et al*., 2013).

Heavy metals exist naturally in the environment and are present in rocks, plants, soil and sediments. Human activities such as mining, smelting, irrigating with sewage water, etc have contributed to the pollution of soil and sediments with heavy metals (Joshua and Oyebanjo, 2009). The heavy metals may present a distortion on soil ecology and ground water quality, and ultimately pose health problems to human population (Guidotti, 2005; Li *et al*., 2007; Gregorauskiene, 2008; Dissanayake and Chandrajith, 2009; Adaikpo, 2013).

The health hazards presented by heavy metals in the environment depend on the level and length of exposure which could be acute or chronic. Acute exposure refers to contact with a large amount of the heavy metal in a short period of time. Under this condition, the health effects may be apparent or delayed. Chronic exposure refers to contact with low levels of the heavy metal over a long period of time. A recipient may even be unaware that the exposure is occurring and that health problems may develop (Baldwin and Marshall, 1999). The main threats to human health from heavy metals are associated with exposure to lead, cadmium, mercury, copper, zinc, arsenic, chromium, iron, manganese and vanadium. These metals have been extensively studied (Centeno *et al*., 2005; Olli and Destouni, 2008; Attia, *et al*., 2014; Abah *et al*., 2014) and their effects on human health regularly reviewed by international bodies such as the WHO (Clarkson, 2001; Lars, 2003).

The assessment of heavy metal contamination in mangrove sediments and leaves from Punta Mala Bay, Pacific coast of Panama was done by Defew *et al*., (2005). The results in parts per million (ppm) from analysis of eight metals (Mn, Cu, Zn, Ni, Pb, Fe, Cr, Cd) showed that Fe with values of 9827 ppm, 105 ppm for Zn and 78.2 ppm for Pb had concentrations high enough to conclude that there was moderate to serious contamination within the bay. In the same year, the trends in heavy metal concentrations were analysed in sediments, finfishes and shellfishes in inshore waters of Cochin, southwest coast of India were carried out by Kaladharan *et al*., (2005). The results obtained showed cadmium concentrations in sediment of estuarine and inshore areas of Cochin. They registered a highest value of 2.4 ppm during 1996 and a lowest value of 0.02 ppm during 1991. Sediment from the inshore area showed a high value of 1.3 ppm compared to 1.2 ppm in the estuarine area. An investigation of heavy metal distribution in marine sediments of the east Adriatic Sea was taken by Ana and Zoran (2010). The findings reported concentrations for Pb, Cd, Cu, Zn and Ni which showed the distribution of metal concentrations decreasing in the sediment samples from SE to NW along the coast. The mass concentrations in the sediment samples range from 10.64 to 24.35 mg/kg for Pb, from 0.0893 to 0.2713 mg/kg for Cd, from 61.43 to 109.40 mg/kg for Zn from 20.46 to 44.30 mg/kg for Cu and from 172.69 to 325.70 mg/kg for Ni. Heavy metal distributions in the coastal sediment of the Chennai coast were measured by Ramanibai and Shanthi, (2012), and their results showed that Pb varied from 0.0225 to 0.0191 mg/kg; Zn from 0.0109 to 0.0863 mg/kg; Co from 0.0730 to 0.0170 mg/kg;

Ni from 0.0711 to 0.0366 mg/kg; Cr from 0.0880 to 0.0437 mg/kg and Cu from 0.0923 to 0.0401 mg/kg.

Understanding the method of transfer and distribution of toxic metals between sediment and water columns is of great importance. Once heavy metals are introduced into the aquatic environment, they are redistributed throughout the water column, and are deposited and accumulated in sediments (Christophoridis *et al*., 2009). Heavy metal concentrations profiles in sediments are used to identify the history and sources of pollution. The sources of major and minor elements in aquatic sediments areas are a combination of natural weathering, run-off and riverine and atmospheric input, affected by anthropogenic impact (Yalcin *et al*., 2008; Zhang *et al*., 2009).

1.4 An overview of the coastline of the Erongo Region

The Erongo region is situated in the western part of Namibia, bordering the Kunene region in the North, the Otjozondjupa Region in the North East, the Khomas Region in the South East and the Hardap Region in the South. It lies partly on the Namibian highlands at an altitude above 1200 m and partly across the central Namib Desert, a 150 km wide coastal plain below 800 m and covers an area of 63579 Sq.Km. The region is also home to six active uranium mines, where commercial exploitation of uranium has been taking place for export purposes (ERC, 2013). Figure 1.3 presents map of the region showing uranium deposits.

Namibia's highest mountain, the Brandberg at 2579 m above sea level is situated in the Erongo Region. Other prominent mountains are Erongo (2319 m) and Spitzkoppe (1759 m). Four ephemeral rivers run from east to west namely Ugab, Omaruru, Swakop/Khan and the Kuiseb River. The region has different climate zones which run parallel to the coastline; these are a foggy coastal zone, a foggy interior zone, a middle desert zone, an eastern desert zone, the escarpment and the Namibian highlands. The annual mean temperature is between 15^{o}C and 22^{o}C (SEA, 2010). South-western winds prevail for most of the year (280 days) starting in early summer. The mean rainfall varies between 0 mm in the west and 350 mm in the east (SEA, 2010).

The coastline of the Erongo Region is also known as a tourist destination with tens of thousands of holiday makers visiting the beaches of the towns of Walvis Bay, Swakopmund and Henties Bay for recreational purposes.

Walvis Bay is located some 30 km South from Swakopmund with latitude 22^{o} 57' 27'' South, longitude 14^{o} 30' 19'' East. Walvis Bay is Namibia's major port and the biggest town along the Namibian coast. An important tourist attraction of Walvis Bay is the natural lagoon. The lagoon at Walvis Bay is an important wetland and is home to a large population of

flamingos and is an internationally designated wetland and a migration point for many thousands of sea birds and waders (ERC, 2013).

Swakopmund, is located at latitude 22^{o} 4’ 59’’ South, longitude 14^{o} 31’ 59’’ East about 30 km to the north of Walvis Bay, is the second biggest town along the Namibian coast and a popular holiday destination. Along the coastline between Swakopmund and Walvis Bay are some holiday resorts, a caravan park, camping sites, swimming pools, beaches and café (ERC, 2013).

Henties Bay is located some 70 km up the coastal road from Swakopmund with latitude 22^{o} 55’ 27’’ South, and longitude 14^{o} 30’ 19’’ East. The small municipality of Henties Bay lies within the Namibian National west coast Tourist Recreation Area. Henties Bay has a linear development pattern along the beach which is typical of a holiday oriented town (ERC, 2013). Figure 1.2 presents map of Namibia showing Walvis Bay, Swakopmund and Henties Bay.

Figure 1.2: Map of Namibia showing Walvis Bay, Swakopmund and Henties Bay (SEA, 2010).

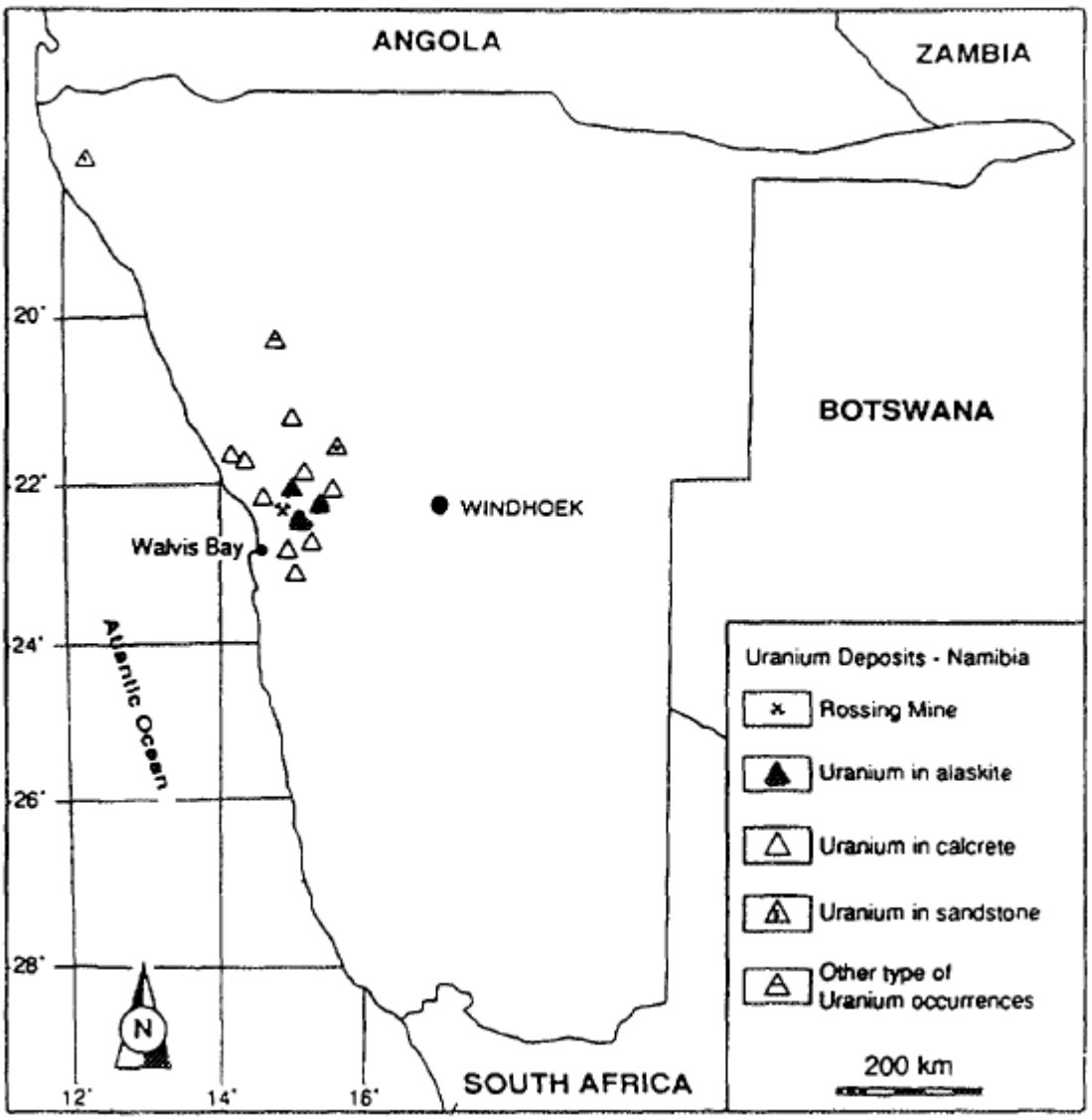

Figure 1.3: Map showing Uranium deposits in Namibia (Roesner and Schreuder, 1992).

1.5 Problem Statement

Natural background radiation is the most common source of human population exposure to radiation and a significant component of the background radiation is generated from natural radionuclides in soil and sediments. It has been confirmed that parts of the Erongo Region of Namibia have high levels of natural background radiation (Steinhauster and Lettner, 1992; SEA, 2010). There are different human activities that cause emission of additional levels of natural radioisotopes and heavy metals into the environment. Some of these sources include; industrial mining and milling of mineral ores, ore processing and enrichment. Also, the release into the ocean and sea of level waste from nuclear activities has given rise to contamination in the marine coastal ecosystem (Akram, *et al*., 2007).

The accumulation of these radionuclides in sediments can present a health risk to the human population living in the region, especially because the region is an important recreational area and tourist destination. The absence of baseline data that can be used in carrying out an assessment of the impact of radiation on the coastline in the region points to the need to determine the natural radioactivity and hazards as well as the occurrence of heavy metals in shore sediments along the coastline.

1.6 Justification of Study

A field study on the radiological and heavy metals impacts of human activities is essential because of the potential pollution due to these activities. This study will unearth the variation in shore sediment radioactivity levels and occurrence of heavy metals as a result of human activities around the coastline of the Erongo region. Radiation dose assessment and heavy metals concentration will be considered. The availability of the data from this study is vital to all stake holders as the study will address the limited data on radioactivity in this area which will form the basis for addressing these challenges to humans and the environment.

1.7 Research Aim and Objectives

1.7.1 Aim

The aim of this project was to measure the occurrence and concentration of natural radioactivity and heavy metals in shore sediments along the coastline of the Erongo region of western Namibia.

1.7.2 Objectives

The specific objectives for the project were:

(i) To assess the levels of natural radionuclide concentrations in the shore sediments.

(ii) To evaluate the baseline activity concentration trend along the coastline shore sediments.

(iii) To re-evaluate the occupancy factor for effective dose estimation for the coastline.

(iv) To evaluate the absorbed dose rate and annual effective dose from the shore sediments that may accrue to human population at the beach.

(v) To evaluate the hazard indexes due to natural radionuclides and their decay products from sediments of the shoreline of the Erongo Region.

(vi) To determine the baseline data of the levels of some heavy metals of environmental and human impacts along the coastline shore sediments.

1.8 Summary

This chapter has provided a summary of the general background of current literature available on NORMs and heavy metal measurements in shore sediments around the world. The summary shows the absence of research data on these topics on the coastline of Namibia compared to the number of studies that have been undertaken internationally. The coastline of the Erongo region is a holiday hotspot, a destination for both local inhabitants and international tourists; the region is however rich in uranium bearing ore and this has necessitated research in natural radioactivity. It was pointed out that there have recently been reports of NORMs from a number of ambient Namibian soils; Oyedele *et al*., (2010) provided the concentration of natural radionuclides in the soils around the Rossing Uranium Mine and its neighbouring town of Arandis while Shimboyo (2013) examined the natural radioactivity in soils of the Walvis Bay and Henties Bay coastal town of Namibia. These are the two most recent works on NORMs in the Erongo region of Namibia and neither examined the concentration of radionuclides and heavy metals in the beaches along the coastline which are only few kilometre from active uranium mines. Most reports on radiological dose received by members of the public from sediment samples all around the world have employed the UNSCEAR factors in the evaluation of the effective dose estimation which may not be a true dose representation to the general public. One objective of the research is to re-evaluate the occupancy factor for effective dose estimation in the coastline.

CHAPTER TWO

BASICS OF NUCLEAR DECAY

2.1 Introduction

This chapter discusses the different types of decay and gives a comparative study of the different environmental sources of radioactivity.

2.1.1 Radioactivity and radioactive decay

Radioactivity is a statistical process in which an unstable parent nucleus decays into a more stable daughter nucleus (NCRP, 1985; Lilley, 2001). In some cases, the daughter nuclei may also be unstable and the process continues unabated in a chain-like process called a decay chain until such time as a more stable daughter is attained. Atomic disintegration during radioactivity is completely independent of every other disintegration or decay episode, and the time interval between decay is not a fixed process. For a given number of atoms of a particular radionuclide decaying randomly, the frequency of the disintegration is given by Poisson's distribution: if $\bar{n}$ is the mean rate of decay, the probability, P, that the number of atomic nuclei, μ, will decay in a given time interval is:

$$P(\mu) = \frac{\bar{n}^{\mu}}{\mu!} \exp(-\bar{n}) \qquad (Eq.2.1)$$

The strength or intensity of radioactive decay is called activity and is defined as the number of atoms that disintegrate per unit time (Faire and Boswell, 1981). The probability per unit time for the disintegration of a given nucleus is a constant called the decay constant (λ) (Krane, 1988; Ike, 2008). The number of atoms that disintegrate in unit time is related to the activity and is given by.

$$A = -\frac{dN}{dt} = \lambda N \qquad (Eq.2.2)$$

As presented in Equation 2.2, A is the activity of an isotope, with values equal to the number, dN, of radioactive nuclei which decays with time, dt, and is directly proportional to the number, N, of the radioisotope present at the given time, t (L' Annunziata, 2007; Ike, 2008). The decay constant is denoted by λ and the negative sign is indicative of the number of radioactive nuclei that decreases with an increase in time.

The reciprocal of the decay constant is the mean lifetime, τ, of the radioactive nuclei, the mean lifetime of an atom before nuclear decays is.

$$\tau = \frac{1}{\lambda} \qquad (Eq.2.3)$$

The time in this case, represents a decay of the source by a factor of *e* (i.e. 2.718). For convenience, we refer to the half-life, $t_{1/2}$, of the radioactive nuclei as the time during which the activity decreases to half its original value.

$$t_{1/2} = \frac{\ln(2)}{\lambda} = 0.693 \qquad (Eq.2.4)$$

Integrating Equation 2.2, leads to the exponential law of radioactive decay which relates the number of atoms $(N(t))$ at a time (t) and half-life $(t_{1/2})$:

$$N(t) = N_o e^{-\lambda t} \qquad (Eq.2.5)$$

Where N_o is the number of atoms present at time $t = 0$,

This is the fundamental equation of radioactive decay. According to the equation, the number of radioactive atoms decreases exponentially with time (Figure 2.1). Practically, it is important to change the number of atoms with activity, if we bear in mind that activity is directly proportional to the number of atoms, then

$$A(t) = A_o e^{-\lambda t} \qquad (Eq.2.6)$$

Following the discovery of radioactivity, the curie (Ci) was used as the unit of activity and it is defined as the activity of 3.7 x 10^{10} disintegration per seconds. However, in recent times, the International Committee on Radiological Unit (ICRU) adopted the Becquerel (Bq) as the standard unit of activity and is defined as the activity of one disintegration per second. Thus, 1 Ci is equal to 3.7 x 10^{10} Bq (Knoll, 2000).

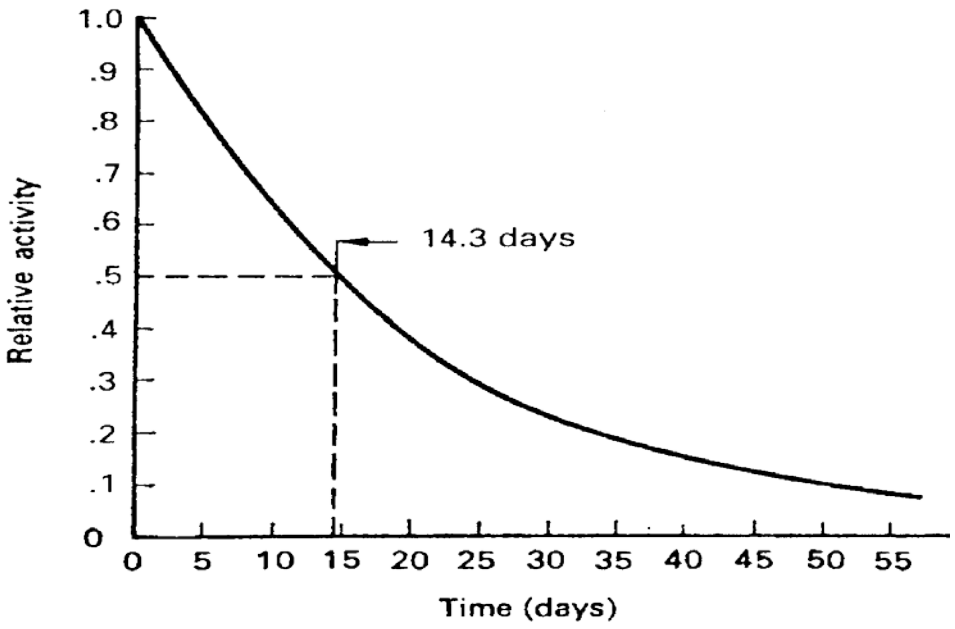

Figure 2.1: The exponential radioactive curve of ^{32}P with half-life, $T_{1/2}$ of 14.3 days (Cember and Johnson, 2009).

2.1.2 Radioactive decay series

In situations where a radioactive material in the decay series of a nuclide is not stable, the progeny after decay may be unstable as well. The natural decay series of ^{238}U, ^{235}U and ^{232}Th are examples of natural radioisotopes in the decay series. The process often occurs in a number of daughter progenies which are also radioactive and subsequently, terminates in a stable atom as describe below.

$$W(\lambda_y) \longrightarrow X(\lambda_x) \longrightarrow Y(Stable)$$

If we assume that at time $t = 0$ we have N_{W_0} atoms of the parent element and no atoms of the decay product are originally present, the number of the parent nucleus decrease with time. From Equation 2.5.

$$N_W = N_{W_0} e^{-\lambda_W t} \qquad (Eq.2.7)$$

Since the number of radioactive progeny increases as a result of the disintegration (decay) of the parent radionuclide and also decreases following its own decay, then:

$$\frac{dN_W}{dt} = \lambda_W N_W - \lambda_X N_X \qquad (Eq.2.8)$$

The solution of the first order differential equation $(dN_X / dt) + \lambda_X N_X = \lambda_W N_{W_0} e^{-\lambda_W t}$ is of the form $N_X = We^{-\lambda_W t} + Xe^{-\lambda_X t}$ and substituting this into the above equation when the initial conditions described are maintained we find:

$$N_X = \frac{\lambda_W N_{W0}}{\lambda_X - \lambda_W}(e^{-\lambda_W t} - e^{-\lambda_X t}) \qquad (Eq.2.9)$$

From Equation 2.7 and Equation 2.9 we can calculate the relative activity ratio of the two species

$$\frac{\lambda_X N_X}{\lambda_W N_W} = \frac{\lambda_X}{\lambda_X - \lambda_W}[1 - e^{-(\lambda_X - \lambda_W)t}] \qquad (Eq.2.10)$$

with λ_W << λ_X . In situations where the half-life of the nuclide W is much greater than the half-life of nuclide X , the parent nuclide decays at a fixed rate.

$$\lambda_X N_X = \lambda_W N_{W0}(1 - e^{-\lambda_X t}) \qquad (Eq.2.11)$$

2.1.3 Radioactive equilibrium

Radioactive equilibrium is used to describe a steady state when constituents of the radioactive chain decay at the same rate as they are produced. In this state, the disintegration of the parent nuclide is equal to the decay process of its progeny (Prince, 1979).There are three main state of radioactive equilibrium namely; secular equilibrium, transient equilibrium and no equilibrium.

2.1.4 Secular equilibrium

This is a steady-state condition where the half-life of the parent radionuclide is far much greater than the half-life of the daughter nuclei. Therefore, λ_W << λ_X and from $Eq.2.8$, λ_W << λ_X and $\lambda_W \approx 0$ it follows that $e^{-\lambda wt} \approx 1$. Hence, at equilibrium, the parent nuclei and daughter nuclei activities are equal, i.e.,

$$\lambda_W N_W = \lambda_X N_X \qquad (Eq.2.12)$$

In practice, when secular equilibrium is attained, the activity of the radioactive progeny becomes equal to the activity of the parent nuclei (Cember and Johnson, 2009). Radioactive equilibrium is a chain process. In a decay chain process, the numbers of nuclei of the constituent daughters present at radioactive equilibrium are inversely proportional to

their decay constants and the rate at which they are formed and the disintegration rate of every daughter nucleus equal to the decay rate of its parent nucleus (Cember and Johnson, 2009). One example which illustrates the attainment of the state of secular equilibrium is the sequence of ^{226}Ra with half-life of 1600 years which decays to ^{222}Rn with half-life of 3.8235 days. Figure 2.2 represents a state of build-up and attainment of secular equilibrium of daughter ^{222}Rn from long-lived parent nuclei ^{226}Ra.

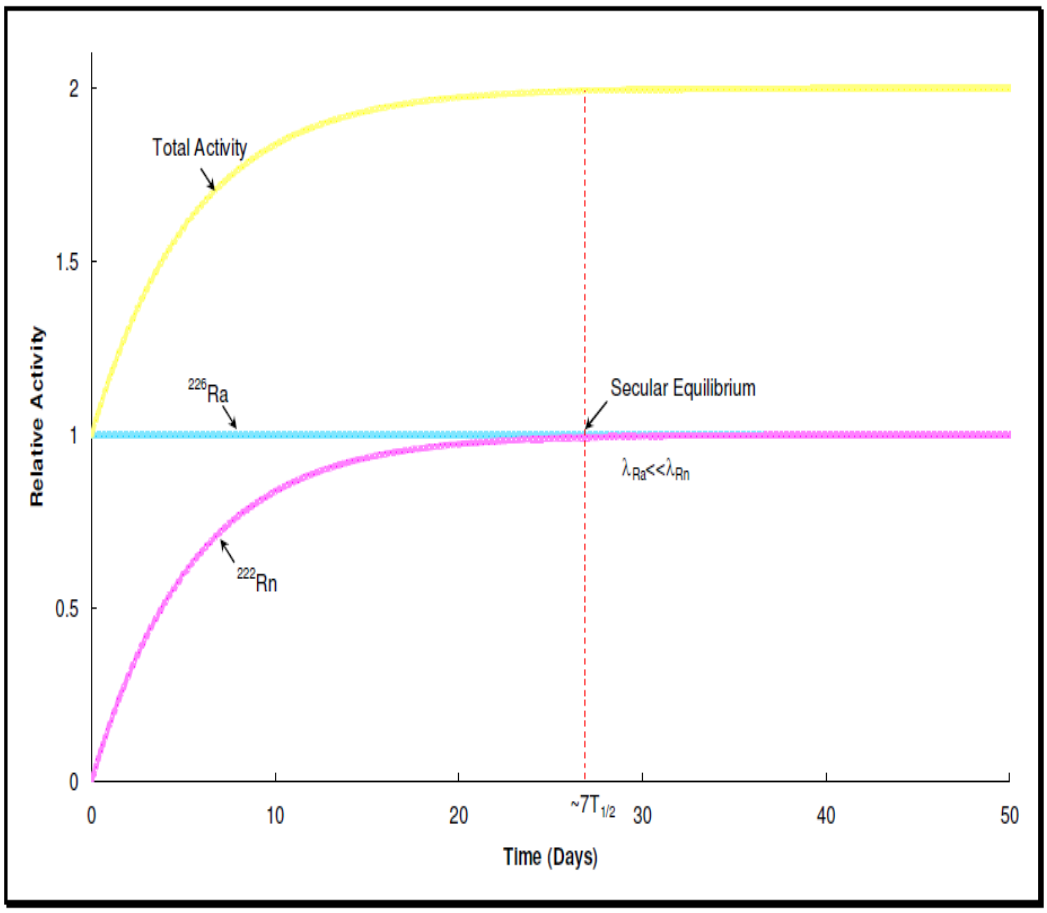

Figure 2.2: Growth of short-lived daughter nuclei (^{222} Rn) from a long-lived parent (^{226} Ra) until the attainment of Secular Equilibrium (Magill and Galy, 2004).

2.1.5 Transient equilibrium

In transient equilibrium the half-life of the radioactive progeny is of the same order but much smaller than that of the parent nucleus (Havey, 1969) i.e., where $\lambda_W < \lambda_X$. In these circumstances, the exponential term in the decay equation, tends to be small and the

activities ratio A_W / A_X approaches the limiting constant value $\lambda_X /(\lambda_X - \lambda_W)$. This can be expressed as;

$$N_X / N_W = \lambda_W / \lambda_X - \lambda_W \qquad (Eq.2.13)$$

One example of transient equilibrium is the decay of ^{140}Ba (half-life of 12.75 d) to ^{140}La (half-life of 1.68 d) as shown in Figure 2.3.

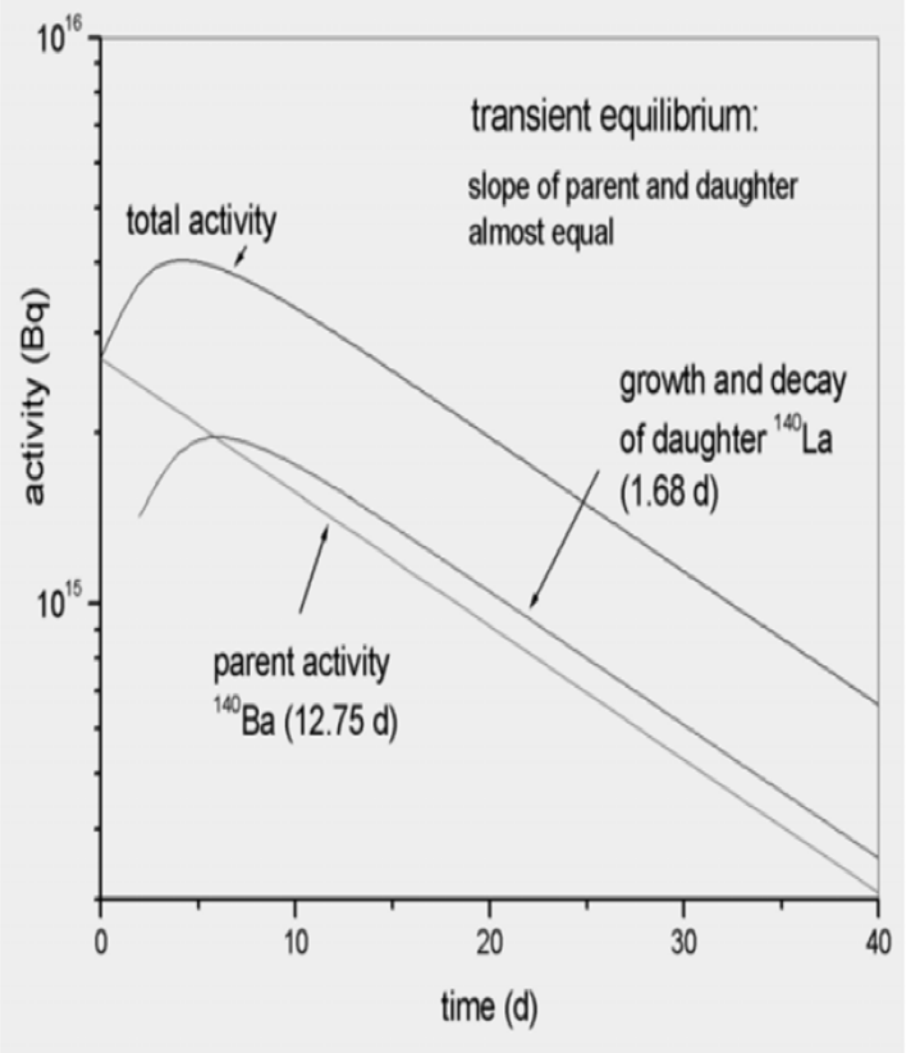

Figure 2.3: Typical transient equilibrium between ^{14}Ba and ^{140}La (Magill and Galy, 2004).

2.1.6 No equilibrium

When the parent radionuclide has a shorter half-life compared to that of its progeny, then the state of equilibrium will not be attained $(\lambda_W > \lambda_X)$ (Figure 2.4). In this case, the daughter activity rises to a maximum and then decays with its characteristic decay constant.

If the time of decay is very long then the term $e^{-\lambda_W t}$ becomes negligible. The daughter nuclei decay can then be calculated using $Eq.2.14$.

$$N_X(t) = N_w \frac{\lambda_W}{\lambda_X - \lambda_W} e^{-\lambda_X t} \qquad (Eq.2.14)$$

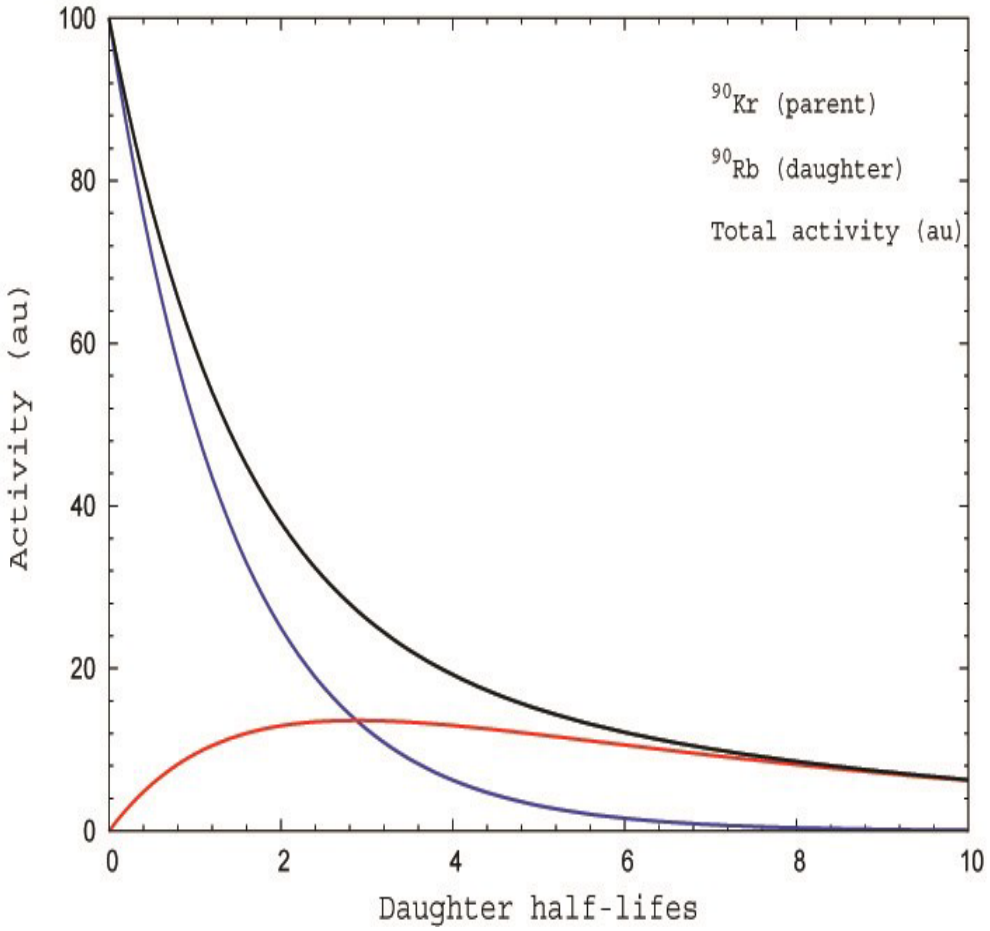

Figure 2.4: No equilibrium: the growth and decay of ^{90}Rb (of half-life 158 s) from ^{90}Kr (of half-life 33.33 s) (Magill and Galy, 2004).

2.2 Types of decay

Radioactive decay is the spontaneous nuclear disintegration of unstable radioisotope that results in the production of new stable progeny. The process results in the emission of both particulate and electromagnetic radiations. There exist three principal types of radiation emitted by radioactive substances (Lilley, 2001). These are;

2.2.1 Alpha decay

An alpha particles, α, are positively charged helium atoms. It has two protons and two neutrons bound together, with a total spin zero. Alpha emission occurs principally with nuclei that are too large having atomic number ($Z > 83$) hence, their instability. When a nucleus emits an alpha particle, its number of neutron, N, and its atomic number, Z, each decreases by 2 and its mass number, A, decreases by 4. Schematically, alpha decay can be written as:

$$ {}^{A}_{Z}X \rightarrow {}^{A-4}_{Z-2}Y + {}^{4}_{2}He + Q \qquad (Eq.2.15) $$

where X and Y are the initial and final nucleus species: One example is the disintegration of the radioactive isotope of ^{226}Ra to ^{222}Rn (part of the ^{238}U decay chain):

$$ {}^{226}_{88}Ra \rightarrow {}^{222}_{86}Rn + {}^{4}_{2}He + Q \qquad (Eq.2.16) $$

where Q is the amount of energy released, and is equal to the difference in mass-energy between the parent nuclei and its progeny. The disintegration energy (which is equivalent to Q) can be evaluated by accounting for the total mass/energy change in the disintegration process using the expression below.

$$ Q = (m_W - m_X - m_\alpha)c^2 \qquad (Eq.2.17) $$

where m_W, m_X and m_α are the nuclear masses of the parent radionuclide, the progeny and the released α particle, respectively. Alpha decay is a process found mainly in proton-rich, high atomic number nuclides owing to the fact that electrostatic repulsive forces increase more vigorously in heavy nuclides than the cohesive nuclear force. Equally, the emitted particle must have high energy to overcome the potential barrier in the nucleus as illustrated in Figure 2.5.

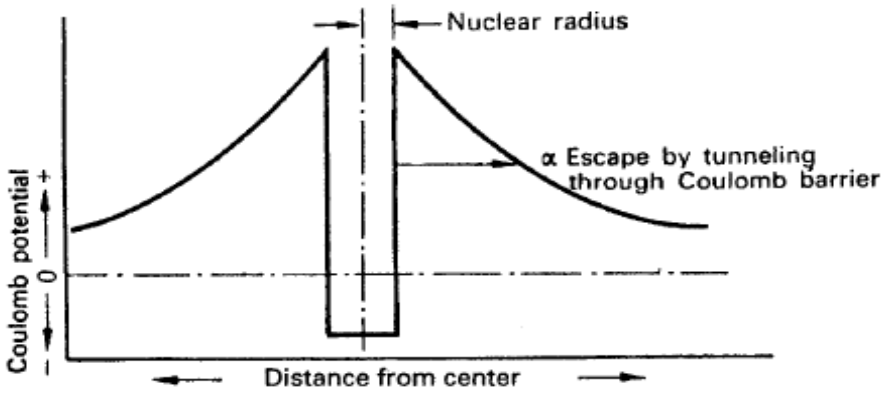

Figure 2.5: Potential inside and in the vicinity of a nucleus (Cember and Johnson, 2009).

The potential barrier has a height of about 25 MeV. At this height, alpha particle of about 4 MeV can still be released through the barrier by a process called quantum tunnelling. When an alpha particle interacts with matter, it losses all its energy and thus become a helium atom. The range of alpha particle in solids and liquids is small somewhat of the order of micrometres hence; they do not pose any external health hazard to human population. However, internally, the risk is high because of their high linear energy transfer (LET). The amount of LET values of ionising radiation imparted into a biological medium will increase sufficiently with mass and charge of the particle (Lamarsh and Bell, 2009). It is for this reason that the alpha particle decay will impart more amount of LET radiation and hence, produce a greater biological damage on an absorbing medium.

2.2.2 Beta decay

A beta particle (β) originates from the nucleus of the neutron-rich or proton-rich unstable nuclei (Lilley, 2001). The beta particle is an electrically charged particle with the same mass as an ordinary electron (Cember and Johnson, 2009). There exist three types of beta decay: beta-minus, beta-plus, and electron capture (Harvey, 1969; Lilley, 2001). Beta-minus particles (β^-) are negatively charged electron. The emission of β^- involves the nuclear transformation process where the neutron is transformed into a positively charged proton, a negatively charged electron, and a third particle called an antineutrino (Lilley, 2001). The process of reducing neutron number in nucleus, involves a neutron decaying into a proton, an electron and the third particle called the antineutrino which takes an average time of about 15 minutes for this transformation to occur.

Beta particles are released with a continuous spectrum of energy. This would not be possible if the two particles were the β^- and the recoiling nucleus, since energy and

momentum conservation would then require a definite speed for the β^-. Thus there must be a third particle involved. From conservation of charge, it must be neutral, and from conservation of angular momentum, it must be a spin-1/2 particle.

Antineutrino is the antiparticle of neutrino, ν_e. Both have no charge and their masses are negligible (zero). They therefore produce very little observable effect when passing through biological matter (Young and Freedman, 2008). Neutrinos have three different varieties each having its associate antineutrino. One corresponding to beta decay and the remaining two has an association with the decay of two unstable particles, the muon and the tau particles. The antineutrino that is released in β^- decay is denoted as $\overline{\nu_e}$. The main process involving β^- decay is

$$n \rightarrow p + \beta^- + \overline{\nu_e} \qquad (Eq.2.18)$$

In cases where the neutron-to-proton ratio, N/Z is too large for nuclear stability, beta-minus decay usually occurs. In decay process involving β^- decay, N decreases by 1, Z increases by 1 and A remains change. Radioactive nuclides for which N/Z is too small for the attainment of stability, positrons are emitted. Positrons are electron's antiparticle, which share identity with electron but have positive charge. Beta-plus decay therefore, occurs whenever the mass of the original neutral atom is at least two electron masses larger than that of the final atom. The basic process, called beta-plus decay (β^+), is

$$p \rightarrow n + \beta^+ + \nu_e \qquad (Eq.2.19)$$

The third type of beta decay called the electron capture. There are some but very few radionuclides for which the emission β^+ is not energetically possible but in which the K shell orbital electron can easily combine with a positively charged proton in the nucleus to produce a neutron and neutrino (Adloff and Guillaumont, 1993; Young and Freedman, 2008). The neutrons don't leave the nucleus only the neutrinos are emitted. Electron capture thus occurs whenever the mass of the original uncharged atom is larger than that of the final atom. The basic process is

$$p + \beta^- \rightarrow n + \nu_e \qquad (Eq.2.20)$$

2.2.3 Gamma decay

Gamma radiations are electromagnetic radiation emitted by atomic nuclei and are electrically neutral. This radiation can travel in the form of waves (Gilmore, 2008). Although gamma radiations are electromagnetic radiation they differ from all other electromagnetic

radiation on the basis of their short wavelength, frequency and origin (Krane, 1988). The energy of internal motion of a nucleus is quantized. There exist a set of allowed energy levels in a nucleus, a ground state also called the lowest energy state and a number of excited states. The strength of nuclear interactions are enormous hence, excitation energies of nuclei are typically of the order of 1 MeV, when compared with only a few eV for atomic energy levels. In a nuclear transformation involving both physical and chemical reactions, the nucleus always remains in its ground state. During the process of bombardment, the nucleus is placed in an excited state, either with high-energy particles or by the process of radioactive transformation, it thus, disintegrates to the ground state by releasing one or more photons called gamma-ray photons, having energies of 10 keV to 5 Mev (Adlof and Guillaumont, 1993; Young and Freedman, 2008). This process is called gamma (γ) decay. For example, alpha particles released from ^{226}Ra only have two possible kinetic energies, either 4.784 MeV or 4.602 MeV. Including the recoil energy of the resulting ^{222}Rn nucleus, these correspond to a total released energy of 4.871 MeV or 4.685 MeV, respectively. When an alpha particle with the smaller energy is emitted, the ^{222}Rn nucleus is left in an excited state.

2.3 Environmental sources of radioactivity

Natural occurring radioactive materials (NORM) are categorized as arising from two origins; these are namely, cosmogenic and terrestrial. Other sources arise from human activities concerned with the use of radiation and radioactive materials from which release of radionuclides into the environment may occur (Klement, 1982; Eisenbud and Gesel, 1997).

2.3.1 Cosmogenic origin

Cosmic rays are composed mainly of highly energetic positively charged particles (mostly protons), and high energy photons (UNSCEAR, 2000). The upper atmosphere shields the earth and blocks most of the cosmic rays that approach the earth. However, some radionuclides are generated by the interactions of cosmic rays with the earth's upper atmosphere (Eisenbud and Gesell, 1997; Knoll, 2000). These nuclear interactions are formed mainly from secondary neutron capture and high-energy nuclear spallation (Klement, 1982; UNSCEAR, 2000). Spallation refers to a process in which a heavy nucleus emits a large number of nucleons as a result of being hit by a high-energy particle (UNSCEAR, 2000). The majority of the target atoms in the earth's atmosphere are those from argon, oxygen, and nitrogen gases.

There exist a large number of cosmic-ray produced radioactive isotopes that can be found on the earth surface (Table 2.1). There are several cosmogenic radionuclides with a

wide range of half-lives from minutes to millions of years. However, studies have shown that only four of them contribute a significant measurable dose of radioactivity to human population (NCRP, 1975; Eisenbud and Gesell, 1997; UNSCEAR, 2000).

From environmental hazards point of view, the main cosmogenic radionuclides are tritium (^{3}H), beryllium-7 (^{7}Be), carbon-14 (^{14}C) and sodium-22 (^{22}Na) (NCRP, 1975 Eisenbud and Gesell, 1997; Watson *et al*., 2005). Of all these, ^{14}C is the most significant cosmogenic radionuclide because it can be taken up by plants and hence, become part of the food chain (Watson *et al*., 2005). Some other heavy radioactive elements such as thorium and uranium have also been detected in meteoritic material (Klement, 1982; Kathren, 1998). The average radiation exposure to cosmic rays according to UNSCEAR (2000) is 0.4 mSv (Table 2.2).

Table 2.1: Cosmogenic radionuclides of natural origin (UNSCEAR, 2000)

Elements	Isotope	Half-life	Decay mode and γ-line energy (kev)
Hydrogen	^{3}H	12.33 y	$\beta^{-}(100\%)$
Beryllium	^{7}Be	53.29 d	EC (100%) and $\gamma(477.612)$
	^{10}Be	1.51 x 10^{6} y	$\beta^{-}(100\%)$
Carbon	^{14}C	5730 y	$\beta^{-}(100\%)$
Sodium	^{22}Na	2.602 y	$\beta^{+}, and \gamma(1279)$
Aluminium	^{26}Al	7.4 x 10^{5} y	EC (100%)
Silicon	^{32}Si	172 y	$\beta^{-}(100\%)$
Phosphorus	^{32}P	14.26 d	$\beta^{-}(100\%)$
	^{33}P	25.34 d	$\beta^{-}(100\%)$
Sulphur	^{35}S	387.51 d	$\beta^{-}(100\%)$
Chlorine	^{36}Cl	3.01 x 10^{5} y	$EC(1.9\%), \beta^{-}(98.1\%)$
Argon	^{37}Ar	35.04 d	$EC(100\%)$
	^{39}Ar	269 y	$\beta^{-}(100\%)$
Krypton	^{81}Kr	2.29 x 10^{5} y	$EC(100\%)$

Table 2.2: Average radiation exposure from natural sources (UNSCEAR, 2000)

Source	Worldwide average annual effective dose, mSv	Typical range
<u>External</u>		
Cosmic ray	0.4	0.3 – 1.0
Terrestrial rays	0.5	0.3 – 0.6
<u>Internal</u>		
Inhalation (radon)	1.2	0.2 – 10
Ingestion	0.3	0.2 – 0.8
Total	2.4	1 - 10

2.3.2 Terrestrial origin

Terrestrial radionuclides are widely distributed in rocks, soil, water, oceans and also in building materials (UNSCEAR, 2000; Xinwei *et al*., 2006). These radionuclides were present at the creation of the planet. Such radionuclides are commonly referred to as primordial radionuclides. Primordial radionuclides have very long decay half-lives, which are comparable to the age of the earth (Wilson, 1994; Lilley, 2001; Tzortzis, 2005). Studies have shown that primordial radionuclides can be subdivided into the series and non-series radionuclides (NCRP, 1975; Eisenbud and Gesell, 1997). Table 2.3 presents a list of primordial radionuclides.

Table 2.3: List of primordial radionuclides (Eisenbud and Gesell, 1997; UNSCEAR, 2000)

Nuclide	Decay Mode	Half-life (years)	Isotopic Abundance (%)	Stable Disintegration Products
^{40}K	β, ε, γ	1.3×10^{9}	0.0117	^{40}Ar, ^{40}Ca
^{50}V	β, ε, γ	1.4×10^{17}	0.25	^{50}V, ^{50}Ti
^{87}Rb	β	4.9×10^{10}	27.83	^{87}Sr
^{113}Cd	β	7.7×10^{15}	12.22	^{113}In
^{115}In	β	4.4×10^{14}	95.71	^{115}Sn
^{123}Te	ε	6.0×10^{14}	0.89	^{123}Sb
^{138}La	β, ε, γ	1.1×10^{11}	0.09	^{138}Ba,
^{144}Nd	α	2.4×10^{15}	23.80	^{138}Ce
^{147}Sm	α	1.1×10^{11}	14.99	^{140}Ce
^{148}Sm	α	7.0×10^{15}	11.24	^{143}Nd
^{152}Gd	α	1.1×10^{14}	0.20	^{144}Nd
^{174}Hf	α	2.0×10^{15}	0.16	^{148}Sm
^{176}Lu	β, γ	3.8×10^{10}	2.59	^{170}Yb
^{186}Os	α	2.0×10^{15}	1.59	^{176}Hf
^{187}Re	β	4.1×10^{10}	62.60	^{182}W
^{190}Pt	α	6.5×10^{11}	0.014	^{187}Os
^{238}U(series)	α	4.5×10^{9}	99.27	^{186}Os
^{235}U(series)	α	7.0×10^{8}	0.72	^{206}Pb
^{232}Th(series)	α	1.4×10^{10}	100	^{207}P

2.3.3 Series radionuclides

Uranium, Thorium and Actinium make up the three main radioactive decay series (Lilley, 2001). There exist also the Neptunium series but due to the non-existence of the head of the Neptunium series and owing to its short half-life daughters, the series does not count as part of the natural radioactive decay chain on earth (NCRP, 1975). The heavy isotopes of ^{238}U , $^{232}Th,$ and ^{235}U heads the chain of series radionuclides. These three chains of radionuclides decay through sequences of radioactive daughter nuclides that have varying ranges of half-lives. This process continues until a stable isotope of lead at the end of each decay chain is reached. Figures 2.6-2.8 present the decay schemes of series radionuclides.

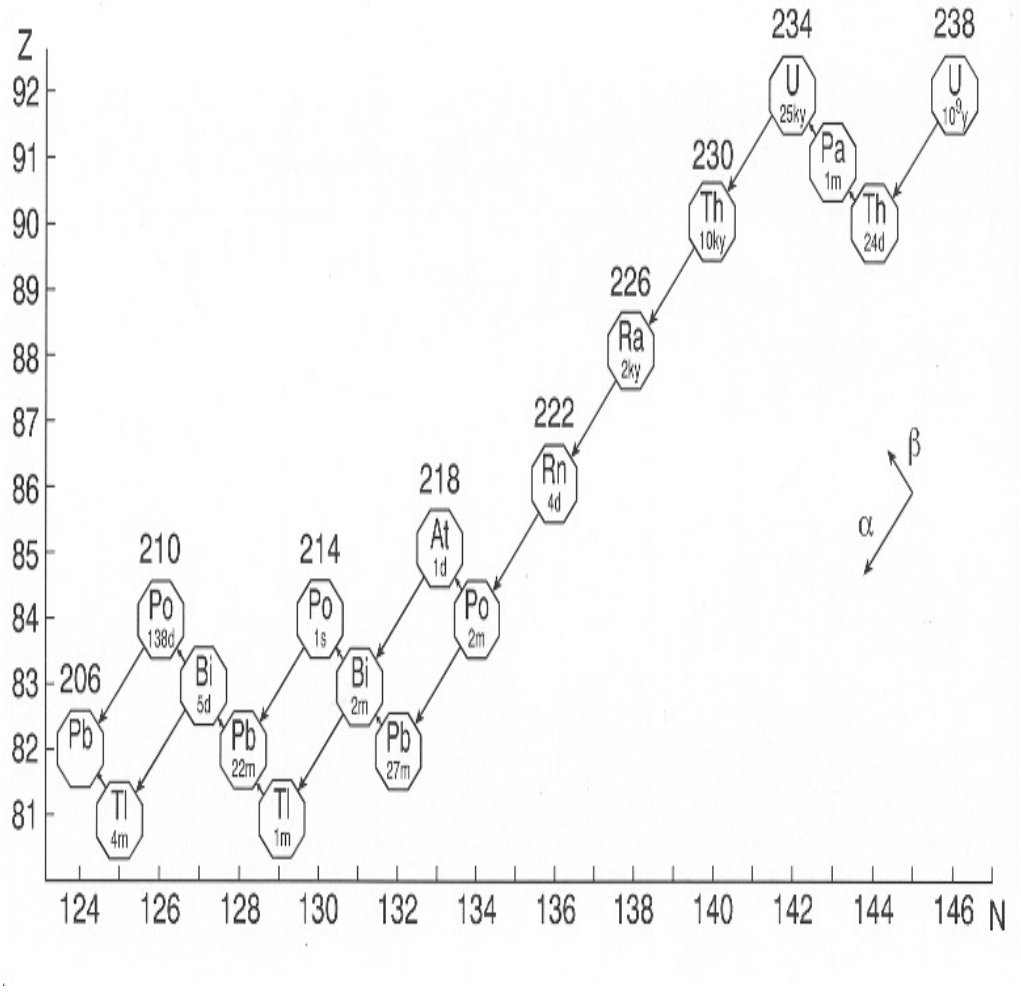

Figure 2.6: Schematic of ^{238}U decay chain and its decay products (Huda, 2011).

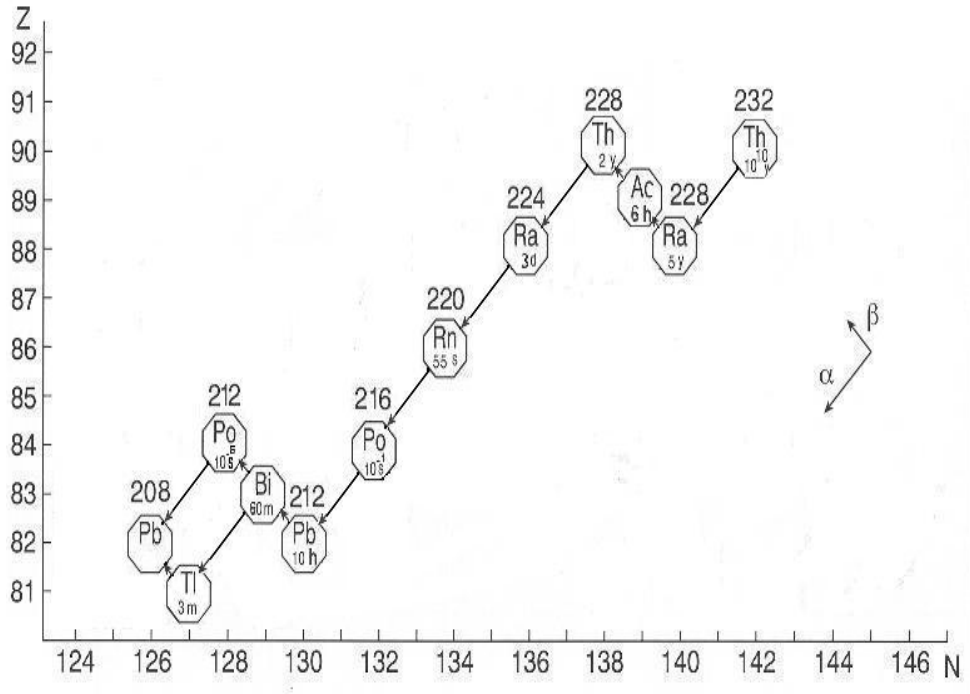

Figure 2.7: Schematic of the ^{232}Th decay chain and its decay products (Huda, 2011).

.

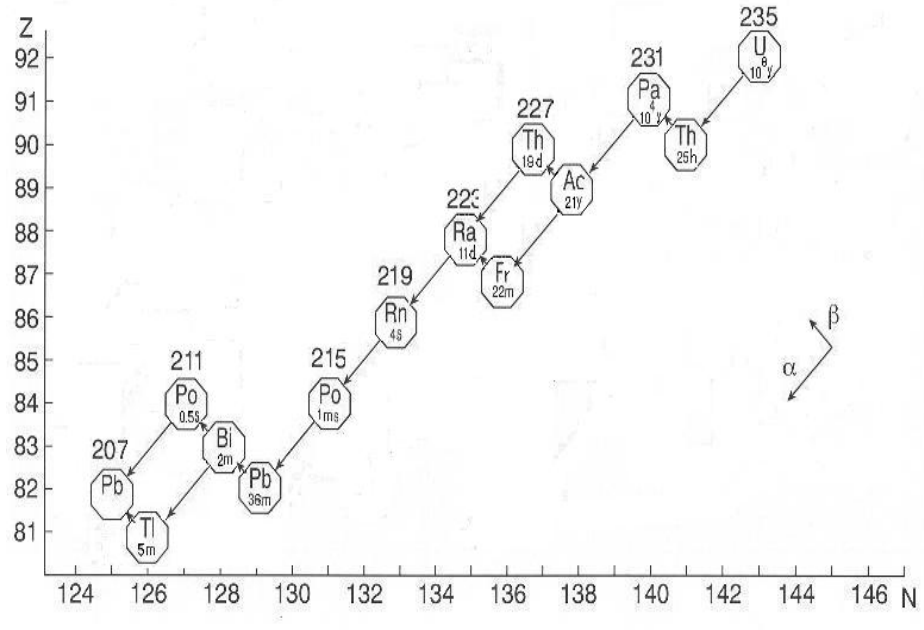

Figure 2.8: Schematic of the Actinium ^{235}U decay chain and its decay products (Huda, 2011).

2.3.4 Non-series radionuclides

Primordial radionuclides that decay directly to stable nuclides are termed non-series radionuclides. From Table 2.3, it is seen that some of these radionuclides have extremely long half-lives and an insignificant isotropic abundances. Hence, they have negligible activities and as such are not considered radiologically significant to humans. Nevertheless, ^{40}K and ^{87}Rb that are members of the group have significant sources of natural radiation (Sood, 1981; NCRP, 1975; Watson *et al*., 2005). ^{40}K can decay by beta followed by gamma-ray emission whereas ^{87}Rb is a pure beta emitter (NCRP, 1975; Paul, 1979; Watson *et al*., 2005). Figure 2.9 gives a schematic representation of ^{40}K decay.

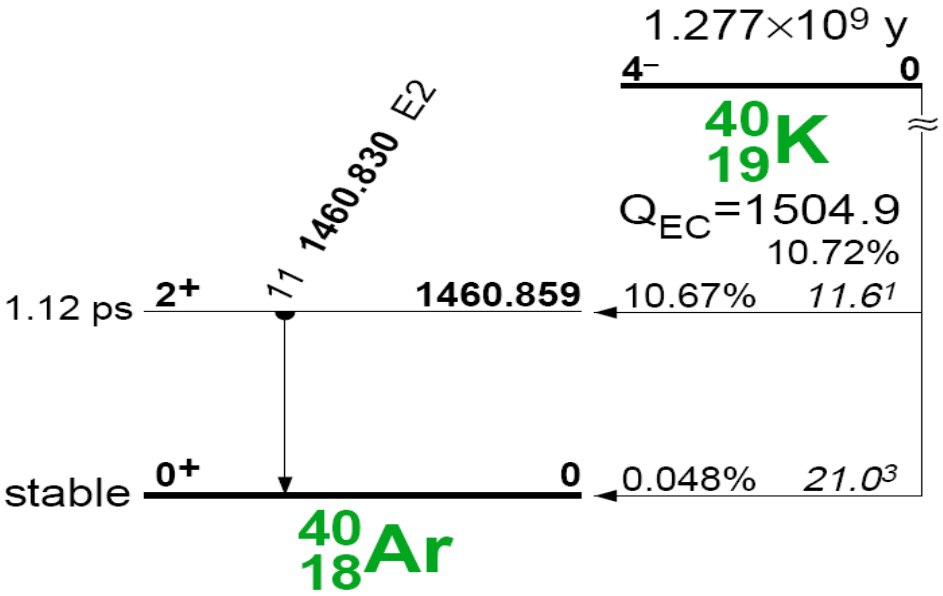

Figure 2.9: Schematic of the ^{40}K decay (Browne et al., 1986).

2.3.5 Anthropogenic sources

Some human endeavours such as mining and extraction of ores, processing and transportation often lead to emission of radioisotopes into the environment. There exist several ways by which radioisotopes can reach human body and these are categorized as on-site and off-site respectively. On-site exposure are those that affect mainly human population that work with radioactive materials and those who are living within the vicinity of mining activities where NORM could be present in excavated raw materials, industrial waste piles, storage tanks, build-up of contamination on equipment and in pipes. These are direct exposure to external gamma irradiation or internal exposure resulting from inhalation of radioisotopes in dust (O'Brien and Cooper, 1998). On the other hand, off-site exposure is that exposure to human population who live within or near the vicinity of mining environment.

This is characterised by indirect exposure. External exposure to the general public can result from exposure to gamma radiation from cosmic rays passage from the upper atmosphere, reconstituted radioisotopes in suspended particulate matter, and the use of industrial waste containing NORMs or through ingestion of radioisotopes that are incorporated in the food chain (Dahlgaard, 1996).

2.4 Summary

In this chapter the basic physics of environmental radioactivity was given. The presentation shows that radioactivity is a statistical phenomenon where an unstable 'parent' nucleus is transformed into a more stable nuclide called the daughter (NCRP, 1985; Liley, 2001). This process is called radioactive decay which is the spontaneous nuclear transformation to form new stable elements. The different types of decay have also been presented.

CHAPTER 3

PRINCIPLES OF GAMMA-RAY SPECTROMETRY AND INSTRUMENTATION

3.1 Introduction

This chapter discusses the interaction of gamma rays with matter and gives a comparative study of the different techniques used to measure environmental radioactivity and the reasons for the choice of high purity germanium detector in this present study.

3.2 Interaction of gamma rays with matter

A gamma ray can be defined as an electromagnetic radiation which has both wave-like and particle characteristics. The properties of gamma radiation are distinct, hence, they have differentiated it from the massive alpha and less-massive negatively charged beta particles. Gamma radiations are characterized by a much greater penetration power and longer range at very high energy. The photon energies for gamma rays are typically ~ 100 keV to ~ 5 MeV (Knoll, 2000).

When an uncharged gamma-ray photon interacts with electrons in an absorbing medium, it can lose all or part of its energy to the electrons during the process leading to indirect ionization. Although there are various possible interaction mechanisms for gamma rays in matter, only three most important mechanisms play a significant role in radiation measurement (Knoll, 2000). These are the photoelectric absorption, Compton scattering, and pair production.

3.2.1 Photoelectric absorption

The photoelectric absorption process involves the interaction of an incident photon with a bound electron in an absorber medium. During this process, the incident photon releases all of its energy to a bound electron. Then an energetic electron called a photoelectron is ejected from one of the electron shell (K shell) as shown in Figure 3.1. The vacancy shell will be filled quickly through the process of capturing of a free electron from other shells of the atom. The de-excitation process of the atom may lead to electron rearrangement from higher shells to fill in a vacancy leading to the emission of characteristic X-ray. The outgoing electron is ejected with an energy given by,

$$E_{e^-} = h\nu - E_b \qquad (Eq.3.1)$$

where hv and E_b represents the energy of the photon and the binding energy of the electron to the atom (Knoll, 2000). Photoelectric effect is generally the dominant attenuation mechanism involving an incident photon and bound electrons with energies $\leq 200keV$. Characteristic x-rays may appear from the gamma spectrum. The probability of photoelectric absorption (τ) varies approximately with the atomic number (Z) of an absorbing medium and photon energy (E_γ), according to,

$$\tau \cong \text{constant x } \frac{Z^n}{E_\gamma^{3.5}} \quad , \; n = 4\text{-}5 \qquad (Eq.3.2)$$

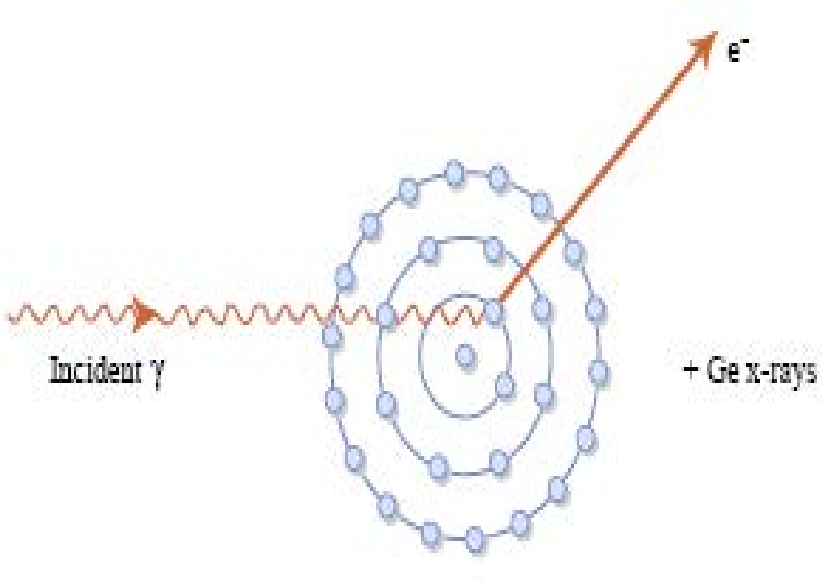

Figure 3.1: Schematic of photoelectric absorption process (Knoll, 2000).

3.2.2 Compton scattering

In a Compton scattering process, part of the energy of an incident gamma-ray photon is transferred to a free or a loosely bound electron of the absorbing medium (Omole and Akanbi, 1997). During this process, only a portion of the photon energy is transferred to the electron. This result in the degradation of energy of the incoming photon of the gamma-ray after which, it is deflected from its original path and subsequently emits a recoil electron. The Compton effect is one of the major ways in which a beam of X-rays and γ-rays is attenuated in passing through matter. From the principle of conservation of energy, the energies of the scattered photon and recoil electron are related to the angles at which they are emitted. Figure 3.2 shows a schematic diagram of the Compton scattering effect.

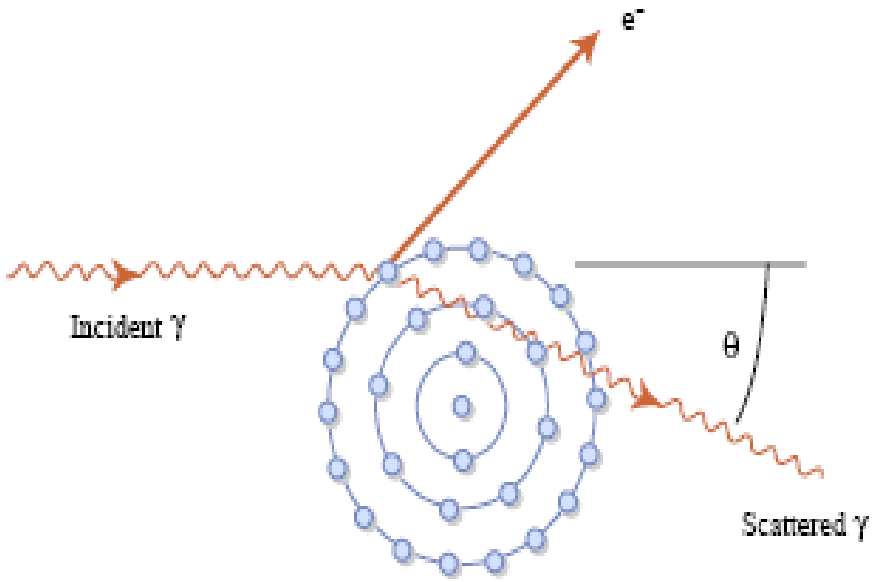

Figure 3.2: Schematic of Compton scattering process (Knoll, 2000).

The energy of the scattered photon $h\nu'$ is related to the scattering angle θ by the expression (Kaplan, 1962)

$$h\nu' = \frac{h\nu}{1+\left(\frac{h\nu}{m_0c^2}\right)(1-\cos\theta)} \qquad (Eq.3.3)$$

where $m_0c^2 = 511$ keV represents the rest mass energy of the bound electron. It thus, follows that the kinetic energy of the recoil electron is given by;

$$E_{e^-} = h\nu - h\nu' = h\nu\left(\frac{(h\nu/m_0c^2)(1-\cos\theta)}{1+(h\nu/m_0c^2)(1-\cos\theta)}\right) \qquad (Eq.3.4)$$

The energy associated with the recoil electron can change from zero $(\theta = 0)$ up to a maximum value $(\theta = \pi)$ depending on the scattering angle. The maximum energy of the recoil electron is given by

$$E_{e^-} = \frac{2h\nu}{2+m_0c^2/h\nu} \qquad (Eq.3.5)$$

The probability of Compton scattering taking place depends on the number of electrons per unit mass of the interacting material and the incoming gamma-ray energy as a function of $\frac{1}{E_\gamma}$ (Lilley, 2001).

3.2.3 Pair production

This process occurs only within the coulomb field of the nucleus given rise to the conversion of gamma-ray into an electron-positron pair. Pair production process is only possible when the gamma-ray photon has energy twice greater than the rest mass energy of 511 keV $(2m_0c^2 = 1.022MeV)$. This process takes place only under the control of the field of a nucleus, but the probability is much lower and the energy threshold is twice greater than (2044 keV). This makes its contribution much smaller and hence, not considered in gamma-ray spectrometry analysis. The electron and positron so created share in the excess gamma-ray energy equally, losing it to the detector medium as they are slowed down.

$$E_e = E_\gamma - 2m_0c^2 \qquad (Eq.3.6)$$

Once, the positron slows down, it can combine with an atomic electron in the surrounding material and subsequently annihilate to form two photons referred to as annihilation photons, each having energies $m_0c^2 = 0.511MeV$.

For linear momentum to be conserved, the two photons must be emitted in opposite directions as shown in Figure 3.3.

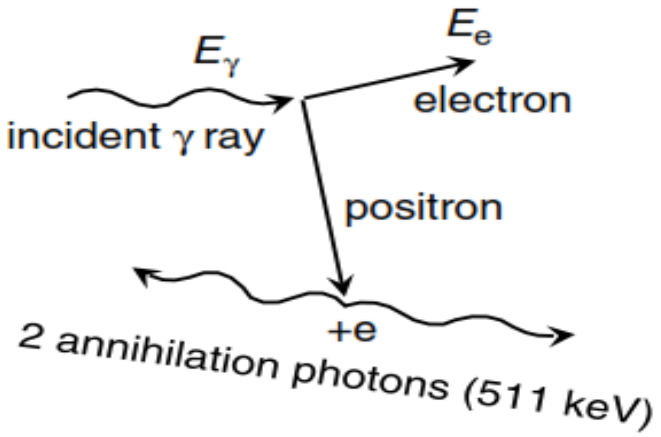

Figure 3.3: Mechanism for pair production and annihilation (Knoll, 2000).

There exist no simple expression for the probability cross section of pair production per nucleus, K, but its size varies approximately as the square of the absorber atomic number.

$$K \approx Z^2 f(E_\gamma, Z) \qquad (Eq.3.7)$$

The variation of the K with the atomic size is dominated by the Z^2 term. The function $f(E,Z)$ is only slightly dependent on Z and increases continuously with energy from the

threshold 1022 keV. At energies greater than 10 MeV, pair production is the most prominent of all the interaction mechanisms. Figure 3.4 represents the relative importance of all the three interaction processes and shows that these interactions are a function of gamma-ray energy and the value of Z absorber.

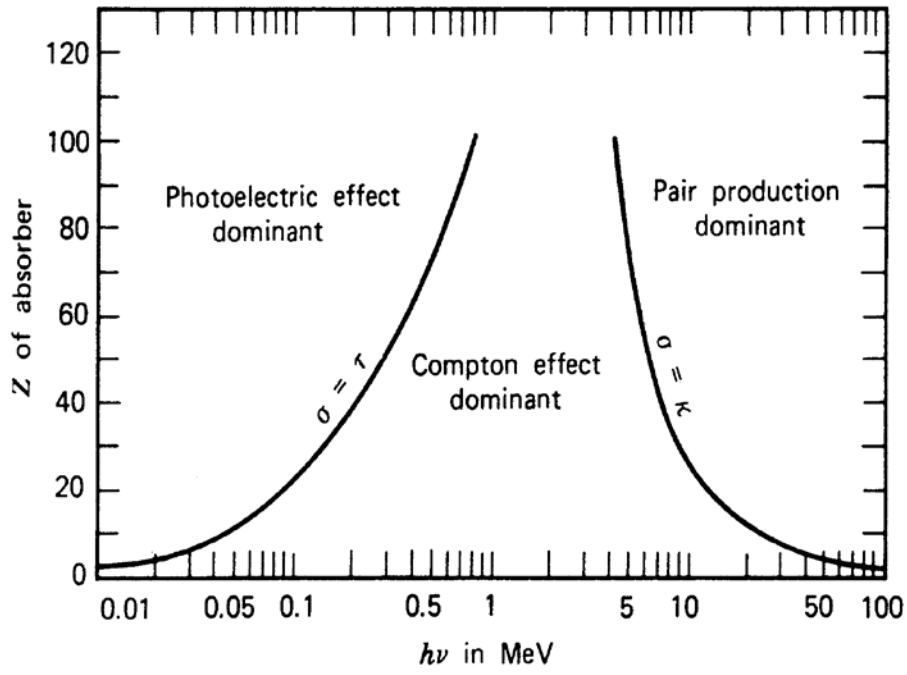

Figure 3.4: The three gamma-ray interaction Processes (Knoll, 2000).

3.3 Instruments for measurement of natural radioactivity in the environment

Radiation detectors operate by detecting a change in the absorbing medium which is caused by the transfer of energy from the ionizing radiation to the medium. There are many different types of instruments available for measuring ionizing radiation in samples. Some of these instruments include: gas filled detectors (ionization chamber counters, proportional counters and Geiger-Muller counters); scintillation counter; and solid state detectors (semiconductor detectors).

Any radiation detector requires two basic elements namely the sensing and indicating elements – the sensing elements, which converts the energy of the incident radiation into electrical energy. These sensing elements for the detection of radiation rely upon the formation of ions as in Geiger counters, ionization counters and proportional counters. When these ions are formed, an indicating element e.g. a scaler, recorder or rate meter is required to measure the resultant electrical energy form.

For any radiation to be detected or measured by any detector, it has to give up its energy to the medium of the detector either by ionising it directly or by causing it to emit a

charged particle which later produces ionisation of the medium. Electromagnetic radiation gives rise to energetic electrons by one of the three types of processes, namely photoelectric effect, Compton scattering and pair production as discussed in section 3.2.

Gas-filled detectors are the most suitable detectors only for measurement of low energy electrons, ions and photons due to their poor stopping capacity as detection medium for gamma rays. To this end, the means of improving the absorption probability of a detecting medium, a higher atomic and/ or higher density liquid or solid material is employed to measure highly penetrating radiation (Krane, 1988; Gilmore, 2008).

Detectors which are based on the principles and practice of scintillation can be used for the detection and measurement of ionising radiation. For example, in gamma spectrometric analysis, thallium-activate sodium iodide scintillator $(NaI(Tl))$ is the most frequently used detector. This is because of its high efficiency for the detection of gamma rays and also because it does not require cooling. This is not the case with scintillation detectors because they do not provide the energy discrimination (Knoll, 2000; Cember and Johnson, 2009) to deal with a complex gamma radiation spectrum occasioned by their poor energy resolution as shown in Figure 3.5. To achieve a good energy resolution, semiconductor detectors are used. To this end, this project employed the use of high purity germanium semiconductor detectors.

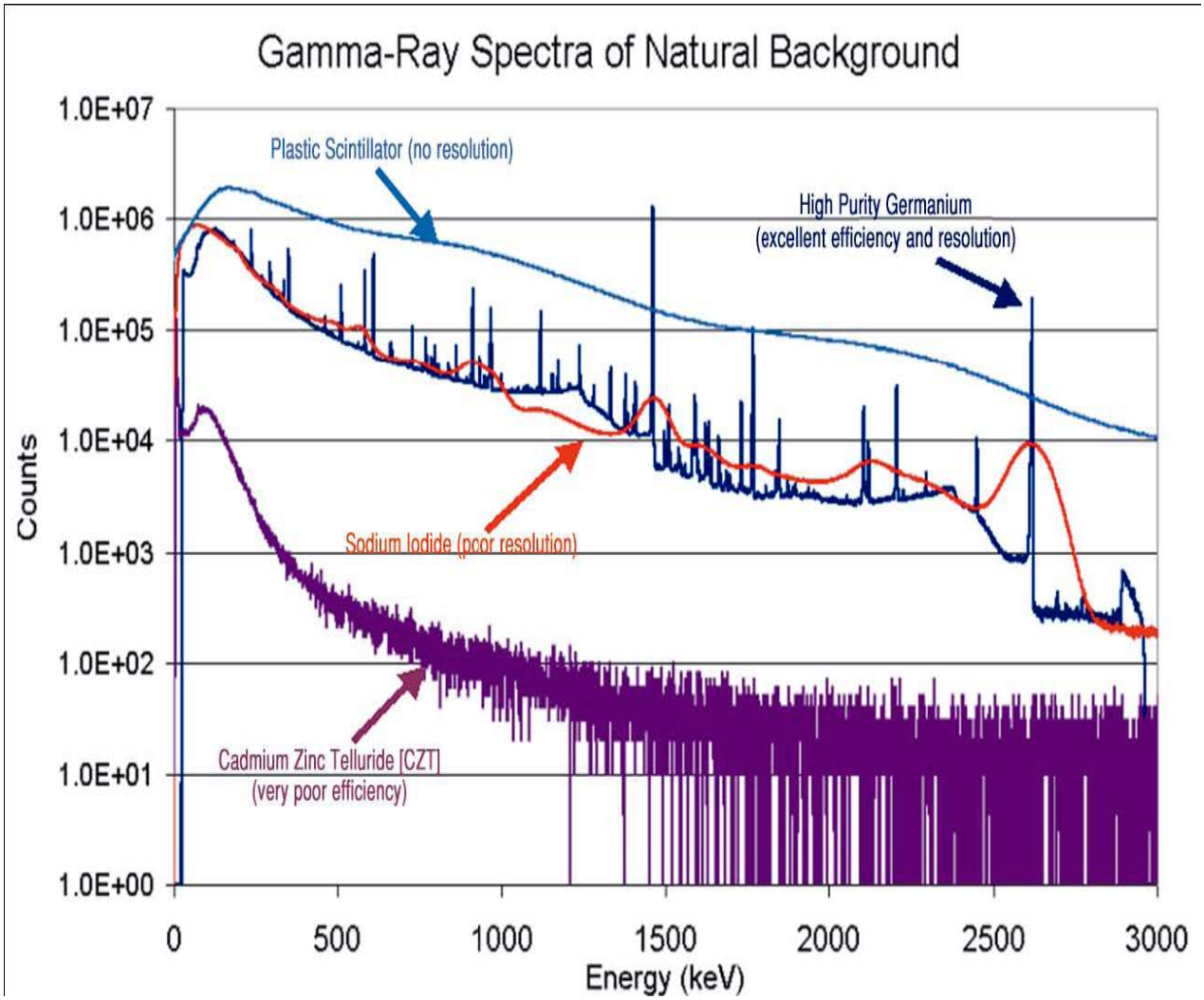

Figure 3.5: Comparison of natural background radiation collected by different radiation detectors (Ortec, 2003).

3.3.1 Semiconductor detectors

The amount of energy that is required to produce an ionisation event in a semiconductor detector is 3.5 eV. This value is in contrast to the gas filled detectors which require a mean high energy of 30-35 eV to produce an ionising event (Cember, 1996). A semiconductor is a substance that has electrical conducting properties in the midway between a conductor and an insulator. Silicon and germanium are the commonly used semiconductors. These are elements in group IV (has four (4) valence electrons) of the periodic table. They form crystals that are made up of a lattice of atoms that are linked together by covalent bonds. Table 3.1 presents some common physical properties of silicon and germanium.

Table 3.1. Some properties of intrinsic germanium and silicon (Lilley, 2001; Knoll, 2000).

	Silicon (Si)	**Germanium (Ge)**
Atomic number, Z	14	32
Atomic weight, A	28.09	72.60
Density (300 K) in g/cm ^{3}	2.33	5.32
Forbidden energy gap in eV at:		
300 K	1.115	0.665
0 K	1.165	0.746
Electron mobility in cm^2/V s at:		
300 K	1350	3900
77 K	21000	36000
Hole mobility in cm^2/V s at:		
300 K	480	1900
77 K	11000	42000
Energy per electron-hole pairs in eV at:		
300 K	3.62	-
77 K	3.76	2.96

3.3.2 Electrical conductivity and band theory

Solids materials are subdivided into conductors, semiconductors and insulators. This is based on the availability of conduction electrons within the structure of the solid material. Band theory provides an understanding into these differences in electrical properties and gives accounts for the presence, or absence, of those conduction electrons.

Each atom has defined allowed energy levels for its electrons; in situation where a large number of atoms are joined together forming a solid mass the energy levels become restructured in a way that there will be bands of possible energy levels (Figure 3.6). This restructuring process is referred to as the tight binding approximation.

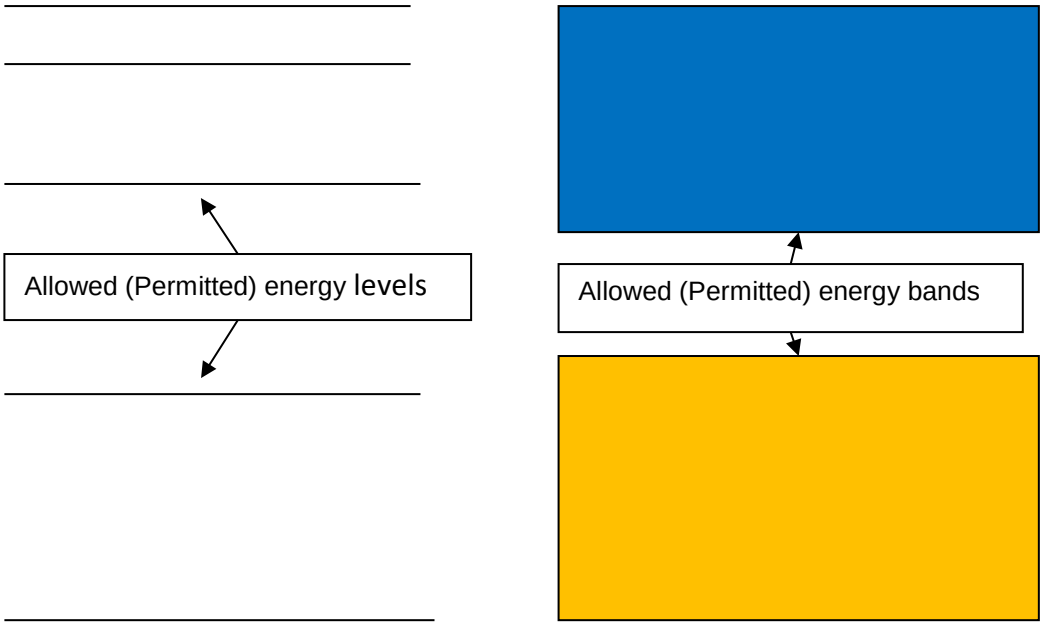

Figure 3.6: Discrete energy levels within an atom (left) and bands of allowed energy levels within a solid material (right) (LTS, 2011).

There exist electrons in solid materials. The bands are filled if the discrete energy levels exist in solid. They can be described as valence and conduction band though many permitted energy bands are available in that solid. Figure 3.7 shows the band description of solid.

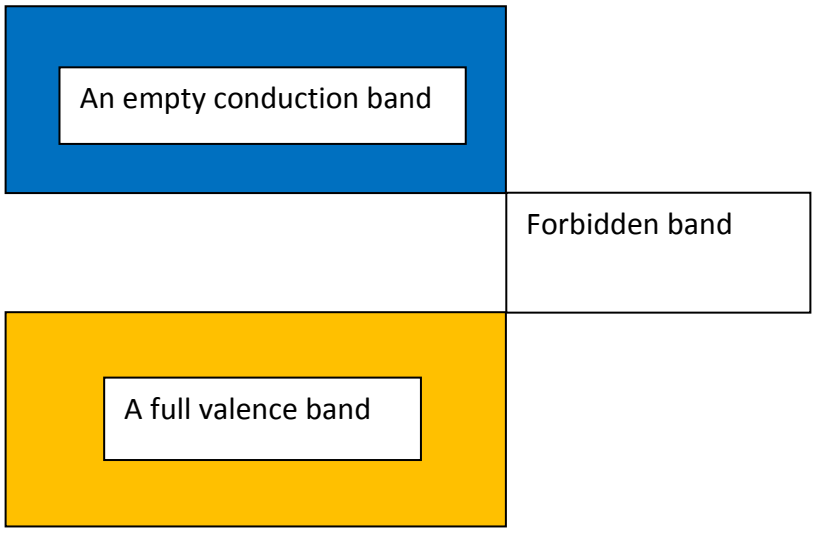

Figure 3.7: Conduction and valence bands in an insulator (LTS, 2011).

The electrons that have lower energy occupy the valence band. They are considered as bound electrons which are less influence by nearest atom with

specific energy levels. The valence bound electrons move from one atom to another and will not contribute to the conduction. The lowest level to the highest level is only filled by electrons in the valence band. The uppermost level of the valence band is filled by the available electrons at absolute temperature. The valence band of insulator and semiconductor is completely filled with electrons but the conduction band is empty. Due to the difference in the available electrons in different band, insulator and semiconductor form a gap between conduction and valence band called the forbidden gap (Figure 3.8).

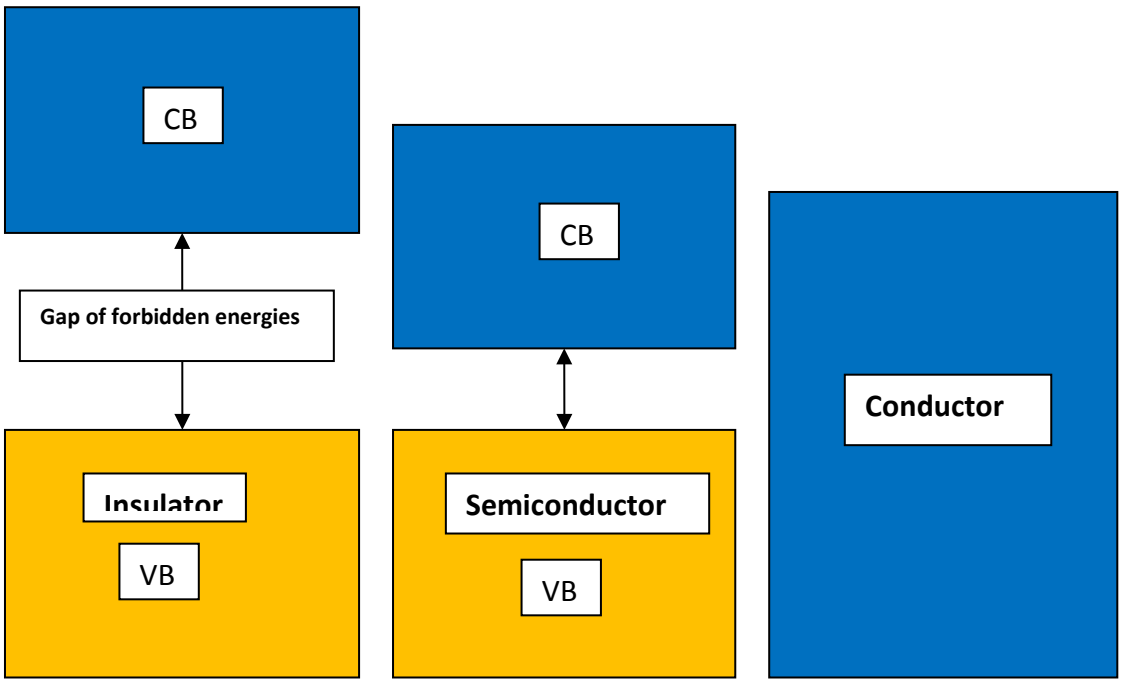

Figure 3.8: Conduction bands (denoted with blue) and valence bands (denoted with yellow) for insulators, semiconductors and conductors (LTS, 2011).

Forbidden gap is more in insulator and it gives clear separation between valence band and conduction band. The energy gap is nearly of 1eV .For different products this gap is different. So electrons cannot easily migrate from valence band to conduction band.

But in semiconductors, valence band is completely filled. The forbidden gap is very small for example, in silicon and germanium this energy gap is nearly 1.1 eV and 0.72 eV respectively and it is very much possible for electrons to move from valence band to conduction band with minimum amount of energy. With increased temperature, or thermal excitation, more number of electrons is available in the conduction band. Therefore, the increase of conductivity of semiconductors, by the process of doping is necessary.

3.3.3 Intrinsic semiconductors

The group IV element of the periodic table such as silicon and germanium are the intrinsic semiconductors having the tetrahedral structure. They are undoped semiconductors. In this case, electrons are thermally excited easily and migrate to the conduction band. So vacancies are created by electrons in the valence band with a small amount of energy. The created electron vacancy can easily be available for conduction (Gilmore, 2008) (Figure 3.9).

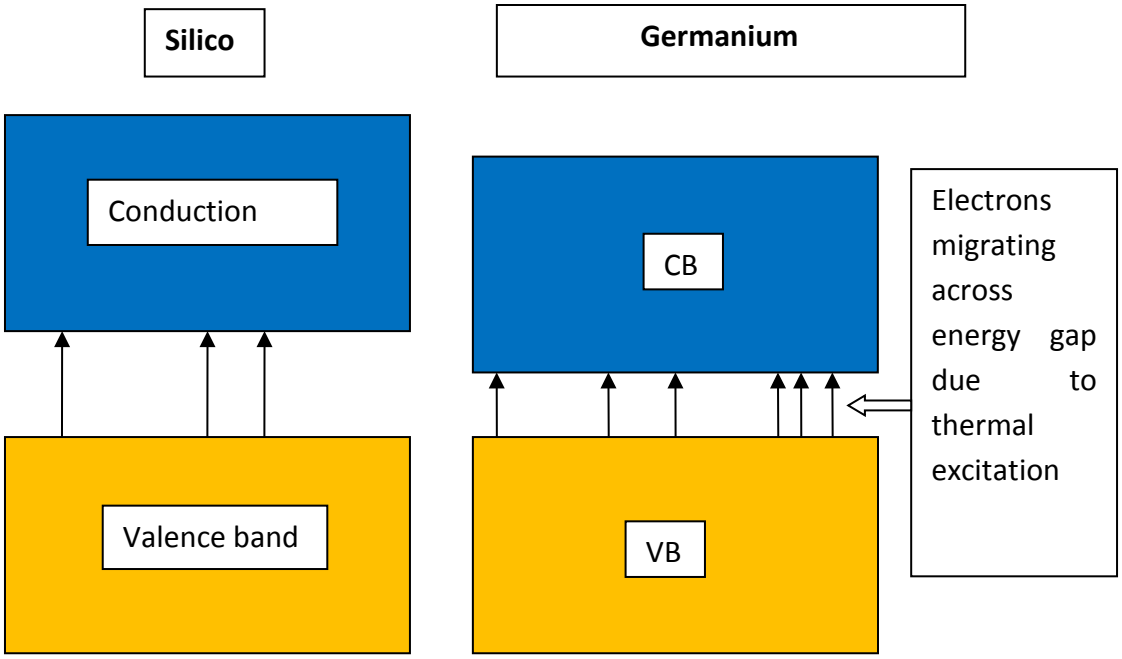

Figure 3.9: A significant numbers of electrons to crossing the energy gap in semiconductors (LTS, 2011).

The valence electrons move to the conduction band creates a hole in the valence band due to formation of hole and other valence electrons fill its position. So holes acts as a positively charged carrier. Therefore, in this semiconductor, hole travels instead of electrons.

3.3.4 Extrinsic semiconductors

It is an improved intrinsic semiconductor where we intentionally change the properties of semiconductors with the addition of small amount of impurities. The conductivity can be controlled by the introduction of different impurity atoms. Based on the conductivities, the majority charge carriers are either electrons or holes. The Figure 3.10 gives an indication of doped semiconductor which has only three electrons in its outer shell. They are unable to form covalent bond with nearest group four elements. Therefore, hole is created to fill the position and make a new semiconductor crystal. Therefore, this type of semiconductor is called P-type semiconductor where holes are the majority charge carrier. We can enhance the conductivity of the semiconductor by doping which will give energy to flow the charge inside the semiconductor easily. In p-type semiconductor, conduction occurs in the valence band. This is called acceptor band due to the addition of impurity atom to an energy level created just above the valence band.

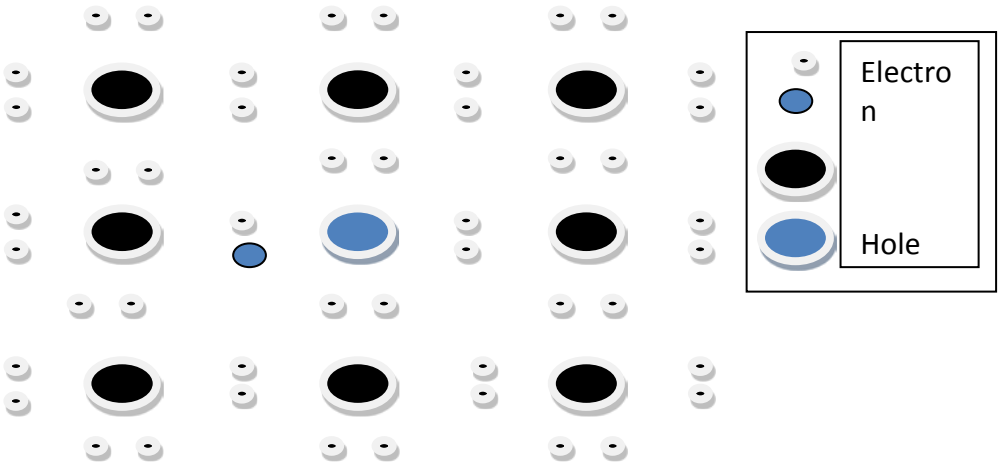

Figure 3.10: Impurity atom introduced into a silicon lattice leaves holes built into the valence band (LTS, 2011).

Similarly, n-type semiconductor can be formed by doping group five elements to give an extra electron for conduction process. Here, a donor band is created due to formation of an extra energy level below conduction band.

3.3.5 P-N junction

When p and n-type semiconductors are interfaced with each other, p-n junction is formed with one end p-type and the other end n-type with different behaviours. In the junction, electron move from n-type to p-type boundary and hole from p-type to n-type boundary form a small region called the depletion layer (Gilmore, 2008) (Figure 3.11)**.** Due to the formation of depletion layer, p-n junction contributes heavily to the conduction process. This process is due to the movement of majority electrons and holes towards opposite sides; no further diffusion of electrons and holes takes place due to formation of depletion layer. Such a process results in there being no further diffusion of electrons or holes owing to Coulomb attraction and repulsion (Figures 3.11 and 3.12).

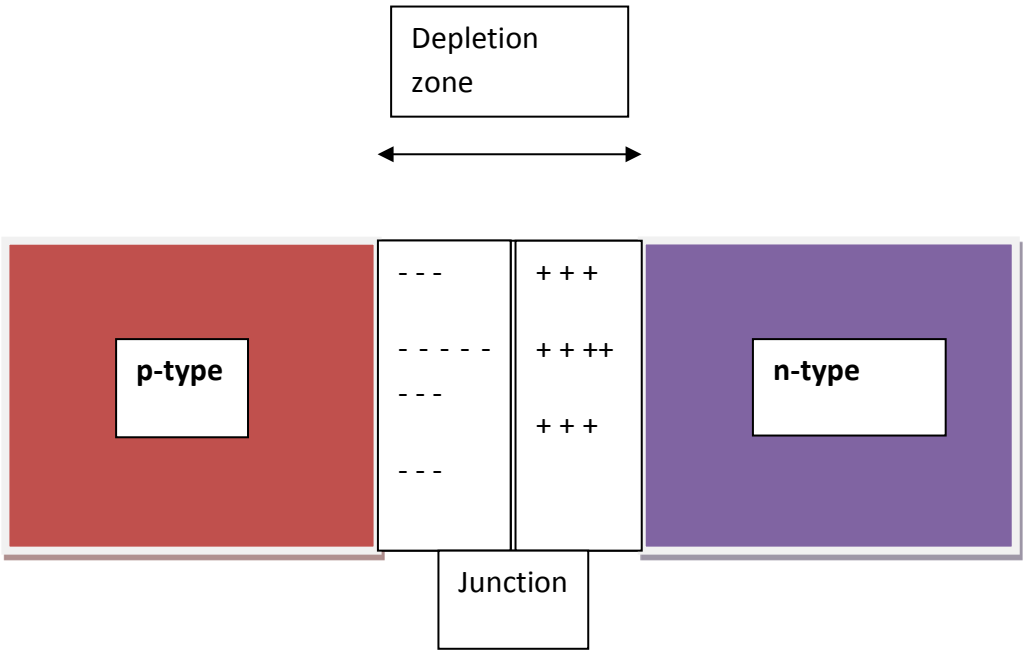

Figure 3.11: Schematic of a p–n junction forming a depletion zone by the diffusion of electrons from the n-type material into the p-type material (LTS, 2011).

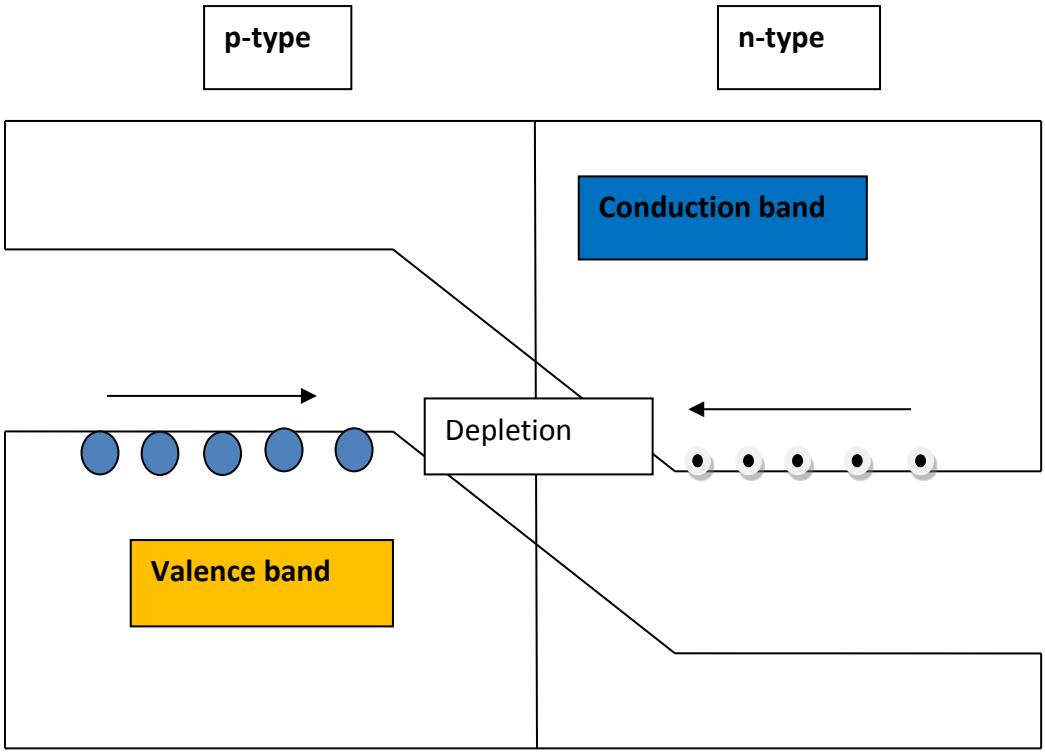

Figure 3.12: Holes and electrons diffuse towards the junction in their different bands under the condition of applied forward biased (LTS, 2011).

In p-n junction current will flow when it is forward biased. In this case, the negative terminal is connected to the n-type material. Electrons from the depletion zone are push with sufficient potential difference.

P-n junction is reversed biased when n-type material is connected to positive terminals when the depletion region is barrier for conduction.

3.3.6 High purity germanium detector (HPGe) in gamma-ray spectrometry

The Germanium semiconductor detector was first designed in 1962 (Tavendale and Ewan, 1963). This detector has earned its place amongst researchers as the detector of choice for high energy-resolution gamma-ray spectrometric analysis. The principle of its operation is characterized by the direct collection of charges originating from the ionization process of the semiconductor material. On average, an electron-hole is developed on the average for every 3 eV absorbed from the radiation. Subsequently, the pair of electron-hole move under the influence of electric field to the electrodes where a pulse is generated. Some information carriers are responsible for small numbers of percentage fluctuation that produces high resolution in the detector. It should be noted that these detectors do not consist only of semiconductor material and two electrodes but there exist a number of

impurities atoms in these materials. The elements, Si and Ge have a valence 4 thus, when an impurity atom of valence 3 (acceptor) or 5 (donor) exists in the crystal, this tends to lower the energy necessary to create electron-hole pairs and this results in the creation of much noise. In order to overcome this, p-n junctions are created at one electrode and then polarize it to prevent the passage of current through it when there is no ionizing radiation. This process is referred to as reverse bias. This process creates a region called the depletion layer. A step forward was ultimately achieved when high Ge material could be fabricated (Hansen, 1971; Khandaker, 2011), with impurity concentration of 10^{10} atoms/cm $^{-3}$ as against the 10^{13} atom/cm ^{3}, eliminating the need for Li compensation. This gives rise to high resistivity which is proportional to the square of the depletion layer's thickness. This achievement paved the way for the development and manufacture of a more efficient detector (Figure 3.13). Some major characteristics of HPGe detector are high atomic number, low impurity atom concentration, low ionizing energy requirement to generate electron-hole pair, compact size, high conductivity, high resolution, first time response and the simplicity of operation (Khandaker, 2011).

For effective decay counting, a closed end co-axial dipstick detector is employed. This presents a detector with uniformly, cross-sectional volume space to samples making counting more efficient even at a short distance from the detector.

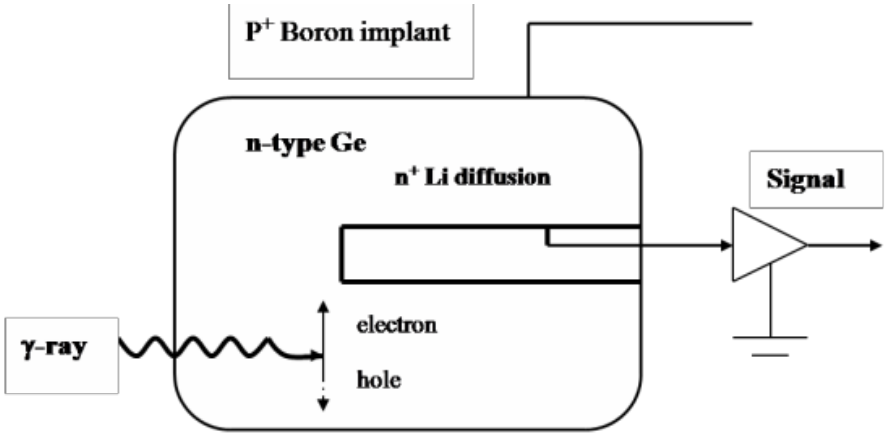

Figure 3.13: The configuration of n-type intrinsic germanium closed-end co-axial detector (Khandaker, 2011).

3.3.7 Detector assembly

All germanium detectors of any type have a deficiency of operation at room temperature. This is so because of their small band gaps (0.7 eV) which give rise to a large thermally-induced leakage current (Gilmore, 2008). In order to overcome this leakage

current, the germanium detector must be cooled by a reservoir of liquid nitrogen as represented in Figure 3.14

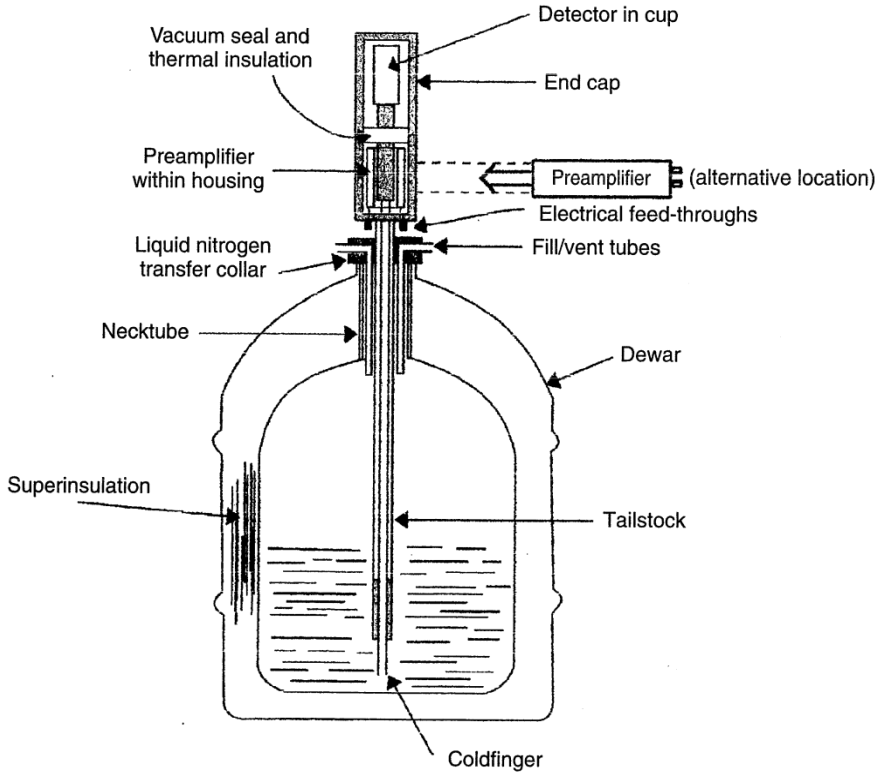

Figure 3.14: A schematic of a typical germanium detector cooled by a reservoir of liquid nitrogen (Gilmore, 2008).

3.3.8 Energy resolution

Energy resolution is the most important characteristic of a germanium detector. Gamma-ray spectrometric analysis using HPGe detector has the major advantage of excellent energy resolution which helps to separate and resolve many close energy gamma-ray peaks even in cases of complex energy spectrum. The full width at a level of half maximum of the full energy peak also referred to as FWHM is measured and it is sometimes called the measure of the energy resolution. The units of FWHM are expressed in (keV) for germanium detector and defined at specific, characteristic full energy peaks associated with standard radioactive sources. These are; 662 keV for ^{137}Cs source or 1332 keV for ^{60}Co source. However, energy resolution of germanium detector is affected by three factors. These factors are the number of electron-hole pairs created in the detector, incomplete charge collected, and electronic noise contributions. These factors are

dependent on the properties of the detector and the gamma-ray energy (Gilmore, 2008).

3.3.9 Experimental set up and counting system for HPGe detector

The detector and experimental set up was done following the illustration in Figure 3.16.

(a) Bin and power supply
(b) HPGe detector
(c) Amplifier
(d) Detector bias supply
(e) Pulse
(f) Multichannel analyser (MCA) and personal computer

The interaction of incident gamma-ray with HPGe detector undergoing any of the three significant interaction processes generates a number of electronic secondary charges. The charge generated is proportional to the amount of gamma-radiation deposited in the detector. The output electrical charge from the detector will be collected and counted on electronic counting system as shown in Figure 3.16. This is then displayed in form of the gamma-ray spectrum.

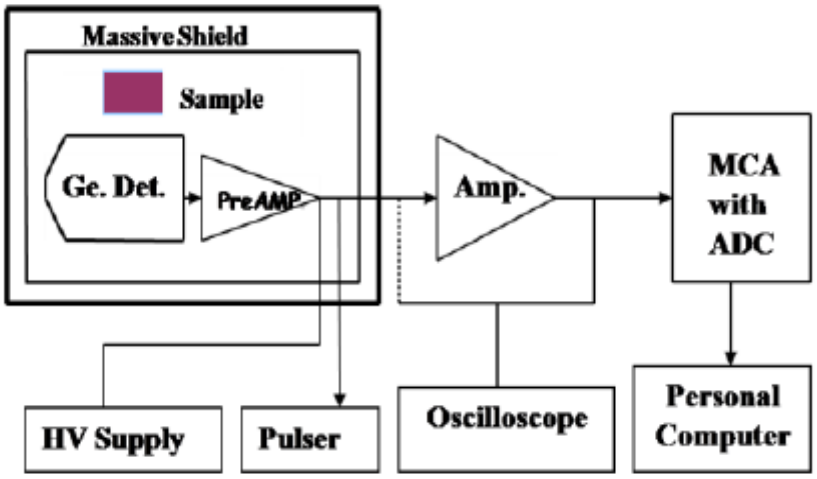

Figure 3.16: Electronic block diagram for gamma-ray spectrometry (Khandaker, 2011).

A detector bias supply is connected to a HPGe detector in order to remove the electron-hole pairs which was created within the depletion region of the detector

and then all charge carriers will be collected by the preamplifier. The preamplifier functions as a converter of the collected charge pulse to a voltage pulse. The size and shape of the preamp pulse are modified to be suitably processed by the amplifier. As a result of the linearity of the amplifier, its pulse height is proportional to the gamma-ray energy which was absorbed. The pulses from the amplifier are simply sorted out by their pulse height and later converted to a digital number by the analog-to-digital converter (ADC) in the multichannel analyser (MCA).

3.4 Inductively coupled plasma optical emission spectrometry (ICP-OES)

The ICP-OES is a scientific technique in which the composition of elements in mostly water-dissolved samples can be determined using plasma and a spectrometer.

The principle governing the ICP-OES involves a procedure where the solution to be analyse is conducted by a peristaltic pump through a nebulizer into a spray chamber where aerosols are produced. The generated aerosols are lead into argon plasma.

Matter exists in four states which are solid, liquid, gas and plasma. In the ICP-OES the plasma is generated at the end of a quarts torch by a water-cooled induction coil through which a high frequency alternate current flows. As a result, an induced alternate magnetic field is produced which accelerates electrons into a circular trajectory. Following collision interaction between argon atom and electrons the process of ionization occurs resulting to stable plasma. The plasma is extremely hot, in the range of 6000-7000 K. In the induction zone it can even reach 10000 K. In the torch desolvation, the process of atomization and ionization occurs due to thermic energy taken up by the electrons, they the reach a higher excitation state. When the electrons drop back to the ground level, energy is liberated as light (photons). Each element has its own characteristic emission spectrum. By means of an Echelle grating, a prism, and a focusing mirror these emitted photon in various frequencies are captured simultaneously on a charge coupled device (CCD).

3.5 Summary

This chapter has discussed the interaction of gamma rays with matter and the different techniques used to measure environmental radioactivity. A comparative study between the different techniques and the reasons for the choice of high purity germanium detector was discussed. Also, the principle of inductively coupled plasma-optical emission spectrum used in the analysis of heavy metals was explained.

CHAPTER 4

BIOLOGICAL EFFECTS OF IONISING RADIATION AND TOXICOLOGY OF SOME HEAVY METALS

4.1 Introduction

The purpose of this Chapter is to discuss the biological effects of ionising radiation and the toxicity of heavy metals. When ionising radiation interacts with biological specimens such as human tissue, the DNA may be damaged (Gerrado, 1974; Nour, 1982). Equally, heavy metal poisoning has been known to induce blindness, organ damage and respiratory related problems. The mechanism of direct and indirect action of ionising radiation on the DNA molecule and toxicity of heavy metals which depends on the chemical form and the species of the element will be discussed.

4.2 Biological effects of ionizing radiation

The exposure of human population to ionizing radiation leads to a process of ionisation and excitation of atoms and molecules in cells. This can lead to an “interphase death”, a breakdown of the complete cell metabolism, which cannot be related to a defined initial process (Neimann, 1983). The degree of biological damage from ionising radiation depends on the type of radiation charge carried, and the amount of energy impacted to tissues and organs (Eisenbud and Gesell, 1997; Lilley, 2001). A long chain of events occurs when ionising radiation passes through biological materials. In ionising or exciting an atom, energy is released from the particle as it passes the atom. The photon losses its energy and eventually comes to rest at which point, it is no longer radio-biologically significant. The energy released per unit length along this track is called Linear Energy Transfer (LET) (UNSCEAR, 1998).

The LET is a term used in dosimetry to describe the action of radiation upon matter. It is identical to the retarding force acting on a charge ionizing particle travelling through matter. The stopping power of a medium toward a charge particle refers to the energy loss to the particle per unit path length in the medium. Alpha particle has a low speed (because of its large mass) and it has a positive charge of +2e. A beta particle has high speed (owing to its small mass) and it has a charge of minus one (- 1). Hence, the LET of alpha particle is much greater than that of beta particle.

Therefore, as the LET increases, with increasing number of ionising events per unit length, the lethal effect of radiation also increases. Each time ionising events occur, there is a reduction in the energy of the charged particle, and hence, the particle travels more slowly (Azu and Ike, 1998). There are two ways in which ionizing radiation acts on cells: the direct action and the indirect action.

(a) Direct action

The effect of ionizing radiation in which no threshold doses are postulated could be thought to be as a result of direct ionisation and excitation of molecules with the consequent dissociation of the molecule (Cember, 1996). The dissociation of an atom can induce changes in the sequence of bases of the genes and therefore alter genetic code on the deoxy-ribonucleic acid (DNA) (Gerrado, 1974). This alteration in genes is called mutation and there exist a kind of mutation called point mutation (replacement of one nucleotide by another) which may occur in germinal cell and be passed onto the next generation or may occur in the somatic cells which results in a point mutation in the daughter cell (Hendee, 1973). Other possible alterations that may occur include the clastogenic mutation (addition or removal of any piece of DNA from one base pair) and inversion (excision of a portion of the double helix followed by its re-insertion in the same position but in a reversed orientation) (Hendee, 1973).The structure of a DNA is shown in Figure 4.1.

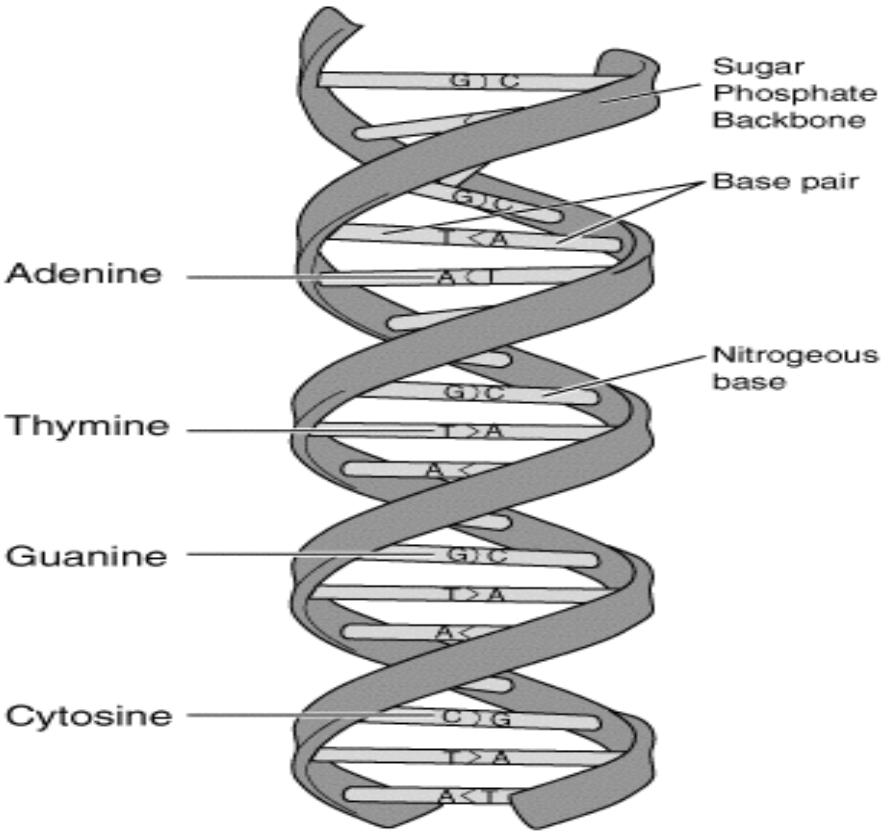

Figure 4.1: Structure of the DNA molecule (IAEA, 2014).

(b) Indirect action

This is when a molecule reacts with another molecule or the product of a molecule that had undergone direct radiation. This indirect irradiation explains a number of physical and chemical events that lead to cell death.

Water being the main constituent of all biological systems is of importance in the evaluation of free radical formation after irradiation (Forstner and Wittman, 1983). Water absorbs energy from ionising radiation when irradiated to become either ionised or excited as shown below:

$$H_2O \rightarrow H_2O^+ + e^- \qquad (Eq.4.1)$$

$$H_2O^+ \rightarrow H^+ + OH \qquad (Eq.4.2)$$

The free electron in equation (4.1) interacts with neutral water as follows;

$$H_2O + e^- \rightarrow H_2O^- \qquad (Eq.4.3)$$

$$H_2O^- \rightarrow H + OH^- \qquad (Eq.4.4)$$

All the H^+ and OH^- ions produced from Equation 4.1-4.4 do not pose any hazard since the body fluids already contain significant concentration of these ions. However, the free radicals H^+ and OH^- sometimes combine with like radicals or react with other molecules in the solution (Cember, 1996). The OH free radicals formed may combine with each other leading to the production of toxic hydrogen peroxide as follows:

$$OH + OH \rightarrow H_2O_2 \qquad (Eq.4.5)$$

Equally, the free radicals combine to yield gaseous hydrogen

$$H + H \rightarrow H_2 \qquad (Eq.4.6)$$

Furthermore, if the irradiated water contains dissolved oxygen, the free H radical may equally combine with oxygen to form the hydrogenperoxyl radical as given below

$$H + O_2 \rightarrow HO_2 \qquad (Eq.4.7)$$

This hydroperoxyl that is formed is not so reactive and has lifetime than the free OH radical and is able to combine with free H radical leading to the formation of H_2O_2 as follows:

$$HO_2 + H \rightarrow H_2O_2 \qquad (Eq.4.8)$$

The H_2O_2 formed in Equation 4.5 and Equation 4.8 are relatively stable compounds, very powerful oxidising agent and can pose a threat to cells and molecules that did not suffer irradiation damage directly. The mechanisms of both direct and indirect action are shown in Figure 4.2.

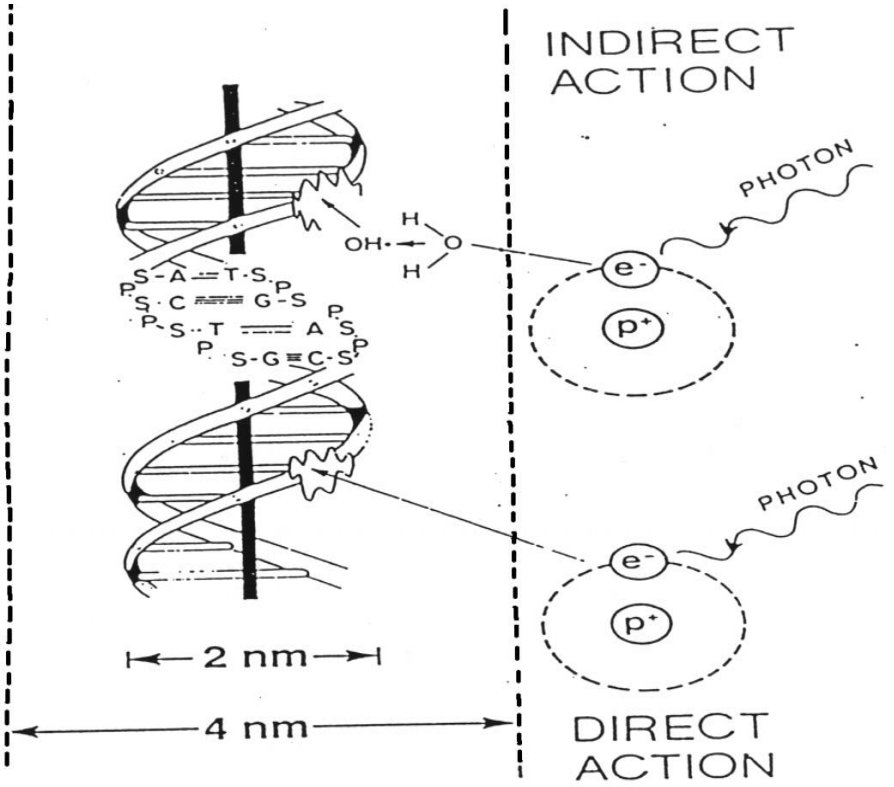

Figure 4.2: Mechanisms of the direct and indirect actions on DNA molecules (IAEA, 2014).

4.3 Radiation dosimetry

Radiation dosimetry deals with calculation, evaluation and assessment of the radiation dose received by the human body. To properly assess radiation dose, basic radiation quantities and unit are used to quantify radiation effects.

4.3.1 Basic radiation quantities and units

(a) Exposure

When radiation interacts with matter, electrons are ejected from atoms through the process of ionization. However, ionization does not have to completely eject an electron off the atom. It can raise the energy of the electron instead, raising the electron energy to a higher energy state. When the electron returns to it normal energy level, radiations are emitted (excitation process). This excitation result in the breaking of molecular bonds leading to damage to living cells.

When considering the interaction of gamma and X-rays in air, the term exposure is used. The basic radiation quantity is exposure, and this is defined as the measure of electric charge produced by electromagnetic radiation in a unit mass of air. Exposure is associated

only with limited energy range X-rays and gamma rays interacting with air (Noz and Maguire, 2007). Exposure is expressed in Roentgen (R) which is defined as the ionization of 2.58 x 10^{-4} C/Kg of air at S.T.P. Exposure is a very important physical term because of the ease with which it is measured. One just has to measure charges produce in air to ascertain the strength of the electrical field. The ionization chamber is an instrument that can be used for this purpose.

(b) Absorbed dose

Although exposure to gamma or X-rays is easily measured in our everyday life, we are confronted with other types of radiation such as alpha, beta, or neutron. Equally, we are also interested in the effects caused by such radiation in other materials like human tissue, cells and organs not only in dry air. Hence, to measure the interaction of all the different radiation with any given material, the term absorbed dose is used. This is denoted by Rad, and is defined as a measure of the amount of energy imparted to matter by ionising radiation per unit mass of the irradiated material at the place of interest. 1 rad = 1 J/kg. This unit has been replaced by the System International unit (S.I) of gray (Gy). 1Gy = 100 rad.

The total absorbed energy is not the only factor which determines the level of damage caused by radiation from a biological point of view. The type of radiation and its energy also have to be considered. Therefore, the biological effect of highly ionising radiation in any given tissue is more severe per unit absorbed dose than the other radiations that produce low ionisation. For this reason, the term relative biological effectiveness (RBE) was introduced as a dimensionless quantity of the amount of absorbed dose of ionizing radiation relative to that of X -ray or γ radiation of a particular energy to provide the same biological response (Lilley, 2001; Noz and Maguire, 2007). Due to the difficulty in applying such complicated functions of energy, RBE has been normalized to a factor known as the radiation weighting factor (w_R) by ICRP AND NCRP (Noz and Maguire, 2007). This factor is obtained from the RBE over a range of energies for any particular type of radiation. Table 4.1 gives a list of radiation weighting factors for various types of ionising radiation.

Table 4.1: Radiation weighting factors for different ionising radiations (ICRP, 1991)

Type of Radiation	Energy range	weighting factor, w_R
Photon, electrons, positrons and muons	All energies	1
Neutrons	< 10 keV	5
	> 10 keV to 100 keV	10
	> 100 keV to 2 MeV	20
	> 2 MeV to 20 MeV	10
	>20 MeV	5
Protons	>20 MeV	5
Alpha particles, fission fragments, non-Relativistic heavy nuclei		20

(c) The skin erythema dose (SED)

This is the dose of radiation that causes skin erythema i.e., the redness of the skin. This particular reaction was at one time used as a standard to measure the quantity of radiation to which human population had been exposed to. 1SED = 10Gy

(d) Committed dose

The committed dose is the total dose delivered during a certain period of time the radioisotope remains in the body.

(e) Collective dose

This is the summation of the products of the mean dose in the various groups of people and the total number of individuals in the group.

(f) Equivalent dose

To determine the effect of the nature of the radiation by the weighting factor in Table 4.1, a unit commonly referred to as equivalent dose (H_T) is specified. This is the total amount of dose $(D_{T.R})$ absorbed over a tissue or organ (T) due to radiation (R) and is given by the expression (Noz and Maguire, 2007):

$$H_T = \sum_R w_R D_{T.R} \qquad (Eq.4.9)$$

The Sievert (Sv) is used to express the equivalent dose. In addition to the types of radiation and energy, the biological effect of radiation is concerned with the sensitivities of irradiated organs and tissues. Organs and tissues of the human body respond differently to the effects of radioisotopes. It is for the reason, that the term effective dose and tissue weighting factor w_T was introduced which takes into account all contribution of radionuclides to the human body.

(g) The effective dose

The effective dose is defined as the sum of the equivalent doses weighted by the tissue weighting factor for each tissue, as given by Equation 4.10. (Ike, 2008).

$$E = \sum_T w_T H_T \qquad (Eq.4.10)$$

Consider Equation 4.9 and Equation 4.10,

$$E = \sum_T w_T \sum_R w_R D_{T.R} \qquad (Eq.4.11)$$

Some tissue weighting factors for human organs and tissues are listed in Table 4.2.

Table 4.2: Tissue weighting factors (ICRP, 1991)

Tissue or Organ	Tissue weighting factors, (w_T)
Gonads	0.20
Colon	0.12
Lung	0.12
Red bone marrow	0.12
Stomach	0.12
Bladder	0.05
Breast	0.05
Oesophagus	0.05
Liver	0.05
Thyroid	0.05
Skin	0.01
Bone surface	0.01
Remainder	0.05

4.4 Radiation protection and dose limits

Human population survivals of nuclear accidents and other related anthropogenic sources of ionizing radiation in the environment have largely provided the knowledge base of the effects of ionising radiation to mankind (Noz and Maguire, 2007). The Biological Effect of Ionising Radiation (BEIR) has defined a relationship between biological damage and exposure to ionising radiation. A study was carried out by the United Nation Scientific Committee on the Effect of Atomic Radiation (UNSCEAR) in partnership with the International Commission on Radiological Protection (ICRP) to determine the extent of biological damage occasioned by ionising radiation. In the current study, the absorbed dose limits relevant are those below 51 nGy.h^{-1}, for hazard indexes it should be $\leq$ 1, and 370 Bq.kg^{-1} for radium equivalent activity and 70 $\mu Sv.y^{-1}$ for AEDE outdoor factor. Deterministic effects and the stochastic effects are two terms frequently used to describe the effect of radiation to humans (IAEA, 1998).

4.4.1 Deterministic effects

Deterministic effects develop due to cell killing by high dose radiation. They appear only after a certain threshold dose is exceeded. Normally, this dose is considered higher than doses from background radiation or from occupational exposure at normal operation. The severity of the effects depends on the dose. At a given high dose the effects are

observed in severe form in all exposed cells, at higher doses the effects cannot increase. The threshold doses for some deterministic effects are presented in Table 4.3-4.4.

Table 4.3: Threshold doses for some deterministic effects in case of acute total radiation exposure (IAEA, 1998)

Doses	Effects
0.2 Gy	increase of number of the chromosomal aberration in bone marrow and lymphocytes
0.3 Gy	temporary sterility for man
0.5 Gy	depression of haematopoiesis
1.0 Gy	acute radiation syndrome
2.0 Gy	detectible opacities
5.0 Gy	visual impairment
2.5-6.0 Gy	sterility for woman
3.5-6.0 Gy	permanent sterility for woman
3.0-10.0 Gy	skin injury

Table 4.4: Threshold doses for some deterministic effects in case of radiation exposure for many years (IAEA, 1998)

Dose	Effects
0.1 Gy	detectible opacities
0.2 Gy	sterility for woman
0.4 Gy	visual impairment
0.15 Gy	temporary sterility for man
0.4 Gy	depression of haematopoiesis
1.0 Gy	chronic radiation syndrome
2.0 Gy	permanent sterility for man

4.4.2 Stochastic effects

These effects develop due to mutation effect at low dose radiation, the threshold dose is not known accurately. It was observed by Noz and Maguire, (2007) that different types of cancers appear above different dose ranges, the severity of the effect does not depend on the dose, but the frequency of the appearance of the effect (the probability) in the exposed population group is dose dependent (in most case linearly increasing with the dose). To prevent unwanted exposure to radiation by human population, all doses must be kept as low as reasonably achievable (ALARA). This recommendation was given by the International Commission on Radiological Protection (ICRP) (Noz and Maguire, 2007). Dose limits recommended by ICRP and the nominal probability coefficients for stochastic radiation effects are presented in Table 4.5-4.6.

Table 4.5: Recommended effective dose limits. (Cember and Johnson, 2009)

Application	Dose limit	
	Occupational	Public
Whole body	20 mSv[a] per year, averaged over a period of 5 years[b]	1 mSv[a] in a year
Annual equivalent dose in		
Lens	150 mSv	15 mSv
Skin	500 mSv	50 mSv
Hand and feet	500 mSv	-

[a] To find the recommended limit in rem, 1 mSv = 0.1 rem
[b] Maximum dose in any single year do not exceed 50 mSv

Table 4.6: Nominal probability coefficients for stochastic radiation effect (IAEA, 1998)

Detriment (10^{-2} Sv^{-1})				
Exposed population	Fatal cancer	Non-fatal cancer	Severe heredity effects	Total
Adult worker Only	4.0	0.8	0.8	5.6
Whole population (All age groups)	5.0	1.0	1.3	7.3

[1] Rounded values
[2] For fatal cancer, detriment coefficient is equal to probability coefficient

4.5 Toxicity of some heavy metals

An elevated concentration of heavy metals increases the potential of adverse health effects to inhabitants in a given environment (Duffus, 2002; Ogwuegbu and Duruibe, 2005). Some common health effects associated with heavy metal poisoning include blindness, organ damage and breathing related problems (Moja and Mnisi, 2013). The toxicity of heavy metals depends on their chemical form and the species of the elements. For some metals, the most toxic form is that having alkyl groups attached to the metal since most of such compounds are soluble in animal tissues and can pass through biological membranes. For example, uptake of arsenic can cause skin lesions, neurotoxicity and other cancerous problems of different form. Cadmium (Cd) has high soil mobility than any other metal to plant system (Alloway, 1995). In human, only about 5-50% of the inhaled element ever enters the lungs. Also, only 1-10% Cd gets into the digestive system via ingestion of food and water intake. Chronic exposures to Cd result in renal tubular damage, bone deformities, and heart related diseases (Goyer and Clarkson, 2001; MacFarland, 1979). Ingestion and inhalation of high levels of nickel Ni induces lung damage in man (Goyer and Clarkson, 2001). Ni dermatitis is the most common effect of the element to human population. Toxicological effects of lead on man include; inhibition of haemoglobin formation, sterility, hypertension and mental retardation in children (Amdur et al., 1991).

Mercury (Hg) has low solubility in water (Steinnes, 1995). Mercury compound (HgS) has been used for many centuries in cave painting and skin beautifications (Jarup, 2003). Chronic exposure due to ingestion of methyl mercury is of great concern (Goyer and Clarkson, 2001). Hg causes brain damage, chest pain, stomach ache and cough (Alloway, 1995). Aluminium (AI) though not regarded as a heavy metal because its density is less than 5mg/cc of water is one of the frequently analysed metals in soils, sediments, sludge, rocks, minerals and plant and animal tissues. Mineral soils contain between 1 – 12% AI, while organic soils contain between 0.05 – 0.5% AI. Despite its abundance in soil, only a small fraction is mobile (Alloway, 1995). The leaching of AI from soils into ground waters could be a concern, as an association between AI and Alzheimer's disease has been demonstrated (Radojevic and Bashkin, 1999). Total Mn concentrations in soils are variable (1 – 3000mg/kg). Soluble Mn^{2+} ions are the most readily available of all the different forms of Mn in soil. The availability of Mn is influenced by pH. Reducing the pH and other conditions could lead to excessive Mn^{2+} in the soil which could have toxic effect (Rasheed and Awalallah, 1998; Radojevic and Bashkin, 1999).

Zinc is an essential element in the human diet because it is required to maintain the proper functions of the immune system. The Recommended Daily Allowance (RDA) for zinc is 15mgZn/day for men and 12mgZn/day for women. Ingestion of large doses (390mgZn/day for 3 – 13 day, or about 27mgZn/day) of Zn can cause death. If doses of 10 – 15 times

higher than the RDA are taken over a long period, anaemia and damage to the pancreas and kidney can develop. Vomiting, diarrhoea, abdominal cramping, and in some cases, intestinal haemorrhage can occur from long-term exposure to high (i.e. >85mg/kg/day) doses of zinc (ATSDR, 1994; Murphy, 1970). Iron is the fourth most abundant element in the earth's crust and it is a constituent of many soils. Ingestion of high levels of Fe may act as a phyto-toxin (Radojevic and Bashkin, 1999).

Copper is one of the essential elements for living organisms. Copper concentrations in soils are generally < 100mg/kg, while in sludge, levels as high as 17000mg/kg have been reported (Radojevic and Bashkin, 1999). Exposure to excessive level of Cu can result in a number of adverse health complications including liver and kidney damage, anaemia, immunotoxicity, and developmental toxicity (Radojevic and Bashkin, 1999).

4.6 Bio-accumulation of metals in living systems

Bio-accumulation is a process where living systems store up metals acquired from their surrounding into their tissue by chelation process. The accumulation of a metal in a living system is the product of equilibrium between the concentration of the metal in the living system's environment and its rates of ingestion and excretion (Ademoroti, 1996).

Studies have shown that there are two main mechanisms associated with bio-accumulations of toxic metals in the ecosystem namely:

i) Direct absorption
ii) Food chain distribution

Direct absorption is common in aquatic environment where all organisms are exposed to the same concentrations of the substance present in the environment and all have equal opportunity to accumulate substances by absorption into their tissues (Ademoroti, 1996).

In the terrestrial environment, the food chain distribution mechanism constituted the pathway of bio-accumulating toxic metals (Jarup, 2003).

4.7 Summary

This chapter has reported on the variation of biological effects of radiation. It was pointed out that these depend on the types of radiation, the energy transferred to the living tissue and the toxicology of some heavy metals. This Chapter also summarised the direct and indirect action of ionising radiation on the DNA structure which inevitably induces DNA damage. The bio-accumulation of metals in living systems and attendant effect on human organs has been looked at. The chapter also summarised the procedure for the calculation and assessment of radiation dose.

CHAPTER 5

MATERIALS AND METHODS

5.1 Introduction

This chapter provides detail of the Erongo region in which the study was performed. The arid region of Erongo, which encompasses the Namib Desert, the towns of Walvis Bay, Swakopmund and Henties Bay was selected for the study. A brief description of the study location has been provided in Chapter 1. The sampling locations, relevant maps, measurement schedules and scientific objective for selection are covered in this chapter.

This chapter also has a further objective to detail the methodology and analytical techniques used throughout the study. Some instruments employed in this study and questionnaire administration for the modelling of the occupancy factor are also discussed here.

5.2 Study area

The study was undertaken along the beaches of Walvis Bay, Swakopmund and Henties Bay. These towns lie in the coastline of Erongo region of Namibia. Statistics released by Namibia 2011 National Population Census, indicated that the region has a population of 150,400 and covers a total land mass of 63,549 Sq.Km (NPC, 2011). The study areas are located on latitude 22^{o} 57' 22'' South and longitude 14^{o} 30' 19'' East for Walvis Bay; latitude 22^{o} 4' 59'' South and longitude 14^{o} 31' 59'' East for Swakopmund and latitude 22^{o} 55' 27'' South and longitude 14^{o} 30' 19'' East for Henties Bay respectively. Erongo region is situated within the Namib Desert and lies parallel to the coast for about 120 to 150 km (Figure 5.1-5.3). The three major towns of Walvis Bay, Swakopmund and Henties Bay are 60 km, 40 km and 80 km from areas where uranium exploration for export purposes are undertaken as shown in Figure 5.4. The region is, as is most part of the country, arid for most part of the year. Namibia has an average day temperature of 30^{o}C (Roesner and Schrender, 1992). This has caused the migration of people both local and international tourist to the coastline. Several leisure activities thrive at the coastline. Angling is carried out all along the coastline and tracks of off-road driving can be found almost everywhere (ERC, 1999). Tour operators offer leisure activities along the coastline where the ocean meets the sand dunes and most visitors prefer to walk or even relax in the dune field. The lagoon at Walvis Bay is an important wetland and home to a large population of flamingos and is an internationally designated wetland and a migration point for many thousands of birds and waders (ERC, 1999). Four features have dominant effects on the climate of the region and

enhance its aridity. These are the south Atlantic Anticyclonic Cell, the Benguela Upwelling System, the Great Escarpment, and the absence of major topographical features on the 150-km wide plains. These prevalent features make the coastline of Erongo region one of the most climatically stable places in the world (Ward *et al*., 1983; Lancaster, 1989; Tyson and Lindesay, 1992). Little wonder why the coastline play host to large numbers of visitors who spend their time in outdoor activities. The arid nature of the region makes the region to perform poorly in crop farming. Only a small area of land about 10 Sq.Km is suitable for crop production, and these areas include the small scale farming in the Swakop River bed, as well as the settlements of Omaruru and Okombahe. There are a number of industrial activities that thrive in the region, such as fishing and port harbour, tourism, and uranium mining. Also the shore sediments are been used as building materials for making bricks and flooring of houses. Most worrisome, is the proximity of some of these industrial activities to the coastline which portends great challenge to Namibia's Vision 2030 focal area of population and environmental health.

The activities of some of the uranium mines involves open pit mining where some NORM and toxic heavy metals may be washed into the river and sea and consequently, deposited on shore sediments. The accumulation of NORMs and heavy metals can occur in sea and river sediments which are eroded and deposited in shore sediment along the coastline. This can elevate the concentration of natural radioactivity and heavy metals in this area and hence, potentially affect human population that visit the coastline for various activities and also use the sediments as building materials. It is for this reason that the need arose to tackle through relevant research such as the measurement of natural radioactivity and occurrence of heavy metals in beach sediments in the region and to suggest useful mitigation strategies.

Figure 5.1: Map showing the 26 points where sediment samples were collected from the beach of Walvis Bay.

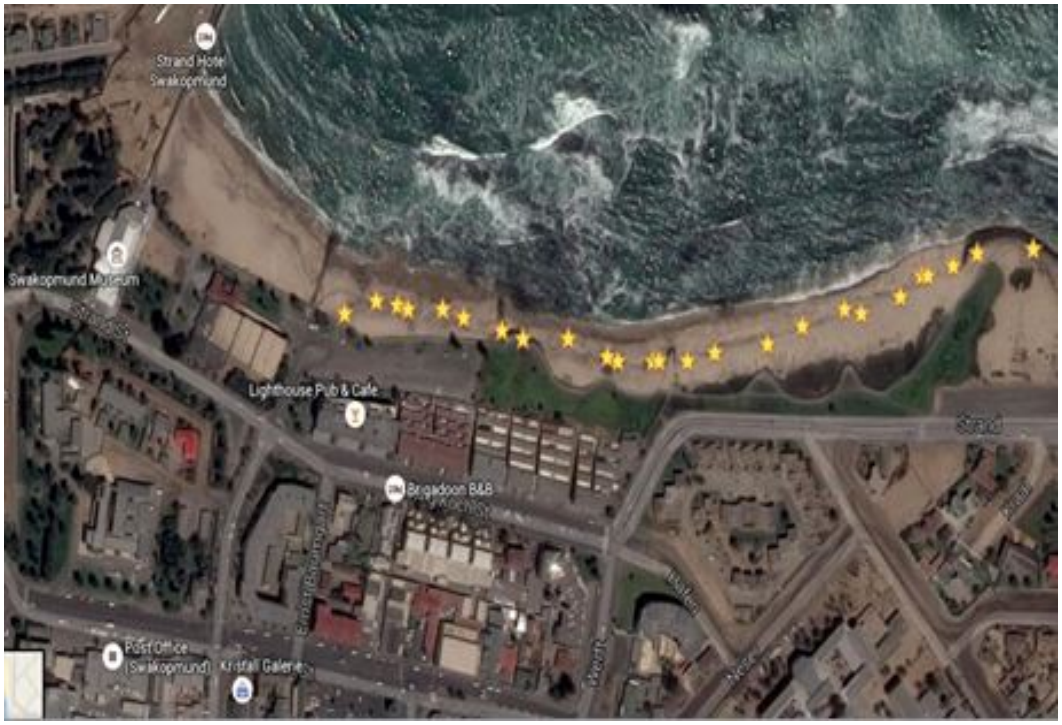

Figure 5.2: Map showing the 26 points where sediment samples were collected from the beach of Swakopmund.

Figure 5.3: Map showing the 26 points where sediment samples were collected from the beach of Henties Bay.

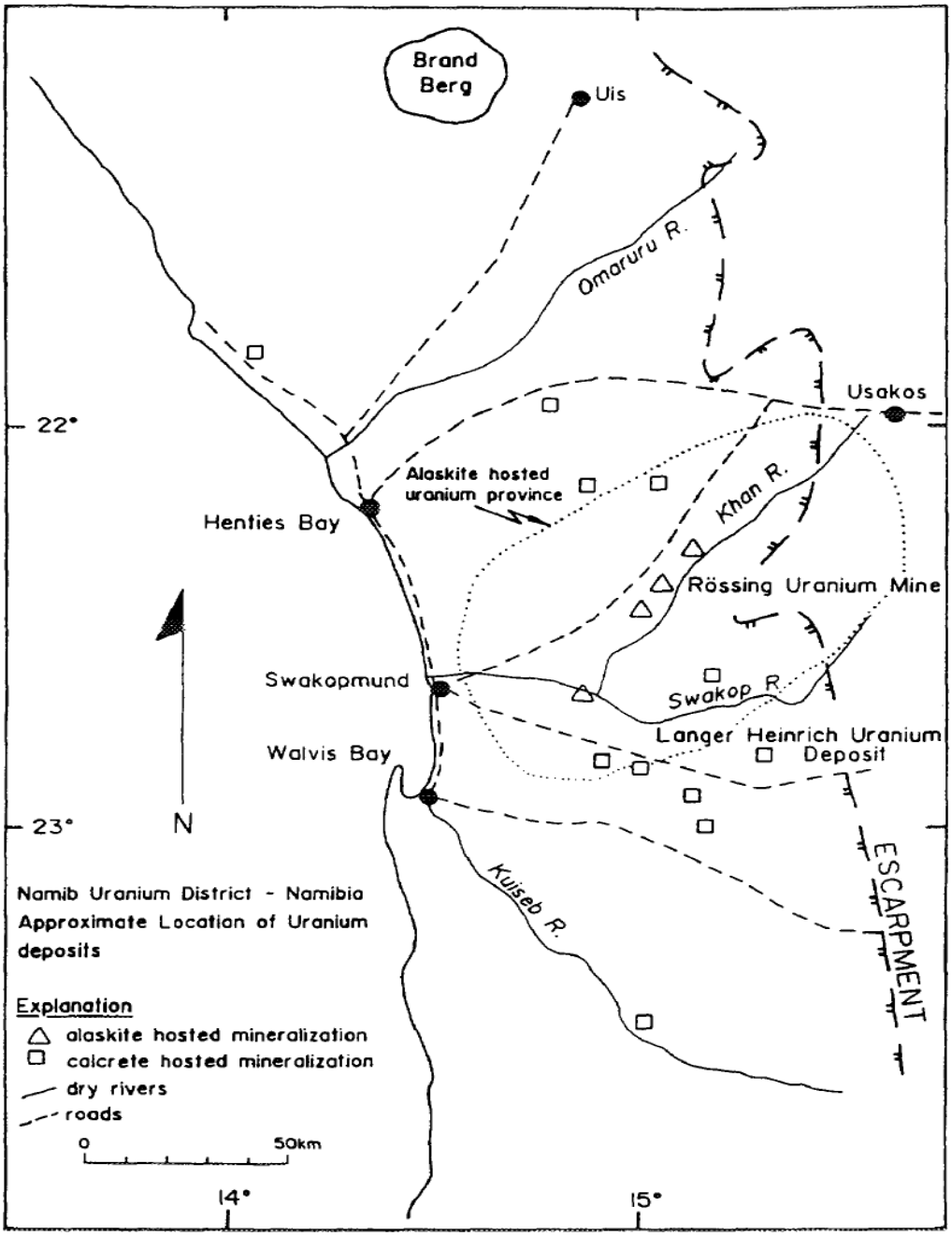

Figure 5.4: Location of uranium deposits in the Namib uranium district of Erongo region (Roesner and Schrender, 1992).

5.3 Sample collection and pre-treatment for gamma counting

Shore sediment samples were collected randomly from 78 points from beaches in the coastal towns of Walvis Bay, Swakopmund and Henties Bay. Samples were collected between October and December 2013 from points marked using a Global Positioning System (GPS) with points designated to be a representation of the levels of natural radionuclides from the sampled locations. Each sampling points were carefully chosen to represent locations where human population is involved in various activities such as; leisure, occupational and others. Samples were collected at a depth of about 20 to 25 centimetres and approximately 7 to 10 meters away from areas of high tide. The shore sediments were scooped using a hand scooper as shown in Figure 5.5. Debris and all other forms of unwanted materials were removed and the samples packed in a zip plastic polythene bags (Figure 5.5) and labelled accordingly to sampling points and geographical coordinates as shown in Figure 5.1-5.3 and Table A1-A3. Samples were later transported to the laboratory at the Namibia University of Science and Technology for further treatments.

Figure 5.5: Photograph of the hand scooper used in the collection of samples.

5.3.1 Sample preparation for counting

The laboratory preparation of samples for gamma counting was carried out by placing each sample in an oven and heated to a temperature of 110^{o}C for 24 hours to allow for a constant weight to be reached and the removal of any residual moisture as shown in Figure 5.6. The dry samples were then shipped to the International Centre for Environmental and Nuclear Sciences, University of the West Indices Mona Campus, Kingston, Jamaica where the dried samples were grounded thoroughly using a mortar and pestle (Figure 5.7.a) to ensure homogeneity, and then filtered through a standard 1 mm mesh size to remove all pebbles as shown in Figure 5.7 (b). After filtration the residue were appropriately discarded. Samples were weighed out (Figure 5.7.d) in polyvials EP 290LG with description 9.5ml-2.57 Drams-1/30z with a lab grade series manufactured with prime polypropylene for lab testing conditions, outside 0.68'' Dia. x 2.25'' Ht and inside 0.61'' Dia. x 2.12'' Ht as shown in Figure 5.7 (c). The vials were filled with samples and the caps heat sealed and wrapped tightly with parafilm for thirty (30) days to prevent the escape of ^{222}Rn and ^{220}Rn from the samples. This process is to allow long-lived parent radionuclide attain secular equilibrium with their short-lived progenies.

(a)

(b)

(c)

Figure 5.6: Oven for drying samples.

(a)

(b)

(c)

(d)

Figure 5.7: The apparatus for sample preparation (a) a mortar and pestle for sample crushing to achieve homogeneity (b) a standard sieve of 1 mm mesh size (c) Polyvials EP 290 LG polyethylene (d) a weighing scale.

5.3.2 Analysis of samples for radioactivity concentration

After the thirty (30) days to attain secular equilibrium, the samples were then counted for 28800 seconds (8 hours) in the gamma spectrometric assembly with a high purity germanium detector (HPGe) detector of 70% efficiency and a resolution of 1.8 keV at the 1.3 MeV of Cobalt-60 source.

The HPGe detector was calibrated using standards of known concentration of radioisotopes for energy and efficiency before measurements were taken. The background was monitored and subsequently subtracted from the spectrum of gamma radiation from each samples in order to obtain net counts for the samples. The spectrum of each standard was later used to obtain energy calibration.

(a) Efficiency calibration

The efficiency calibration for detection efficiency is important for a reliable and accurate result for gamma-ray spectrometry of unknown activity in samples. The absolute, full-energy peak efficiency can be defined according to Equation 5.1.

$$\varepsilon_f = \frac{N_p}{N_\gamma} \qquad (Eq.5.1)$$

where ε_f is the full-energy peak efficiency which represents the number of counts detected for every number of gamma-ray emitted by the source. N_p gives the net gamma-ray count rate in the full-energy peak and N_γ represent the gamma-ray emission rate given by Equation 5.2.

$$N_\gamma = AP_\gamma \qquad (Eq.5.2)$$

where A is the number of nuclear decays per second and P_γ is the probability per nuclear decay.

In this study, the efficiency calibration of the gamma spectrometry was done using four different reference sources and a mixed radionuclide source. The standard sources were contained in beakers having similar geometry as the samples used for counting. Only the full-energy peak was considered for the efficiency calibration.

(b) Determination of detection limits

For a low-level counting system, it is important to determine a limit for which counts are statistically significant. This limit is referred to as detection limit. The decision limit otherwise called critical level and the detection limit were introduced to give certain degree of confidence in measuring and analysing radioactivity level. The critical level L_C is defined as a decision level above which the net counts present represent some detected activity, with some degree of confidence. On the other hand, the detection limit L_D is defined as a level that the true net counts will be detected above the acceptable level with a certain probability in the present of real activity.

The critical level and the detection limit are given by Equations 5.3 and 5.4.

$$L_C = 2.326\sigma_{N_B} \qquad (Eq.5.3)$$

$$L_D = 2.706 + 4.653\sigma_{N_B} \qquad (Eq.5.4)$$

where σ_{N_B} represent the standard deviation of count number when a blank sample is measured to determine the background level.

(c) Minimum detection activity (MDA)

The minimum detection activity is a criterion for measuring performance of gamma-ray spectrometric counting. The minimum detectable amount of activity can be obtained from detection limit in Equation 5.4 and is expressed in equation 5.5 below.

$$MDA = \frac{L_D}{\varepsilon_f P_\gamma T} \qquad (Eq.5.5)$$

where T is the counting time.

5.3.3 Assessment of dose

(a) Absorbed dose rate in air (ADR)

The assessment of radiological hazard following exposure to radiation originating from radionuclides in sediments was determined using Equation 5.6. The determination of the absorbed dose rate is the very first step in evaluating the health related risk. With regards to biological effects, the radiological effects are directly related to the absorbed dose rate in air at 1 meter above the ground surface (Ramasamy *et al*., 2011). The measured activity concentrations of ^{226}Ra (^{238}U), ^{232}Th, and ^{40}K were converted into doses by applying the conversion factors 0.462, 0.604 and 0.0417 for uranium, thorium, and potassium, respectively (UNSCEAR, 2000; Turhan and Gundiz, 2008; Shams *et al*., 2013). These

factors were used to calculate the absorbed dose rate ADR (nGy h $^{-1}$) according to the following formula (UNSCEAR, 2000; Shams *et al*., 2013).

$$ADR(nG.h^{-1}) = (0.462C_{Ra} + 0.604C_{Th} + 0.0417C_{K}) \qquad (Eq.5.6)$$

where ADR is the absorbed dose rate in $nGy.h^{-1}$, C_{Ra}, C_{Th}, and C_{K} are activity concentration (Bq kg $^{-1}$) of ^{226}Ra (^{238}U), ^{232}Th and ^{40}K, respectively.

(b) Annual effective dose equivalent $(AEDE)$

The absorbed dose rate in air at 1 meter above the ground level is not sufficient to provide the radiological risk to which human populations are exposed (Jibiri *et al*., 2007). The absorbed dose can be considered in terms of the annual estimated average effective dose equivalent $(AEDE)$ received by an individual. To calculate $AEDE$, a factor of 0.7 Sv Gy $^{-1}$ is used to convert the absorbed rate to the human effective dose equivalent with an outdoor occupancy of 20% and 80% for indoor (UNSCEAR, 2000). The annual effective dose was determined using the following equations:

$$AEDE.(outdoor)(\mu Sv.y^{-1}) = D(nGy.h^{-1}) \text{ x } 8760\ h \text{ x } 0.7Sv.Gy^{-1} \text{ x } 0.2 \text{ x } 10^{-3} \qquad (Eq.5.7)$$

$$AEDE.(indoor)(\mu Sv.y^{-1}) = D(nGy.h^{-1}) \text{ x } 8760\ h \text{ x } 0.7Sv.Gy^{-1} \text{ x } 0.8 \text{x} 10^{-3} \qquad (Eq.5.8)$$

One of the objectives of this study is to develop a model for the evaluation of the occupancy factors along the coastline. This model will enable us to evaluate the appropriate $(AEDE)$ as the use of the UNSCEAR factor may not represent the true values in the coastline. This model was developed as follows:

(c) Occupancy factor model along the coastline of the Erongo region

Experimental Data Collection

Closed ended questionnaires were administered in the beaches of Walvis Bay, Swakopmund and Henties Bay. A total of 2400 Participants were involved. Some activities that are exposure related such as leisure and work/occupation i.e. fishing, diving, walking, picnic at the shore, horse riding, sun bathing, relaxation at beach house, vendor, shop retailer, sanitation work and others were administered (Appendix D).

Data collected after the administration of the questionnaires were used to calculate the outdoor and indoor occupancy factor for the coastline. Mathematical model relating to time spent for various human activities along the coastline having components for both indoor and outdoor parameters was developed following similar procedure adopted by Arogunjo *et al*., (2007).

Model assumptions

The under listed assumptions were made in the development of the model:

1. The absorption of radiation from naturally occurring radioisotopes is proportional to the amount of time spent during exposure.
2. Each human activity group is assumed to have a time fraction of leisure, occupation and other activities.
3. There is for each human activity group a fraction of the time spent indoor and outdoor.
4. Twenty four (24) hours a day was allocated for the sum of outdoor and indoor activities.
5. All activities are independent of the time.
6. Indoor and outdoor time spent is considered to be linearly dependent on the activities.

If 'I' is taken as the time spent indoor and 'O' represents the time allocated for outdoor activities, and using the assumptions four (4) stated above, we have that;

$$I + O = 24 \qquad (Eq.5.9)$$

The time spent indoor was mathematically arrived at as;

$$I = \sum_{k=1}^{3} \lambda_k A_k = \lambda_1 A_1 + \lambda_2 A_2 + \lambda_3 A_3 \qquad (Eq.5.10)$$

where λ_k = indoor fraction of time parameter for k^{th} indoor activity.

A_k = observed total time allocated for k^{th} activity.

The time spent outdoor was modelled as;

$$O = \sum_{k=1}^{3} \sigma_k A_k = \sigma_1 A_1 + \sigma_2 A_2 + \sigma_3 A_3 \qquad (Eq.5.11)$$

where σ_k = outdoor fraction of time parameter for k^{th} activity.

$$\text{Let } T_k = \left(\frac{\lambda_k - \sigma_k}{2}\right) \qquad (Eq.5.12)$$

where T_k is the total number of the fraction of time parameter for k^{th} activity.

We therefore have that Equation (5.9) + (5.10) – (5.11) gives:

$$I = 12 + \sum_{k=1}^{3} T_k A_k \qquad (Eq.5.13)$$

And similarly, Equation (5.9) – (5.10) + (5.11) lead to:

$$O = 12 - \sum_{k=1}^{3} T_k A_k \qquad (Eq.5.14)$$

The model (Equation 5.13 and Equation 5.14) was employed in MATLAB to calculate the fraction of time estimates for indoor and outdoor occupancy factors.

(d) Radium equivalent activity (Ra_{eq})

Because of the non-uniform distribution of natural radionuclides in the soil samples, the actual activity level of ^{226}Ra, ^{232}Th and ^{40}K in the samples can be evaluated by means of a radiological index referred to as the radium equivalent activity (Ra_{eq}) (Beretka and Mathew, 1985). It is known that 370 Bq.kg $^{-1}$ of ^{226}Ra, 259 Bq.kg $^{-1}$ of ^{232}Th, and 4810 Bq.kg $^{-1}$ of ^{40}K produce the same gamma-ray dose rate. The radium equivalent activity is given by:

$$Ra_{eq}(Bq.kg^{-1}) = C_{Ra} + 1.43C_{Th} + 0.077C_K \qquad (Eq.5.15)$$

Where C_{Ra}, C_{Th} and C_K are the activity concentrations of ^{226}Ra, ^{232}Th and ^{40}K in Bq.kg $^{-1}$, respectively. The permissible maximum value of the radium equivalent activity is 370 Bq.kg $^{-1}$ (UNSCEAR, 1988; UNSCEAR, 2000). This value corresponds to an effective dose of 1 mSv.y^{-1} for the general public (Ajayi, 2009).

(e) Hazard Indices

To limit the radiation exposure attributed to natural radionuclides in soil and sediments samples used for construction purposes to a permissible dose equivalent limit of 1 mSv.y $^{-1}$. Beretka and Mathew (1985) defined two indices H_{ex} and H_{in} that represent external and internal radiation hazards respectively. The prime objective of the indices is to limit the radiation dose accruing to human population to a dose equivalent limit of 1 mSv.y $^{-1}$. The external hazard index (H_{ex}) is determined by using the equation:

$$H_{ex} = \frac{C_{Ra}}{370} + \frac{C_{Th}}{259} + \frac{C_K}{4810} \leq 1 \qquad (Eq.5.16)$$

On the other hand, the internal hazard index (H_{in}) gives the internal exposure due to radon and its short-lived daughters (Ramasamy *et al*., 2011), and it is given by the following formula (Beretka and Mathew, 1985).

$$H_{in} = \frac{C_{Ra}}{185} + \frac{C_{Th}}{259} + \frac{C_K}{4810} \leq 1 \qquad (Eq.5.17)$$

where C_{Ra}, C_{Th}, and C_K are the activity concentration of ^{226}Ra, ^{232}Th and ^{40}K in Bq.kg^{-1}, respectively. Both H_{ex} and H_{in} must be less than unity to have negligible hazardous effect on human population (Al-Hamarneh and Awadallah, 2009).

(f) Excess lifetime cancer risk $(ELCR)$

Excess Lifetime Cancer Risk (ELCR) is calculated using the equations below.

$$ELCR = AEDE \text{ x } DL \text{ x } RF \qquad (Eq.5.18)$$

Where $AEDE$, DL and RF are the annual effective dose equivalent, duration of life taken to be 70 years and the risk factor (Sv^{-1}), fatal cancer risk per Sievert. The International Commission on Radiological Protection (ICRP 60) employed the values of 0.05 for the general public for stochastic effects (Taskin *et al*., 2009).

5.4 Sample collection and pre-treatment for heavy metals

Twenty six replicate beach sediment samples were collected from each of the beaches of Walvis Bay, Swakopmund and Henties Bay following similar collection method for NORMs. Samples were collected in two seasons; winter (May-July 2014) and summer (September-November 2014). Samples collected from each of these sampled areas were thoroughly mixed to ensure homogeneity and filtered through a standard sieve of 1mm mesh size. This sieve fraction was selected because it has been reported that dust particles in this size contains high levels of heavy metal (Ward *et al*., 2004; Ewan *et al*., 2009). Five sub-samples were taken from the large sieved samples and transferred into clean pre-labelled plastic containers and subsequently, transported to Analytical Laboratory Services, Windhoek Namibia, for further processing and analysis. All materials used for holding samples, homogenization and sieving were pre-cleaned with 10% nitric acid to minimize the potential of cross contamination.

5.4.1 Sample digestion for heavy metals

The samples were digested according to the reported EPA method 3050B for Inductively Coupled Plasma-Optical Emission Spectrophotometer (ICP-OES) analysis (Abah *et al*., 2014). A known amount (1.00 g) of each sample was transferred into a digestion vessel and 10 mL of 1:1 nitric acid (HNO_3) was added, mixed thoroughly and covered with a watch glass. Subsequently, the samples were heated to 90^oC and refluxed at this temperature for 10 minutes after which they were allowed to cool for 5 minutes under room temperature. Thereafter, 5 mL of concentrated HNO_3 was added to each, covered and refluxed again at 90^oC for 30 minutes. Then, the solution were allowed to evaporate without boiling to approximately 5 mL each and cooled again for 5 minutes. This was followed by the addition of 2 mL of deionised water plus 3 mL of 30 % hydrogen peroxide (H_2O_2) to each. The vessels were covered and heated just enough to warm the solutions for the peroxide reaction to start (EPA, 1996). This was continued until effervescence subsided and the solutions were cooled. The acid-peroxide digestates were covered with watch glasses and heated until the volume reduced to approximately 5 mL again. Thereafter, 10 mL of concentrated hydrochloric acid (HCl) was added to each, covered and heated on a heating mantle, then refluxed at 90^oC for 15 minutes. After cooling, each digestate was filtered through Whatman No. 41 filter paper into a 100 mL volumetric flask and the volume made to the mark with deionised water (EPA, 1996).

5.4.2 Sample Analysis for heavy metals

Ten (10) mL of each digestate was taken and mixed with equal volume of matrix modifier (EPA, 1996), and then analysed using ICP-OES (ICP: Perkin Elmer Optima 7000 DV) housed in analytical laboratory Windhoek, Namibia for the levels of lead, chromium, cadmium, arsenic, iron, manganese, copper and zinc. Data generated from quadruplicate analyses were expressed as mean concentration of each element and inter-elemental correlation was calculated to determine the degree of association between the heavy metal levels.

5.4.3 Assessment of site contamination with heavy metals

The sediment geochemical quality in an urban environment depends not only on the concentration of pollution sources, but also on time-span of urbanization, industrialisation and poor agricultural practices (Edokpayi *et al*., 2014; Abah, *et al*., 2015). Thus it becomes necessary to compare heavy metal concentrations in shore sediments with guideline limit upon which informed decision about the site quality could be made. In this study, site contamination was assessed using the criteria of, Enrichment Factor (EF), (Foley *et al*.,

2011), Index of geo-accumulation (Igeo) (Tijani and Onodera, 2009), Contamination factor (CF) (Hakanson, 1980) and Pollution load index (PLI) (Tomilson *et al*., 1980). Each of these assessment criteria was calculated using Equation 5.19 to Equation 5.22.

(a) Contamination factor (CF)

The pollution index (CF) gives an indication of the degree of contamination of soil. This is defined as the ratio of concentration of metal in a sample to the concentration of metal in the background. The level of contamination factor of sediment by metal is expressed by Equation 5.19. C_{Sample} is the given metal in shore sediment, $C_{Background}$ is the background value of metal. In this study, the $C_{Background}$ value is equals to the world surface rock average presented in Table 7.1. According to Hakanson (1980) contamination factor can be classified as shown in Table 5.1.

$$CF = C_{Sample} / C_{Background} \qquad (Eq.5.19)$$

Table 5.1: Contamination criteria based on contamination factor (Hakanson, 1980).

Contamination Factor	
Classification	Degree of contamination
$CF < 1$	Low
$1 \leq CF < 3$	Moderate
$3 \leq CF < 6$	Considerable
$CF > 6$	High

(b) Enrichment factor (EF)

The enrichment factor (EF) is based on the standardization of the analysed element against a reference element. The EF is defined as a factor used in assessment of the degree of contamination with heavy metal that point to possible anthropogenic impact in shore sediments. The element which has low occurrence variability was considered suitable for use as a reference element. This present study has used Fe as the reference element of normalisation because natural sources (1.5 %) vastly dominate its input (Tippie, 1984; Foley *et al*., 2011). The EF is defined by Equation 5.20.

$$EF = \frac{C / Fe(sample)}{C / Fe(earth.crust)} \qquad (Eq.5.20)$$

Where C/Fe (sample) is the content of the examined and the reference element in the examined locations, C/Fe (earth crust) is the content of the examined and reference element in the reference environment (World Surface Rock Average) (WSRA) (Table 7.1). Table 5.2 summarises the contamination criteria based on EF.

Table 5.2: Contamination criteria based on EF (Tippie, 1984; Foley *et al*., 2011)

Enrichment Factor	
Classification	Degree of enrichment
$EF < 2$	Deficient to minimal
$2 < EF < 5$	Moderate
$5 < EF < 20$	Significant
$20 < EF < 40$	Very high
$EF > 40$	Extremely high

(c) Index of Geo-accumulation (Igeo)

The index of geo-accumulation (Igeo) is used to assess the degree of metal contamination in terrestrial, aquatic as well as marine environment in comparison to background contents (Tijani and Onodera, 2009). The index of geo-accumulation is defined as:

$$Igeo = \log_2 C_{metal} / 1.5C_{metal(control)} \qquad (Eq.5.21)$$

Where C_{metal} is the measured concentration of element and $C_{metal(control)}$ is the geochemical background value of World Surface Rock Average (WSRA) (Table 7.1). The constant 1.5 allowed for the analysing of the possible natural fluctuations in background value due to lithologic effect. Table 5.3 gives the contamination criteria based on index of geo-accumulation.

Table 5.3: Contamination criteria based on Index of Geo-accumulation (Igeo) (Tijani and Onodera, 2009; Huu *et al*., 2010)

Index of geo-accumulation	
Classification	Degree of contamination
$Igeo < 0$	unpolluted
$0 \leq Igeo < 1$	unpolluted to moderately polluted
$1 \leq Igeo < 2$	moderately polluted
$2 \leq Igeo < 3$	moderately to strongly polluted
$3 \leq Igeo < 4$	strongly polluted
$4 \leq Igeo < 5$	strong to very strongly polluted
$Igeo > 5$	very strongly polluted

(d) Pollution load index (PLI)

Pollution load index (PLI) is used in evaluating the pollution level for an environment. The PLI for this current work was evaluated using the method proposed by Tomlinson et al., (1980) given in Equation 5.22.

$$PLI = (CF_1 \text{ x } CF_2 \text{ x } CF_3 \text{ x } \ldots \ \ldots \ \ldots \text{ x } \ CF_n)^{1/n} \qquad (Eq.5.22)$$

Where, CF is the contamination factor and n is the number of metals investigated. If PLI value is > 1 it means polluted while PLI value < 1 indicates no pollution.

5.5 Summary

This chapter focused on the sampling location and gave a detailed description of the region. Sample collection, preparation and analytical techniques used throughout the study have all been described here. Equations for radiation dose assessment and contamination of site with heavy metal have been discussed.

CHAPTER 6

RESULTS AND DISCUSSIONS
SURVEY OF THE EXPOSED COMMUNITIES

6.1 Introduction

This Chapter presents the report on the survey of two thousand four hundred (2400) participants in the beaches of Walvis Bay, Swakopmund and Henties Bay. Namibia is categorised as an arid region with hot to very hot weather conditions all year round except for two to three months of winter season. The hot and dry weather conditions have made the coastline of Erongo region a holiday destination to locals and international tourists.

The exposure related activities of the study population are categorised as leisure occupational and others. For convenience, we have grouped security workers at the beaches under sanitation worker because it was observed that these activities share common job description of making sure the beach is not littered. Similarly, we have classified vendors as individual that are mobile as they engage in the business of rendering services at the shoreline and shop retailer as individual that render services at the shops. The data obtained from the questionnaires were used to calculate the mean time allocated for each activity in order to evaluate the possible exposure to NORMs along the coastline. The results calculated are summarized in Tables 6.1-6.3. The results are also presented to show achievement of objective as presented in Chapter 1.

6.2 Possible exposure in Walvis Bay beach

Table 6.1 present the mean time the surveyed populations are engaged in each activity on the beach of Walvis Bay. The time spent by each population group for different activities showed wide variations. These activities average time can be arranged as follows: Other > Occupational > Leisure. Considering the study population, and the time allocated for each activity, the results showed that the mean time ranged within: leisure 1.00-15.40h, occupational 0.00-10.33h and others 8.60-15.07h.

The comparative average time spent on each activity shows that the average time spent on other activity is higher than the average time allocated for leisure and occupational related activities. The result of the analysis of variance of the survey showed that the mean time spent on leisure activity, is statistically significant ($p > 0.05$) compared to occupation but significantly lower than other activity ($p < 0.05$). This may be attributed to the variation of

time spent in other activities outside leisure and work related activities. Since, individuals do not spent a whole day in leisure and work related business.

Table 6.1: The mean time for each activity in Walvis Bay beach

	Activity		
Group	Leisure (h)	Occupational (h)	Others (h)
Leisure-fishing	15.40	0.00	8.60
Leisure-diving	10.42	0.00	13.58
Leisure-walking	8.93	0.00	15.07
Leisure-picnic at shore	12.34	0.00	11.66
Leisure-horse riding	11.00	0.00	13.00
Leisure- sun bathing	10.33	0.00	13.67
Leisure-Relaxation at beach house	9.00	0.00	15.00
Occupation-vendor	1.70	9.70	12.60
Occupation-shop retailer	1.00	10.33	12.67
Occupation-sanitation worker	1.50	8.87	13.63
Average	7.06	9.63	12.95

6.3 Possible exposure in Swakopmund beach

The mean time allocated for leisure, occupation and other activities are presented in Table 6.2. The mean time spent for different activities at the Swakopmund beach follow similar pattern as the Walvis Bay beach. That is, no occupational related leisure activity. The average time can be arranged as follows: Other > Occupational > Leisure. This showed that more times are allocated for other activities than for leisure and occupational related activities. The mean time spent for leisure activities range from 1.00-17.00h, occupation ranged 0.00-10.20h and other activity ranges from 7.00-17.84h.

Table 6.2: The mean time for each activity in Swakopmund beach

	Activity		
Group	Leisure (h)	Occupational (h)	Others (h)
Leisure-fishing	11.95	0.00	12.05
Leisure-diving	10.29	0.00	13.71
Leisure-walking	6.16	0.00	17.84
Leisure-picnic at shore	12.17	0.00	11.83
Leisure-horse riding	9.00	0.00	15.00
Leisure- sun bathing	10.06	0.00	13.94
Leisure-Relaxation at beach house	17.00	0.00	7.00
Occupation-vendor	1.32	10.20	12.50
Occupation-shop retailer	1.00	9.00	14.00
Occupation-sanitation worker	1.86	9.28	12.86
Average	8.08	9.49	13.07

.

6.4 Possible exposure in Henties Bay beach

The results of the mean time allocated for leisure, occupation and other activities in the Henties Bay beach are presented in Tables 6.3. The analysis of this result showed average time arrangement in the order of: Other > Occupational > Leisure as the findings from Walvis Bay and Swakopmund beaches respectively. These may be attributed to the similarity in the weather conditions along the coastline. The mean time allocated for the different activities ranges from 0.00-17.00h with the highest mean time allocated to leisure activity in relaxation at the beach house. The lowest value of 0.00 corresponds to occupational related activities which are in good agreement with findings from Walvis Bay and Swakopmund beaches with no time allocated to work related activity.

Table 6.3: The mean time for each activity in Henties Bay beach

	Activity		
Group	Leisure (h)	Occupational (h)	Others (h)
Leisure-fishing	9.67	0.00	11.33
Leisure-diving	10.45	0.00	13.55
Leisure-walking	7.38	0.00	16.62
Leisure-picnic at shore	12.61	0.00	11.39
Leisure-horse riding	0.00	0.00	0.00
Leisure- sun bathing	16.33	0.00	7.67
Leisure-Relaxation at beach house	17.00	0.00	7.00
Occupation-vendor	0.60	11.00	12.40
Occupation-shop retailer	1.00	8.50	14.50
Occupation-sanitation worker	1.00	9.00	14.00
Average	7.60	9.50	12.05

6.5 Comparison of possible exposure to NORMs along the coastline in the different beaches

The results of the mean time for each activity in the three sampled beaches presented as Table 6.1-6.3 have clearly indicated that there are possible exposures to NORMs in the three locations surveyed. In Walvis Bay beach, the highest possible exposure is leisure-fishing with a mean time of 15.4h and the least possible exposure is occupation-shop retailer. This however, is in contrast with the highest possible exposure in Swakopmund and Henties Bay beaches that have leisure-relaxation in beach house as the highest possible exposure with a mean time of 17.00h. The similarity between the results in Swakopmund and Henties Bay may be because of the serenity of the beach houses and their proximity to the ocean. Possible exposure to occupational related activity has vendor having the highest mean time across the three sampled locations. This follows an arrangement in the order of Henties Bay > Swakopmund > Walvis Bay with mean time of 11.0, 10.2 and 9.70h respectively. The reason for vendor having the highest mean time could be as a result of entrepreneurs that engage in enterprising activities at the coastline taking advantage of holiday makers. From Table 6.4, we see that the mean time spent on leisure is significantly higher than that on occupation (mean difference = 5.0851; p-value < 0.0005) but significantly lower than that on other activity (mean difference 4.4409; p-value < 0.0005).

The findings from the survey have shown that there is high possible exposure to NORMs to human population visiting the coastline of the Erongo region and being involved in leisure activity.

Table 6.4: ANOVA post-hoc multiple comparisons of mean time for activity by location

(I) Activity	(J) Activity	Mean Difference (I-J)	Std. Error	Sig.	95% Confidence Interval	
					Lower Bound	Upper Bound
Leisure	Occupation	5.0851*	1.18593	.000	2.7271	7.4430
	Others	-4.4409*	1.18593	.000	-6.7989	-2.0830
Occupation	Leisure	-5.0851*	1.18593	.000	-7.4430	-2.7271
	Others	-9.5260*	1.18593	.000	-11.8840	-7.1680
Others	Leisure	4.4409*	1.18593	.000	2.0830	6.7989
	Occupation	9.5260*	1.18593	.000	7.1680	11.8840

Based on observed means.

The error term is Mean Square (Error) = 21.097.

*. The mean difference is significant at the 0.05 level.

6.6 Modelled results for occupancy factor along the coastline

Table 6.5 presents the weighted mean time spent doing various activities in the sampled areas. Table 6.6 gives the values of the fraction of time allotted for each indoor and outdoor activity. To model the occupancy factor Equations 5.13 and 5.14 in Chapter 5 were used in MATLAB to determine the values of fraction of time spent in different activities engaged by each group and this model was also used to compute the time spent indoor and outdoor. The obtained results are presented in Table 6.7 and 6.8.

The computed time allotted for outdoor activities in the beaches as shown in Table 6.8 was obtained in the range of 18.59 to 8.40 h for leisure related activities and 13.14 to 8.26 h for occupational/work related activities. Leisure and occupation has values in the range 15.60 to 5.41 h, 15.74 to 10.86 h for indoor. The average time an individual spent in outdoor activity was evaluated to be 11.46 h. This value represents 48% of the population likely exposure to natural radionuclides along the coastline. Also, the calculated indoor average time was obtained for 12.54 h. This value points to the fact that the population spent 52% of their total time per day in indoor related activities. The outdoor occupancy factor of 0.48 for an average person who visit the coastline for leisure or occupational purpose is 2.4 times above the value given by UNSCEAR (0.2) which is significant. The values calculated shows that the indoor factor of 0.52 for an average individual along the beaches is 0.65 times lower than the world average factor of 0.8 (UNSCEAR, 1998). This value is significantly low.

Findings from this study are in agreement with previous studies by Arogunjo *et al*., (2004) and Arogunjo and Adekola (2007). The study showed that an increase outdoor factor over UNSCEAR values might have been attributed to differences in behavioural activities and occupational endeavour's. However, the huge differences in the present study with previous ones may be attributed to the prevailing weather conditions of Erongo region which makes people from all over Namibia and international tourists come to the coastline to take advantage of the opportunity to partake in relatively unrestricted leisure activities.

Table 6.5: The weighted mean time allocated for each activity along the coastline

	Activity		
Group	Leisure	Occupational	Others
Leisure-fishing	12.31	0.00	11.69
Leisure-diving	10.38	0.00	13.62
Leisure-walking	7.34	0.00	16.66
Leisure-picnic at shore	12.33	0.00	11.67
Leisure-horse riding	10.00	0.00	14.00
Leisure- sun bathing	10.79	0.00	13.21
Leisure-Relaxation at beach house	13.00	0.00	11.00
Occupation-vendor	1.31	10.18	12.51
Occupation-shop retailer	1.00	9.58	13.42
Occupation-sanitation worker	1.53	9.05	13.42

Table 6.6: Estimated indoor (λ) and outdoor (σ) fractional time parameter

	Activity					
	Leisure		Occupation		Others	
Group	σ	λ	σ	λ	σ	λ
Leisure-fishing	0.76	0.24	*	*	0.79	0.21
Leisure-diving	0.62	0.38	*	*	0.29	0.71
Leisure-walking	0.72	0.28	*	*	0.32	0.68
Leisure-picnic at shore	0.73	0.27	*	*	0.25	0.75
Leisure-horse riding	0.49	0.51	*	*	0.25	0.75
Leisure-sun bathing	0.53	0.47	*	*	0.32	0.68
Leisure-relaxation at beach house	0.49	0.51	*	*	0.46	0.54
Occupation-vendor	0.85	0.15	0.91	0.09	0.22	0.78
Occupation-shop retailer	1.00	0.00	0.45	0.55	0.22	0.78
Occupation-sanitation Worker	0.98	0.02	0.80	0.20	0.24	0.76

***** Not applicable

Table 6.7: Values of the total fractional time parameters

	Activity		
Group	Leisure (T_1)	Occupation (T_2)	Other (T_3)
Leisure-Fishing	-0.26	*	-0.29
Leisure- diving	-0.12	*	0.21
Leisure-walking	-0.22	*	0.18
Leisure-picnic at shore	-0.23	*	0.25
Leisure-horse riding	0.01	*	0.25
Leisure-sun bathing	-0.03	*	0.18
Leisure relaxation at beach house	0.01	*	0.04
Occupation-vendor	-0.35	-0.41	0.28
Occupation-shop retailer	-0.50	0.05	0.28
Occupation-sanitation worker	-0.48	-0.30	0.26

***** Not applicable

Table 6.8: Computed time spent outdoor and indoor along the coastline of Erongo region

Group	Outdoor (Hrs)	indoor (Hrs)
Leisure-fishing	18.59	5.41
Leisure-diving	10.39	13.61
Leisure-walking	10.62	13.38
Leisure-picnic at shore	11.92	12.08
Leisure-horse riding	8.40	15.60
Leisure-sun bathing	9.95	14.05
Leisure-relaxation at beach house	11.43	12.57
Occupation-vendor	13.14	10.86
Occupation-shop retailer	8.26	15.74
Occupation-sanitation worker	11.96	12.54
Average	11.46	12.54
Occupancy Factor	0.48	0.52
Percentage	48%	52%

6.7 Summary

This chapter focused on the survey of the exposed community along the coastline of the Erongo region. Possible exposures to NORMs from all the sampled locations have been discussed. Using MATLAB, a model of the occupancy factor in the coastline has been evaluated. The findings from the survey have shown that the specific objective of re-evaluation of occupancy factor for effective dose assessment has been achieved. This result showed an outdoor factor 2.4 times the UNSCEAR values.

CHAPTER 7

RESULTS AND DISCUSSIONS
ELEMENTAL COMPOSITION OF SHORE SEDIMENTS

7.1 Introduction

Industrial activities, economic development and urbanization in many cities all over the globe have grown very rapidly in recent years and significant amount of contaminants are washed in rivers, estuarine and coastal regions. Among some of these contaminant heavy metals are serious pollutants of aquatic ecosystems. They owe this to their environmental persistence, toxicity and ability to be incorporated into food chains (Santos *et al*., 2005; Nikulina and Dullo, 2009). This chapter presents the findings and analysis of heavy metals from the investigated sites. The results are also presented to show achievement of objectives as presented in Chapter 1

7.2 Assessment of metal concentration

The heavy metals investigated in this study include arsenic (As), lead (Pb), chromium (Cr), cadmium (Cd), cupper (Cu), manganese (Mn), iron (Fe) and zinc (Zn) determined in the shore sediments of Walvis Bay (WB), Swakopmund (SWK) and Henties Bay (HB). Spatial variation in the mean values of their concentration and comparison with reference values of World Surface Rock Average (WSRA) and World Health Organization (WHO) are shown in Table 7.1 and Figure 7.1 and United States Environmental Protection Authority (EPA) presented in Table 7.2.

Table 7.1: Seasonal concentration in (mg/kg) of some heavy metals along the coastline of Erongo region and reference values of World Surface Rock Average (WSRA) and World Health Organization (WHO) (Martin and Meybeck, 1979; Charravarty and Patgiri, 2009; Chiroma *et al*., 2014)

HM	WB		SWK		HB		WHO	WSRA
	Summer	Winter	Summer	Winter	Summer	Winter		
As	6.1	5.3	2.1	2.9	3.5	3.3	20.0	10.0
Pb	3.0	2.7	0.5	2.7	0.6	2.6	100.0	16.0
Cr	12.0	9.2	3.5	6.3	2.2	8.3	100.0	71.0
Cd	1.0	0.8	0.3	0.7	0.6	1.0	3.0	0.3
Cu	5.4	3.9	1.2	3.1	2.4	2.7	100.0	32.0
Mn	38.0	38.0	29.0	50.0	86.0	22.0	2000.0	750.0
Fe	4290.0	8221.0	1587.0	2183.0	2507.0	2124.0	5000.0	35900.0
Zn	7.2	6.7	2.2	4.5	4.1	4.6	300.0	127.0

Table 7.2: EPA heavy metal Guidelines for Sediments (mg/kg) (Ogbeibu *et al*., 2014)

Metals	Not polluted	Moderately polluted	Heavily polluted	Present study
As	ND	ND	ND	2.1-6.1
Pb	<40	40-60	>60	0.5-3.0
Cr	<25	25-75	>75	2.2-12.0
Cd	- - -	< 6	>6	0.3-1.0
Cu	<25	25-50	>50	1.2-5.4
Mn	<300	300-500	>500	22.0-86.0
Fe	ND	ND	ND	1587.0-8221.0
Zn	<90	90-200	>200	2.2-7.2

The study showed the average concentrations (mg/kg) of the metals decreases in the order Fe > Mn > Cr > Zn > As > Cu > Pb > Cd for WB, Fe > Mn > Cr > Zn > Cu > As > Pb > Cd for SWK and Fe > Mn > Cr > Zn > As > Cu > Pb > Cd for HB. The study showed that the trend of distribution of heavy metal is the same for the beaches of WB and HB for both summer and winter seasons (Figure 7.2-7.4).

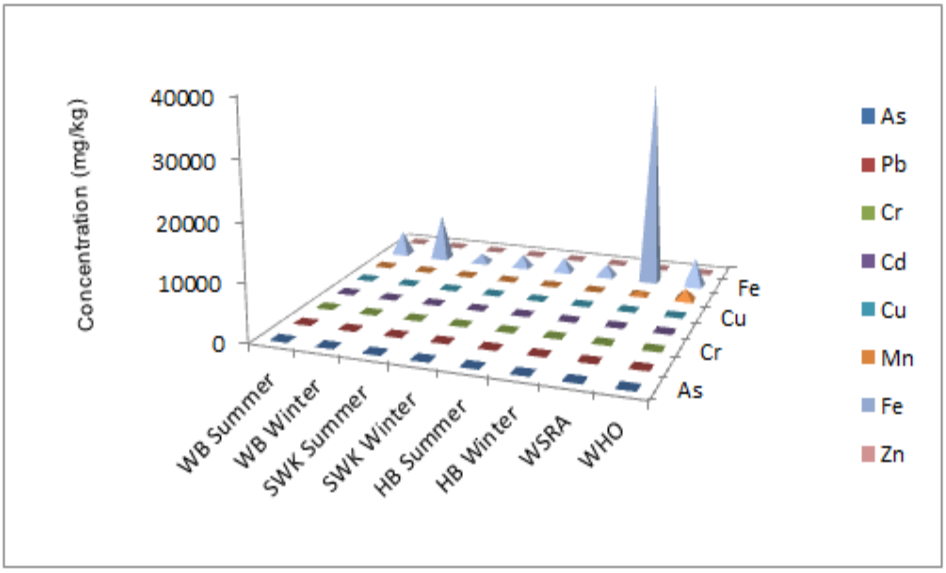

Figure 7.1: Comparison of Heavy metals with reference values of WSRA and WHO.

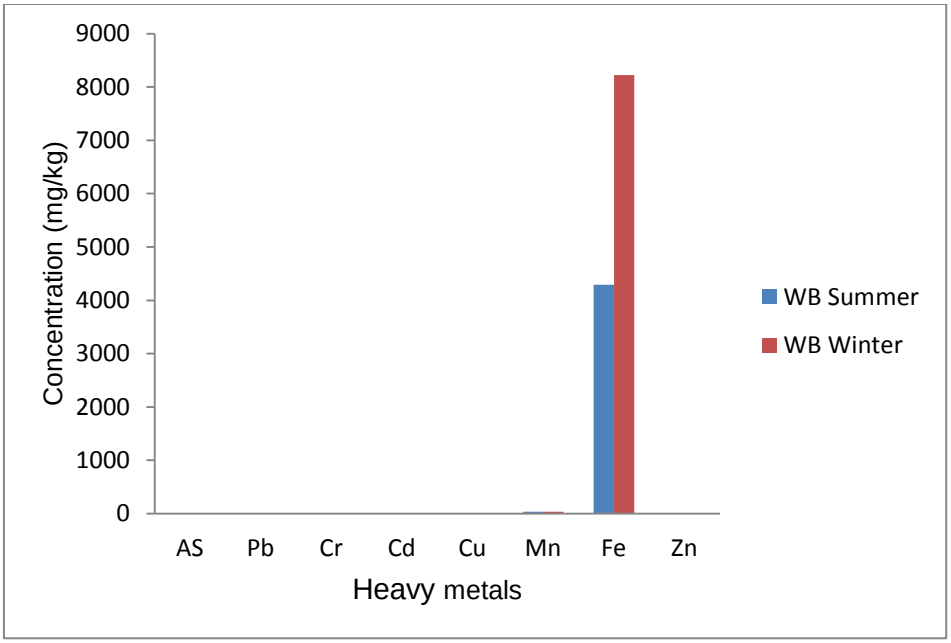

Figure 7.2: Concentration in mg/kg of metals in Walvis Bay Beach.

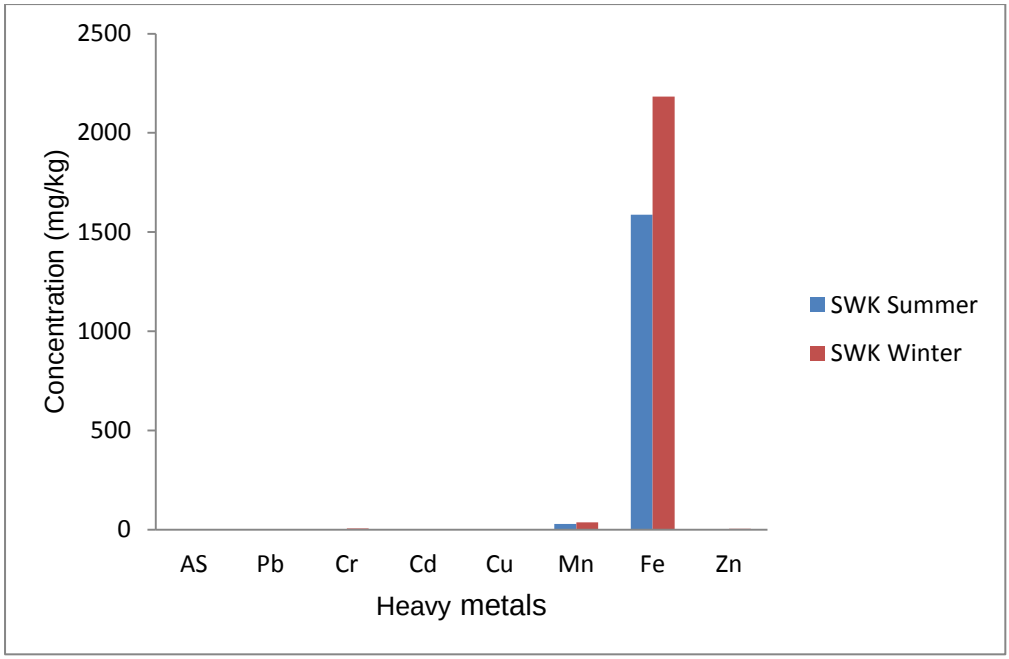

Figure 7.3: Concentration in mg/kg of metals in Swakopmund Beach.

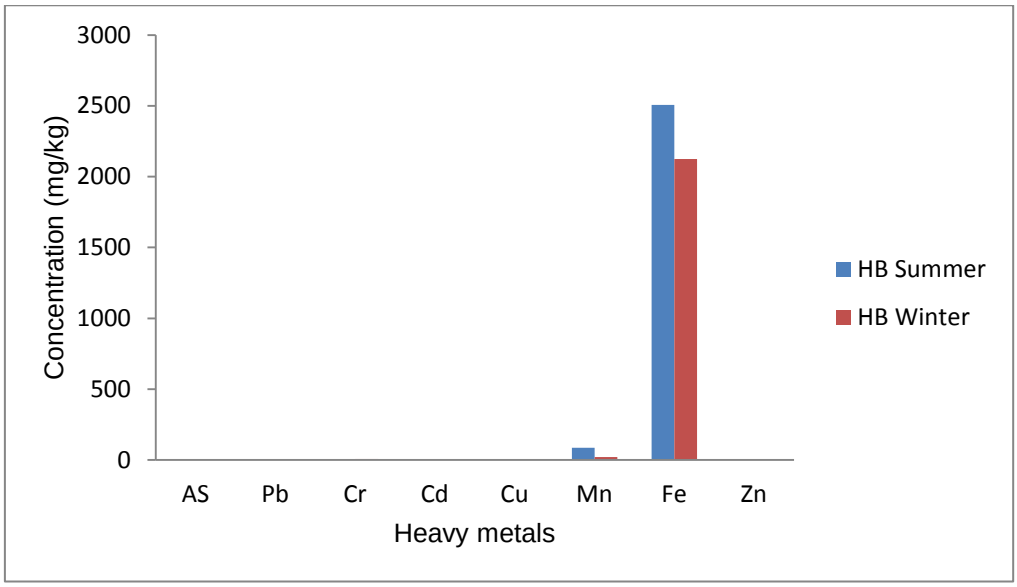

Figure 7.4: Concentration in mg/kg of metals in Henties Beach.

The results obtained showed that Fe recorded the highest concentration in all the sites investigated. This may be because its natural sources (1.5%) vastly dominate its input (Tippie, 1984). The seasonal concentration of heavy metals in Walvis Bay beach ranged from 1.0 to 4290.0 mg/kg in summer and 0.8 to 8221.0 mg/kg in winter (Figure 7.2). The highest was Fe for both seasons and the lowest was Cd which followed similar pattern for both seasons. In SWK Fe was highest (1587.0 mg/kg) in summer and Cd lowest (0.3 mg/kg) (Figure 7.3). In winter, SWK has highest (2183.0 mg/kg) of Fe concentration and the lowest of Cd (0.7 mg/kg). The concentration of metals in HB ranged from 0.6 mg/kg (Pb and Cd) to 2507.0 mg/kg (Fe) for the summer season and highest value of Fe (2124.0 mg/kg) and lowest 1.0 mg/kg Cd values for the winter months. All the elements have concentration below the referenced (WSRA) and (WHO) (Table 7.1) and (Figure 7.1). However, the concentration of Cd has value more than the WSRA in all season investigated across the sampling sites except for SWK where the mean concentration of Cd is below the value for WSRA in summer.

Arsenic concentration varied between 2.1 mg/kg and 6.1 mg/kg with a mean concentration of 3.9 mg/kg. The levels of As decreased in the order WB > HB > SWK for both seasons (Figure 7.5).

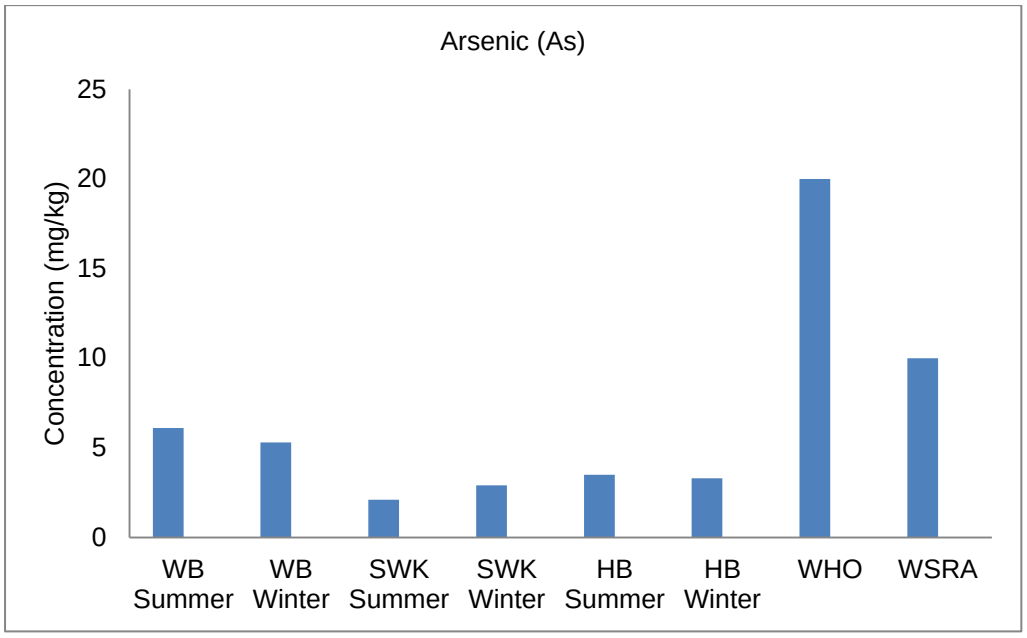

Figure 7.5: Distribution of concentrations of As in summer and winter.

The study showed that the level of As varies with seasons with WB and HB recorded high levels in summer. These values are however, found to be below the critical value of 16 mg/kg (average crustal abundance) (Deneley *et al*., 1976). Arsenic is highly carcinogenic and has no nutritional value for plant and animal (Amadi *et al*., 2012). The concentration of As in all the sampled locations is below the permissible limit set by WHO (Figure 7.5).

Concentration of lead (Pb) in sediment samples ranged from 0.5 to 3.0 mg/kg. The trend of the levels of Pb is similar to those of As (WB > HB > SWK). However, highest levels of Pb are recorded in winter for the sites of SWK and HB while the Pb concentration was highest in WB in summer (Figure 7.6).

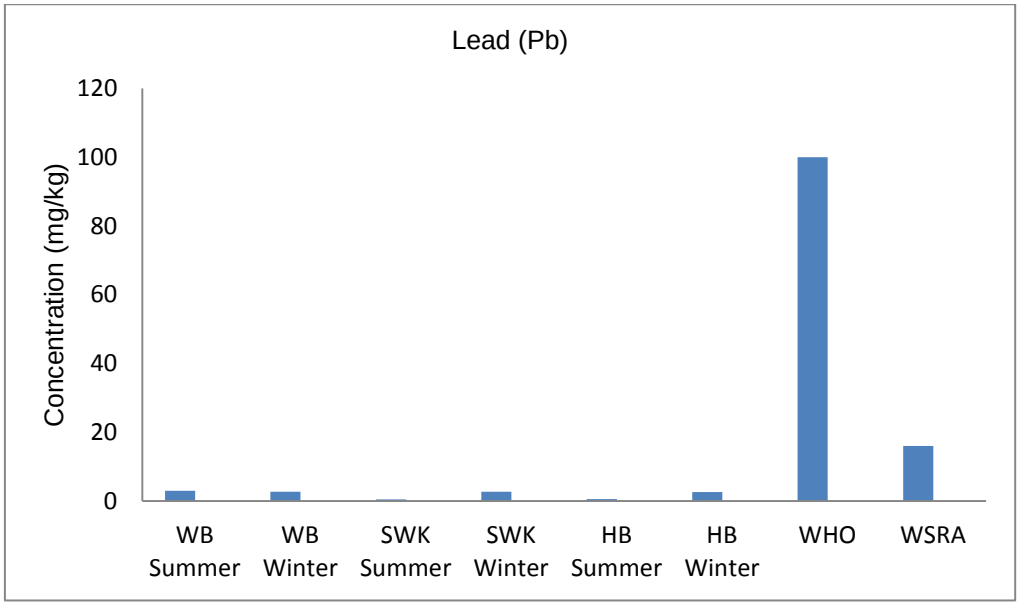

Figure 7.6: Distribution of concentrations of Pb in summer and winter.

Findings from this study have shown that the concentration of lead recorded was below WSRA and indicates that the region is not polluted according to EPA heavy metal guideline for sediments (Tables 7.2). Lead (Pb) as a soil contaminant is a global issue; it accumulates with age in bones, aorta, kidneys, spleen and liver. This metal can enter the body through uptake of food, water and air. The concentration of lead in this study was lower than the values (11.8 to 39 mg/kg and 14.0 to 22.1 mg/kg) obtained by Saikia *et al*., (2014) and Ravichandran and Manickam (2012) in the sediments of the Subansiri River and the Chennai Coast respectively.

Chromium (Cr) in the sediment of all the sampled beaches ranged from 2.2 to 12.0 mg/kg. The concentration of Cr decreased in the order WB > HB > SWK (Figure 7.7).

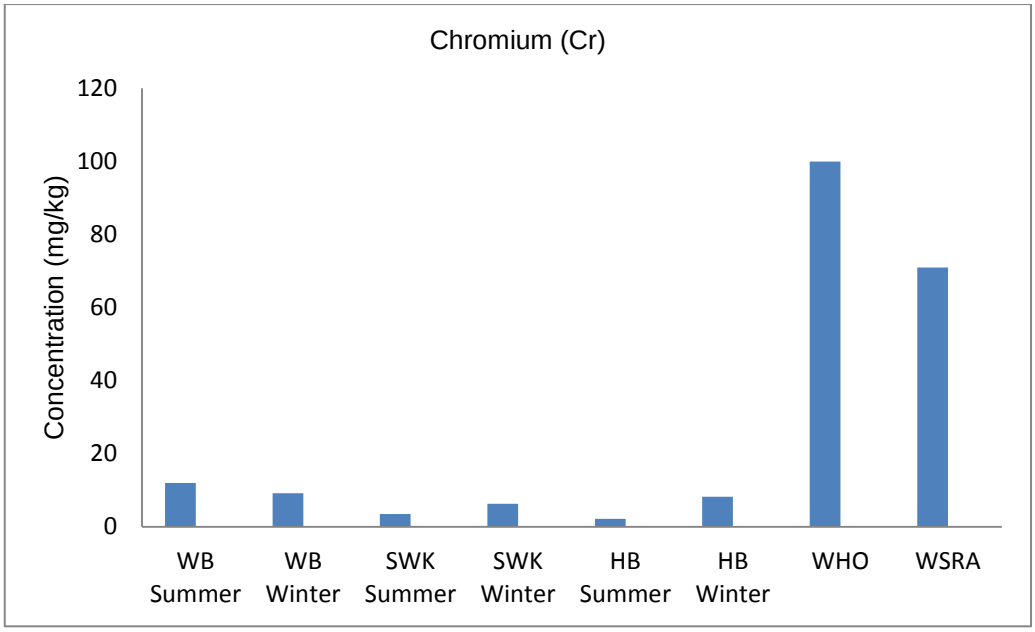

Figure 7.7: Distribution of concentrations of Cr in summer and winter.

Swakopmund and Henties Bay have lower levels of Cr in summer which is in contrast with the high level of Cr in WB during summer. According to the EPA guideline for heavy metal in sediment, the sampled sites are unpolluted with chromium. This metal is carcinogenic and is usually taken in by inhalation; it is also, corrosive to tissue. It is used in alloys, electroplating, pigments, paints manufacture, fungicides, glass, leather tanning industries and photography (Aboud and Nandini, 2009). The values recorded in this investigation were lower when compared to similar studies undertaken by Hu *et al*., (2010) in estuarine sediments near Cua Ong Harbor, Ha long Bay, Vietnam. However, these concentrations of Cr were higher than the levels of 0.25 to 1.68 mg/kg in the Benin River, Nigeria (Ogbeibu *et al*., 2014).

The concentration of Cd in the sediments ranged from 0.3 to 1.0 mg/kg (Table 7.1) and followed the order WB > SWK > HB (Figure 7.8). The highest levels of concentration were in WB in summer and the lowest level was that of SWK in summer. The permissible limit of Cd in soil, recommended by WHO, is 3.0 mg/kg (Table 7.1). The three beaches did not exceed the standard and are therefore not polluted according to EPA guideline (Table 7.2). Cadmium recorded in this study was quite high compared with the values recorded by Hu *et al*., (2010).

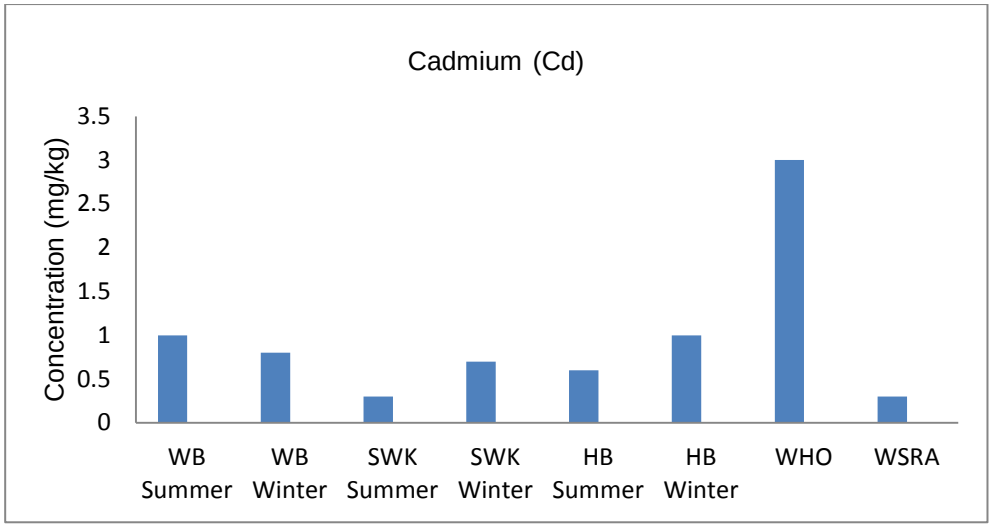

Figure 7.8: Distribution of concentrations of Cd in summer and winter.

The concentration of Cu in the sediments ranged from 1.2 to 5.4 mg/kg (Table 7.1). The trend of Cu in the study sites decreased in the order WB > HB > SWK (Figure 7.9). The permissible limit is 100 mg/kg according to WHO Standards (Table 7.1). The value of Cu in all the samples was found to be below the permissible limits. Contamination of drinking water with high level of Cu which poses a threat to human health was unlikely because a comparison of the level of Cu with EPA indicates that the area is not polluted (Table 7.2). The values of Cu recorded in this investigation were lower compared to similar studies on sediments from Punta Mala Bay Pacific Panama (53.0 to 56.3 mg/kg) Defew *et al*., (2005) and East Adriatic Sea (20.5 to 44.3 mg/kg) Ana and Zoran, (2010).

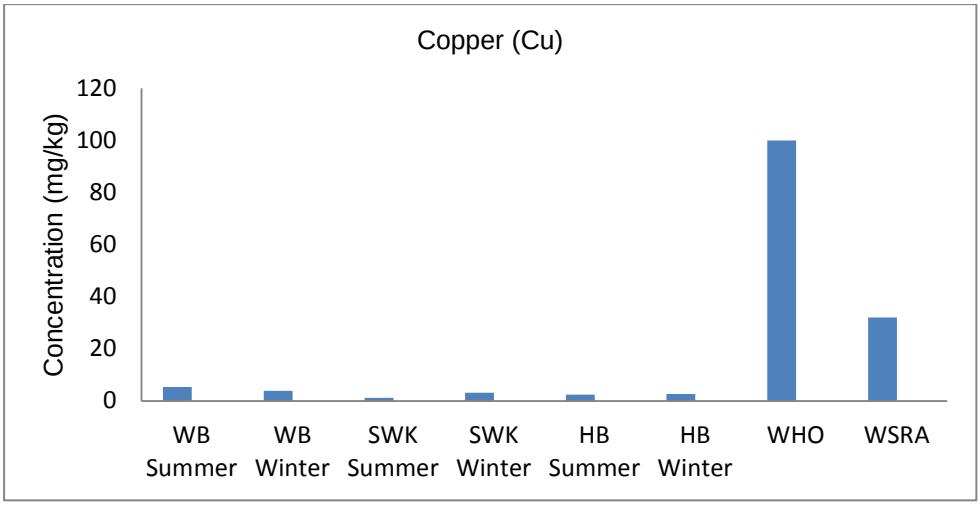

Figure 7.9: Distribution of concentrations of Cu in summer and winter.

Manganese concentrations ranged from 22.0 to 86.0 mg/kg. The level of Mn from the study locations did not follow a similar trend to that of as As. In this case it was HB > SWK > WB (Figure 7.10). A study by Abbasi *et al*., (1998) gave a value of 1000 mg/kg for Mn in an uncontaminated soil. The EPA heavy metal guideline for sediment indicates that the beach is not polluted (Table 7.2). The WHO maximum permissible level in soil is 2000 mg/kg (Table 7.1). Mn is essential for plant and animals but an elevated level can pose threat to life. Mn investigated in this study was quite low compared with the concentration recorded by Defew *et al*., (2005).

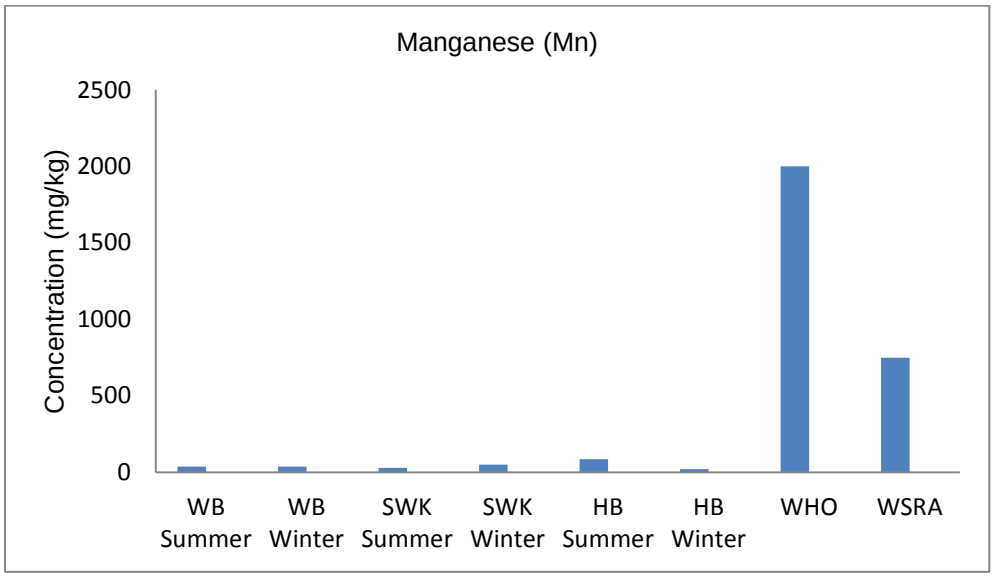

Figure 7.10: Distribution of concentrations of Mn in summer and winter.

Iron exists in water as Fe^{2+} or Fe^{3+} in suspended form. Its presence is evident by staining in clothes and it imparts a bitter taste. Natural geological sources, industrial activities, domestic discharge and other form of by product occasioned the released of Fe into water. WHO recommended safe level of Fe in soil is 5000 mg/kg. Clearly, the level of iron in all the beaches except in Walvis Bay is below the permissible limit recommended (Figure 7.11). However, the elevated concentration of Fe in Walvis Bay may be as a result of industrial wastes from seaport activities, processing companies in the town and from huge domestic waste discharge.

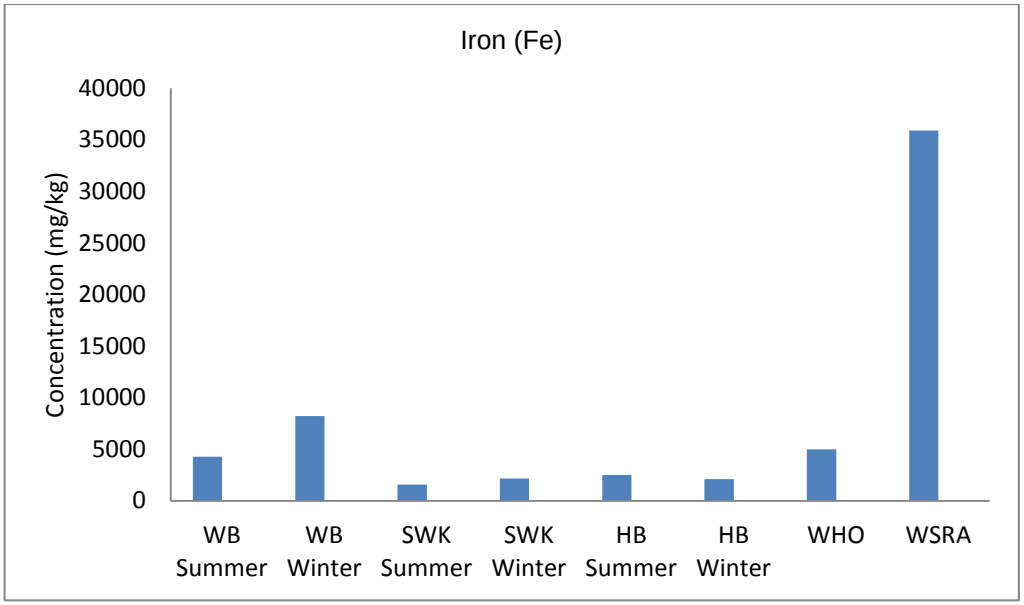

Figure 7.11: Distribution of concentrations of Fe in summer and winter.

Zn as a trace element plays an important role in the physiological and metabolic process of living organisms. However, higher concentrations of Zn can have a negative impact on the organism. Concentration of zinc in the sites monitored ranged from 2.2 to 7.2 mg/kg. The concentrations of Zn decreased in the order WB > HB > SWK (Figure 7.12). WHO, maximum permissible limit of Zn in soil is 300 mg/kg. In all the collected shore sediment samples the concentration of zinc recorded was below the maximum permissible limit. The EPA heavy metal guideline for sediments defines these levels as not polluted (Table 7.2). When the value of Zn is compared with other related studies, the study showed that Zn did not compare favourably with the mean values obtained by Defew *et al*., (2005) and Ana and Zoran, (2010).

A close comparison of the three sampled sites (Table 7.1) showed that the concentrations of heavy metals from the Walvis Bay beach are higher than those of Swakopmund and Henties Bay beaches except for Mn. These changes in concentration may be attributed to the nature of anthropogenic activities carried out on hinterland and within the vicinity of the coastline some of which include; sea port activities and solid waste disposal (open dumps and sanitary landfills). All these represent a significant source of the release of heavy metals into the environment (Abah *et al*., 2015). This study therefore found that human activity can increase the concentrations of heavy metals in the environment.

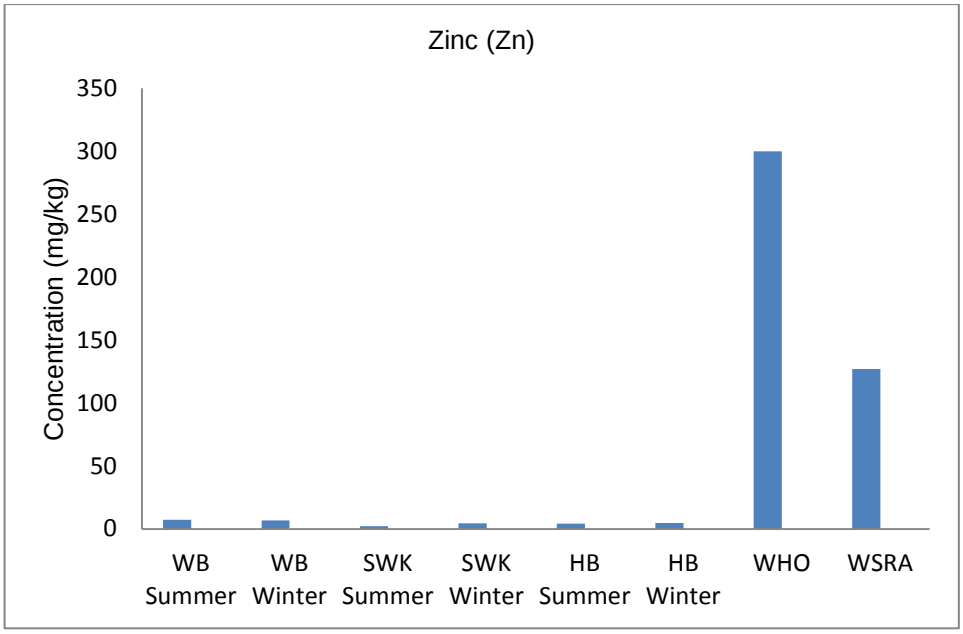

Figure 7.12: Distribution of concentrations of Zn in summer and winter.

7.3 Assessment on contamination status of heavy metals

7.3.1 Correlation analysis of concentrations of the heavy metals

Inter-elemental correlation analyses of the metals content of the shore sediments in summer seasons (Table 7.3) indicated that apart from Mn which showed less negative correlation with As, Pb, Cr, Cu and Fe all the other metals showed strong positive correlation across the sampling areas. This suggests a common source of anthropogenic input across the study area. Thus, Pb-Zn pair may be due to vehicular emission since most of the beaches are closer to access road. The trend of this inter-elemental correlation agrees with a similar study elsewhere in Namibia (Abah, *et al*., 2014) where deposits of heavy metal pollutants are transferred onto residential area. The inter-elemental correlations in the winter seasons (Table 7.4) were Cr-As, Cu-As, Cu-Pb, Zn-Cu, Zn-Cr, Mn-Cd, Fe-Mn, Fe-As, Cu-Mn, Fe-Cu and Fe-Cr. The presence of the association of Cu with Mn and their significant correlation suggests anthropogenic origin presumably from industrial emissions. A similar study elsewhere in the continent (Mmolawa *et al*., 2011) clearly pointed out that Fe and Mn are predominantly lithogenic whereas Cu, Pb and Zn basically originate from various anthropogenic sources.

Table 7.3: Inter-elemental correlation analysis along the sampling locations in summer

	As	Pb	Cr	Cd	Cu	Mn	Fe	Zn
As	1.0000							
Pb	0.9502	1.0000						
Cr	0.8895	0.9876	1.0000					
Cd	0.9960	0.9187	0.8453	1.0000				
Cu	0.9975	0.9700	0.9197	0.9872	1.0000			
Mn	-0.0241	-0.3343	-0.4782	0.0650	-0.0950	1.0000		
Fe	0.9999	0.9536	0.8944	0.9950	0.9982	-0.0349	1.0000	
Zn	0.9994	0.9392	0.8736	0.9985	0.9945	0.0097	0.9990	1.0000

Table 7.4: Inter-elemental correlation analysis along the sampling locations in winter

	As	Pb	Cr	Cd	Cu	Mn	Fe	Zn
As	1.0000							
Pb	0.3592	1.0000						
Cr	0.8348	-0.2139	1.0000					
Cd	-0.0339	-0.9449	0.5219	1.0000				
Cu	0.8825	0.7559	0.4778	-0.5000	1.0000			
Mn	-0.4136	-0.9983	0.1560	0.924	-0.7932	1.0000		
Fe	-0.9931	-0.4664	-0.7644	0.1511	-0.9316	0.5177	1.0000	
Zn	0.9933	0.4647	0.7655	-0.1493	0.9310	-0.5161	-10000	1.0000

7.3.2 Enrichment factors (EF)

The calculation and evaluation of EF values helps to determine whether a certain element has additional or anthropogenic sources other than it's predominate natural sources. Table 7.5 shows the seasonal enrichment factors based on the values of seasonal metal concentrations of some heavy metal investigated in the beaches of WB, SWK and HB. The enrichment factor values for As in the shore sediments stands at 5.1047 for WB in summer and 4.4352 in winter, 1.7573 at SWK in summer and 2.4268 in winter and 2.9289 for HB in summer and 2.7615 in winter. The EF values suggested significant enrichment for the seasons of summer in WB and moderate enrichment for As in WB winter seasons, SWK summer and winter seasons respectively. However, SWK summer seasons registered moderate enrichment based on established environmental site quality criteria (Tippie, 1984; Foley *et al*., 2011), presented in Table 5.2. The EF values for Pb, Cr, Cu, Mn and Zn in all

the sites investigated showed value of EF < 2 in all seasons which is indicative of deficiency to minimum enrichment (Table 5.2). These values were lower compared with the findings of Saikia et al., (2014) from heavy metal EF in suspended sediments of Subansiri River, India.

If the EF value approaches unity, then crustal sources are predominant. In general, if the EF values are > 5, it then implies that a large fraction of the element can be attributed to non-crustal or anthropogenic sources (Wu *et al*., 2007). The EF values for Cd in WB are 27.8943 (summer) and 22.3155 (winter). The EF values for SWK are 8.3683 in summer seasons and 19.5260 for winter seasons. HB has EF of 16.7366 (summer) and 27.8943 (winter). Clearly, the EF in WB indicated very high enrichment for Cd in both seasons and significant enrichment for HB (summer), SWK (winter and summer) beaches respectively. The high EF values for Cd could be as a result of mainly anthropogenic sources such as industrial emissions. This EF values for this present study was higher compared to similar studies on shore sediments where the EF values were moderate enrichment (Hu *et al*., 2010).

Table 7.5: Seasonal enrichment factor (EF) of heavy metals along the coastline of Erongo region

HM	Walvis Bay beach		Swakopmund beach		Hentis Bay beach	
	Summer	Winter	Summer	Winter	Summer	Winter
As	5.1047	4.4352	1.7573	2.4268	2.9289	2.7615
Pb	1.5691	1.4122	0.2615	1.4122	0.3138	1.3598
Cr	1.4144	1.0843	0.4125	0.7425	0.2593	0.9783
Cd	27.8943	22.3155	8.3683	19.5260	16.7366	27.8943
Cu	1.4122	1.0199	0.3138	0.8107	0.6276	0.7061
Mn	0.4240	0.4240	0.3236	0.5579	0.9596	0.2455
Zn	0.4744	0.4415	0.1450	0.2965	0.2702	0.3031

7.3.3 Contamination factors (CF)

The values of seasonal contamination factors for the three sites are presented as Table 7.6. With regards to classifying the degree of contamination, contamination criteria based on contamination factor by Hakanson (1980) was proposed (Table 5.1). This study showed that apart from As that indicated moderate degree of contamination in the summer seasons in WB, all the other sites CF values indicate that the sediments have low contamination in all season. The CF values for Pb, Cr, Cu, Mn, Fe and Zn indicated low contamination in both seasons in all sampled sites. However, for Cd considerable degree of contamination was recorded in WB during the summer season and a moderate degree of contamination in winter seasons. SWK has low contamination of Cd in summer and moderate degree of contamination of Cd in winter seasons. HB followed a similar trend of contamination with Cd as Walvis Bay only that it exhibited moderate contamination in summer and considerably contaminated in winter seasons. The considerable and moderate levels of contamination of Cd in these beaches may be related to improper handling of refuse in the vicinity of the beaches and industrial emissions. These values are in contrast with similar studies (Hu *et al*., 2010) where As is of concern and Cd has low degree of contamination.

Table 7.6: Seasonal contamination factor (CF) values of heavy metals along the coastline of Erongo region

HM	Walvis Bay beach		Swakopmund beach		Hentis Bay beach	
	Summer	Winter	Summer	Winter	Summer	Winter
As	0.6100	0.5300	0.2100	0.2900	0.3500	0.3300
Pb	0.1875	0.1688	0.0313	0.1688	0.0375	0.1625
Cr	0.1690	0.1296	0.0493	0.0887	0.0310	0.1169
Cd	3.3333	2.6667	1.0000	2.3333	2.0000	3.3333
Cu	0.1688	0.1219	0.0375	0.0969	0.0750	0.0843
Mn	0.0507	0.0507	0.0387	0.0667	0.1147	0.0293
Fe	0.1195	0.1195	0.0442	0.0608	0.0698	0.0592
Zn	0.0567	0.0567	0.0173	0.0354	0.0323	0.0362

7.3.4 Geo-accumulation index (Igeo)

The geo-accumulation index (Igeo) has been used extensively in the assessment and evaluation of sediment pollution by heavy metals (Ogbeibu *et al*., 2014; Saikia, *et al*., 2014; Huu *et al*., 2010). Data from this present study has revealed that the beaches of WB, SWK and HB are unpolluted with As, Pb, Cr, Fe and Zn. The negative values in As, Pb, Cr, Cu, Fe, Mn, Cd and Zn indexes of geo-accumulation shown in Table 7.7 are a result of deficient to minimal enrichment (Table 7.5) and/or relatively low levels of contamination (Table 7.6). Table 7.7 revealed moderately polluted beach of WB in summer with Cd, unpolluted to moderately polluted beach of WB in winter with Cd, unpolluted beach of SWK in summer with Cd, unpolluted to moderately polluted beach of SWK in winter with Cd, unpolluted beach of HB in summer with Cd and unpolluted to moderately polluted beach of HB with Cd in winter (Table 5.3).

Table 7.7: Geo-accumulation index (Igeo) values of heavy metals along the coastline of Erongo region

HM	Walvis Bay beach		Swakopmund beach		Hentis Bay beach	
	Summer	Winter	Summer	Winter	Summer	Winter
As	-1.2981	-1.5009	-2.8365	-2.3708	-2.0995	-2.1844
Pb	-3.0000	-3.1520	-5.5850	-3.1520	-5.3219	-3.2065
Cr	-3.1497	-3.5331	-4.9274	-4.0794	-5.5972	-3.6816
Cd	1.1520	0.8301	-0.5850	0.6374	0.4150	1.1520
Cu	-3.1520	-3.6215	-5.3220	-3.9527	-4.3219	-4.1520
Mn	-4.8878	-4.8878	-5.2777	-4.4919	-3.7094	-5.6763
Fe	-3.6499	-2.7116	-5.0846	-4.6246	-1.1030	-4.6641
Zn	-4.7257	-4.8295	-6.4361	-6.4361	-5.5380	-5.3720

7.3.5 Pollution load index (PLI)

The pollution load index (PLI) was calculated using Equation 5.17 and data in Table 7.6. If PLI value is > 1 it means polluted while PLI value < 1 indicates no pollution. The PLI values decreased in the order of WB > HB > SWK (Figure 7.16). The studies showed that the PLI ranged from 0.0660 to 0.2097. The highest index of polluton load was calculated for WB in summer and the lowest value was calculated for SWK also in summer. The present study has shown that the PLI has high values in summer for WB and HB beaches but lower value calculated in summer for SWK beach. The PLI investigated in this study was quite high compared with the values recorded by Ogbeibu *et al*., (2014) in a similar study. The PLI values presented in Table 7.8 clearly indicated values < 1. Hence, according to Tomlinson *et al*., (1980) all the beaches are not polluted with heavy metals.

Table 7.8: Pollution load index (PLI) values of heavy metals along the coastline of Erongo region.

	Seasons	Walvis Bay beach	Swakopmund beach	Henties Bay beach
PLI	Summer	0.2097	0.0660	0.1411
	Winter	0.1975	0.1392	0.1350

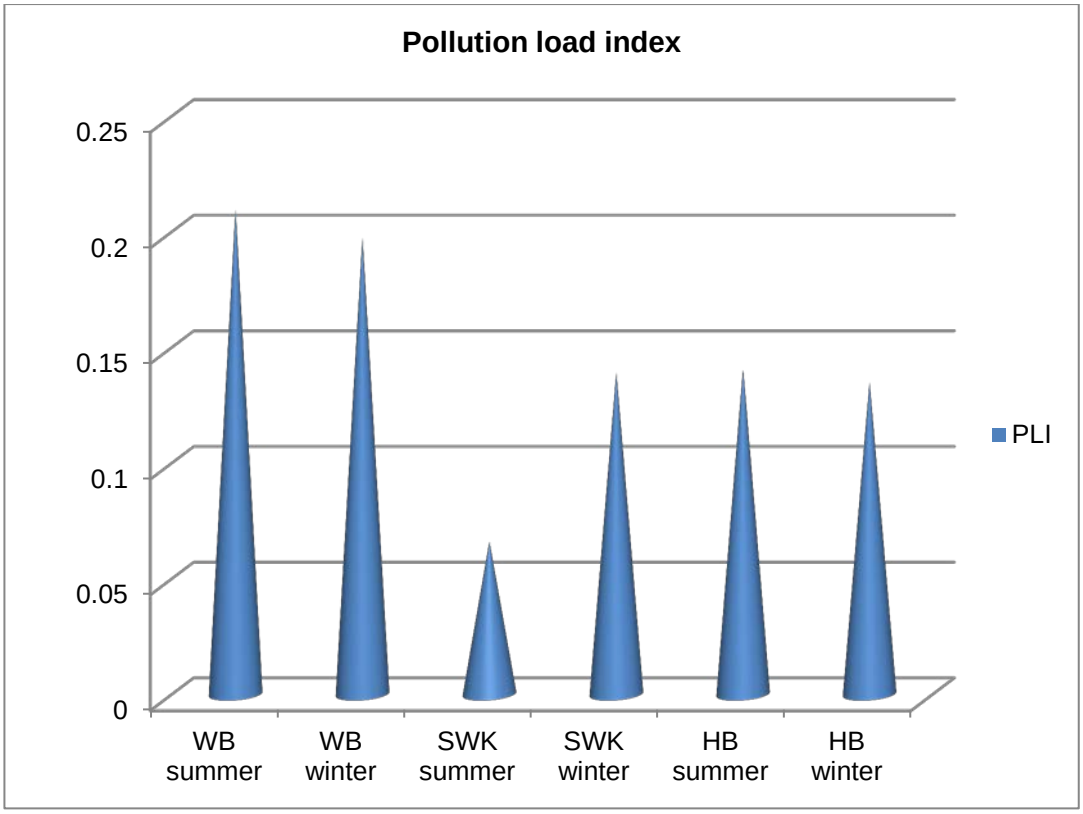

Figure 7.16: Pollution load index (PLI) of heavy metal of sampling site along the coastline of the Erongo region.

7.3.6 Interpretation of heavy metal source using the Principal Component Analysis (PCA)

A factor analysis was carried out in an attempt to further classify the major controlling factors that determine the distribution of heavy metals in the shore sediments. Table 7.9 represents the PCA results used to identify common sources of heavy metals from the different sites during summer and winter sampling periods. PCA results of metals in summer showed two factors accounting for 85% of the total variance. Factor 1 is characterized by low loading which explained 84.6% of the total variance in the winter season. Factor 2 (summer) explained 15.4% of the total variance and correlated with high to very high loadings on Mn. Manoli *et al*., (2002) reported that road dust had high loadings on Mn. Thus, factor 2 is assigned to road and soil dust.

In winter, two factors obtained in the PCA analysis of metals in shore sediments accounted for 65% of the overall variance. Factor 1 (65%) had low loadings for all metals. Factor 2 (winter) (35%) with moderate loadings on Cr and Cd indicated a mixture of industrial emissions, vehicular emissions/oil combustion, and re-suspended road dust from urban areas with high traffic densities (Cd) soil dust origin (Cr)(Samara and Voutsa, 2005; Sham *et al*., 2006).

Table 7.9: PCA loadings calculated for eight chemical variables in Shore sediments along the coastline of Erongo region for summer and winter seasons

Variable	Summer		Winter	
	Factor 1	Factor 2	Factor 1	Factor 2
As	0.3814	0.1125	0.3956	0.2581
Pb	0.3774	-0.1714	0.3190	-0.4100
Cr	0.3612	-0.3082	0.2259	***0.5120***
Cd	0.3756	0.1916	-0.2029	***0.5295***
Cu	0.3839	0.0487	0.4383	-0.0256
Mn	-0.0572	**0.8905**	-0.3362	0.3836
Fe	0.3819	0.1028	-0.4151	-0.1930
Zn	0.3796	0.1426	0.4149	0.1941
Eigen value	6.7668	1.2332	5.1967	2.8033
Percent of variance	84.6%	15.4%	65.0%	35.0%
Cumulative percentage	84.59	1.0000	64.96	1.0000

Note: Bold: high to very high loading (>0.6)

Bold & Italic: moderate loading (between 0.4 and 0.6)

Regular: low loading (<0.4)

7.4 Summary

This chapter has discussed the concentration, trend and seasonal variation of heavy metals along the coastline of Erongo region. The assessment on contamination status and interpretation of metal source has also been presented. The summary of the chapter shows an achievement of the objectives of evaluation of metal concentration and seasonal variation as presented in chapter 1.

CHAPTER 8

RESULTS AND DISCUSSION
RADIONUCLIDE CONCENTRATIONS IN SHORE SEDIMENTS

8.1 Introduction

The objective of this chapter is to present the concentration of natural radionuclides in shore sediments, evaluate the baseline activity concentration and using the modelled factors in chapter six (6) to evaluate the effective dose rate, and hazard index due to natural radionuclides and their decay products from sediment samples.

The results of the mean specific activity concentrations of ^{238}U, ^{232}Th and ^{40}K in beach sediment obtained from Walvis Bay, Swakopmund and Henties Bay are shown in Table 8.1-8.3 respectively.

8.2 Activity concentration of ^{238}U, ^{232}Th, and ^{40}K in shore sediments in Walvis Bay (WB) beach

The mean specific activity concentration of natural radionuclides (^{238}U, ^{232}Th and ^{40}K) from all 26 sampling points in the beach of Walvis Bay is given in Table 8.1. The activity concentrations showed variation from one sampling point to another, because river and sea bottoms can exhibit large variation in chemical and mineralogical properties (Krmar *et al*., 2009). The activity concentration ranges for ^{238}U, ^{232}Th and ^{40}K are BDL – 276.39 Bq.kg^{-1} with a mean of 142.79 Bq.kg^{-1}, BDL – 40.80 Bq.kg^{-1} with a mean of 29.69 Bq.kg^{-1} and 319.26 – 516.45 Bq.kg^{-1} with a mean of 359.78 Bq.kg^{-1} respectively. In all the sampling points, mean activity concentration follows the order ^{232}Th < ^{238}U < ^{40}K (Figure 8.1). The activity concentration of ^{232}Th is lower than other radionuclides. This low concentration of ^{232}Th may be attributed to the low content of monazite (Orgun *et al*., 2007). Comparing this study with a study undertaken by Shimboyo (2010) in the town of Arandis showed that although the town is close to the world's largest open-pit uranium mine, Rössing Uranium Mine, the mean activity concentration of ^{238}U (72.4 $\pm$ 13.5 Bq.kg^{-1}) obtained for Arandis is much lower than that obtained in the present study where the mean activity concentration of ^{238}U is 142.79 Bq.kg^{-1}. This high concentration of ^{238}U in this present study may be due to anthropogenic activities, radioactive dust fall out migration and deposition in rivers and sea and the solubility and mobility of U (VI) O_2^{2+} (Powell *et al*., 2007). The increasing activity concentration trend of ^{40}K is due to the presence of loamy and clay sediments (El – Gamal *et al.,* 2007). The mean activity concentration in this study was higher than the values (7.31

Bq.kg^{-1}, 46.85 Bq.kg^{-1}, and 384.03 Bq.kg^{-1}; 1.42 Bq.kg^{-1}, 1.49 Bq.kg^{-1} and 21.31 Bq.kg^{-1}) obtained for ^{238}U, ^{232}Th and ^{40}K by Ramasamy *et al*., (2010) and Amekudzie *et al*., (2011) in sediment of Ponnaiyar river and Chorkor beach respectively (Table 8.2).

The mean activity concentrations of ^{232}Th and ^{40}K for all measured sampling points in the coastline in the beach of Walvis Bay showed concentration below the world average values (World average values of ^{238}U, ^{232}Th and ^{40}K are 50 Bq.kg^{-1}, 50 Bq.kg^{-1} and 500 Bq.kg^{-1} respectively). The WB-26 has high ^{40}K concentrations. This can be attributed to the mineralogical composition of the sediment at that sampling point (Tsabaris *et al*., 2007). Findings from this study have shown that ^{238}U activity concentrations from all the sampling points are higher than the world average value of 50 Bq.kg^{-1} which suggests that there is an anthropogenic input.

Table 8.1: Mean specific activity concentration due to ^{238}U, ^{232}Th and ^{40}K in the various shore sediment samples in Walvis Bay (WB) beach

Location	^{238}U (Bq.kg $^{-1}$)	^{232}Th (Bq.kg $^{-1}$)	^{40}K (Bq.kg $^{-1}$)
WB-1	140.42	26.67	319.26
WB-2	173.64	35.65	359.95
WB-3	127.70	33.90	425.68
WB-4	153.26	30.33	388.12
WB-5	138.57	28.22	397.51
WB-6	143.14	24.06	338.04
WB-7	134.37	24.32	344.30
WB-8	172.16	31.59	328.65
WB-9	BDL	46.69	338.04
WB-10	172.28	34.19	331.78
WB-11	171.67	37.07	338.04
WB-12	100.90	33.78	366.21
WB-13	BDL	28.58	369.34
WB-14	165.00	22.17	378.73
WB-15	84.72	40.36	359.95
WB-16	106.33	40.07	369.34
WB-17	98.18	31.79	350.56
WB-18	205.13	31.26	400.64
WB-19	226.25	40.80	413.16
WB-20	198.96	33.66	419.42
WB-21	152.15	35.77	375.60
WB-22	116.71	22.86	359.95
WB-23	149.06	26.51	378.73
WB-24	134.49	BDL	350.56
WB-25	171.05	31.71	366.21
WB-26	276.39	BDL	516.45
Mean	142.79	29.69	359.78
Maximum	276.39	40.80	516.45
Minimum	BDL	BDL	319.26

Table 8.2: Comparison of mean specific activity concentration of ^{238}U, ^{232}Th and ^{40}K in the various shore sediment samples in Walvis Bay (WB) beach and other studies in different beaches of the world

Location	^{238}U (Bq.kg $^{-1}$)	^{232}Th (Bq.kg $^{-1}$)	^{40}K (Bq.kg $^{-1}$)	Reference
Walvis Bay	142.79	26.69	359.78	**Present study**
Chorkor beach, Ghana	1.42	1.49	21.31	Amekudzie *et al*., 2011
Ponnaiyar River, India	7.31	46.00	384.11	Ramasamy *et al*., 2010
Osun River, Nigeria	24.00	35.70	162.38	Oyebanjo *et al*., 2012
Red sea, Egypt	95.3-105.6	2.3-221.9	98-1011	El-Mamoney and Khater, 2004
Northeast Coast, Spain	5-19	5-44	136-1087	Rosell *et al*., 1991
Preta beach, Brazil	54-180	128-349	47-283	Freitas and Alencar, 2004
Zircon, Bangladesh	64.39	13.24	47.2	Alam *et al*., 1999
Aegean, Greece	53.0	71.0	877.0	Florou and Kritidis, 1992

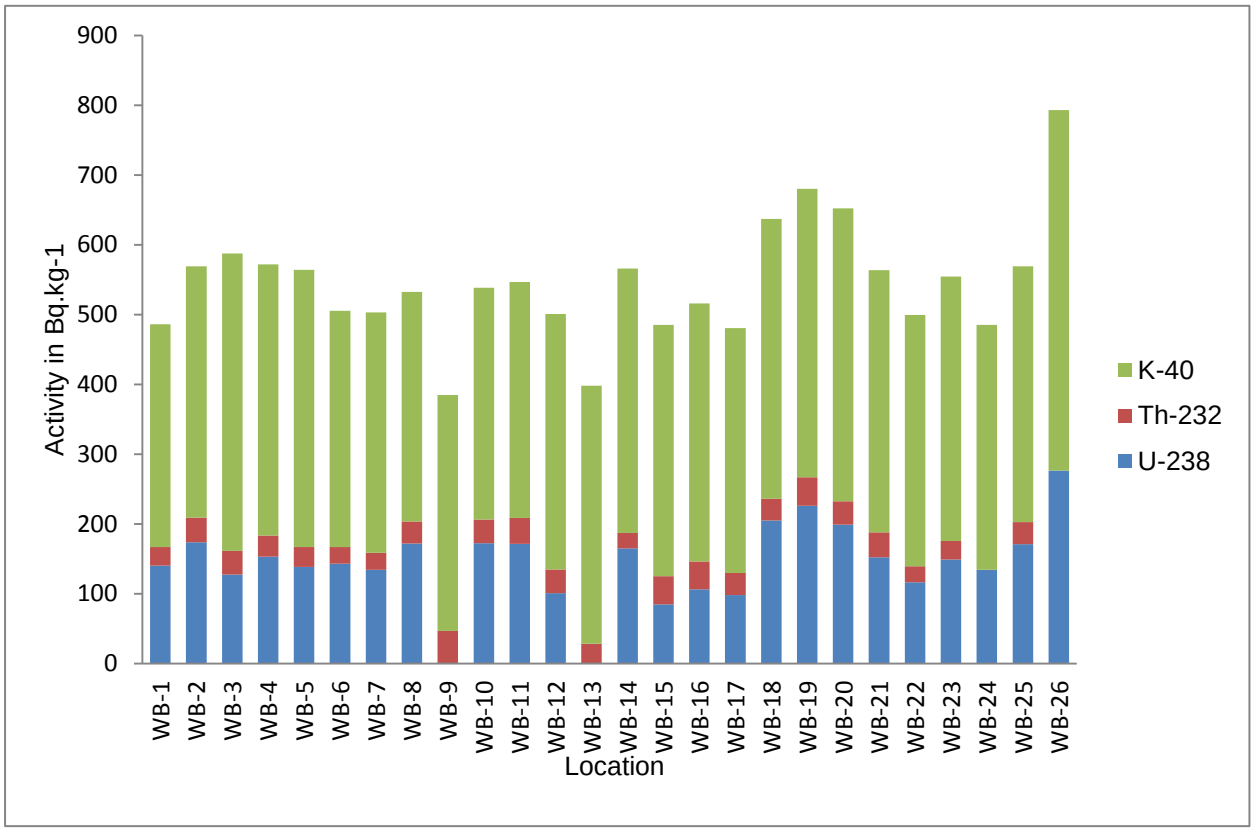

Figure 8.1: Comparison of the mean activity concentrations of ^{238}U, ^{232}Th and ^{40}K for shore sediment samples in Walvis Bay beach.

8.3 Radiological hazards in Walvis Bay beach

Radiation hazard arising from exposure to radionuclides of ^{238}U, ^{232}Th and ^{40}K were employed in the estimation of the dose assessment and human radiological risk. These were done by calculating the absorbed dose rate (ADR), the annual effective dose equivalent (AEDE), the radium equivalent activity (Ra_{eq}), external (Hex) and internal hazard index (Hin) and excess lifetime cancer risk (ELCR). The results are presented in Table 8.3-8.4 respectively.

The absorbed dose rate, ADR(nGy h^{-1}) depends on the activity concentrations of ^{238}U, ^{232}Th and ^{40}K natural radioisotopes. The absorbed dose rate was calculated using $(Eq.5.6)$ on the basis of UNSCEAR (2000) guideline and are given in Table 8.3. The absorbed dose for Walvis Bay ranged from 32.66 to 149.23 nGy. h^{-1} and the calculated mean absorbed dose was found to be 93.27 nGy.h^{-1}. According to UNSCEAR (2000), the average absorbed dose rate value in the world is ~ 51 nGy.h^{-1}. The findings from this study showed that the average absorbed dose rates from the Walvis Bay beach were much higher than the world average value (Figure 8.2). This study is comparable to similar studies undertaken by Ramasamy *et al*., (2009) in which the absorbed dose rate from Ponnaiya river sediments was found to be 73 nGy.h^{-1} and therefore the values are said to be higher than the world average (Table 8.2).

The radium equivalent activity (Ra_{eq}) is a widely used hazard index (Bereka and Mathew, 1985). This index is based on the estimation that 370 Bq.kg^{-1} of ^{226}Ra (^{238}U), 4180 Bq.kg^{-1} of ^{40}K and 259 Bq.kg^{-1} of ^{232}Th produces the same gamma ray dose rate and is expressed as given in $(Eq.5.15)$. The Ra_{eq} calculated using the mean specific concentration for Walvis Bay beach sediments are presented in Table 8.3 and a comparison with recommended value in Figure 8.3. The radium equivalent activity calculated ranged from 69.31 to 316.16 Bq.kg^{-1}. These values are lower than the recommended maximum value of 370 Bq.kg^{-1}.

Hazard Indices (H_{ex} and H_{in}) are two indices that represent the external and internal radiation hazards. These indices are calculated (Table 8.3) using $(Eq.5.16)$ and $(Eq.5.17)$ .The results are compared with safe limit and are presented as Figure 8.4-8.5. The external hazard index (H_{ex}) value ranged from 0.19 to 0.85 with an average value of 0.58 which indicated that all the sampling point are less than unity. This finding is in agreement with a similar study carried out by Oyebanjo (2012) where the H_{ex} values calculated are less than the recommended value of unity. Hence, sediment samples do not pose any significant radiation hazard when used as building component. On the other hand, H_{in} has values ranging from 0.19 to 1.60 with an average value of 0.96. Clearly, it is evident that most of the

sampling points in the Walvis Bay beach exceeded unity (Table 8.3), the limit recommended by ICRP (2000).

The annual effective dose equivalent (AEDE) received by members of the public is calculated from the absorbed dose rate by applying the dose conversion factor of 0.7 $Sv.Gy^{-1}$ and both the occupancy factors for outdoor and for indoor which are 0.2 (5/24) and 0.8 (19/24) respectively UNSCEAR, (2000). The AEDE is determined from $(Eq.5.7)$ and $(Eq.5.8)$ **.** One of the objectives of this present study is to develop a model for the occupancy factor along the coastline of the Erongo region. The calculated indoor and outdoor AEDE values using both UNSCEAR parameters and our current model are presented in Table 8.4. The mean, minimum and maximum value for outdoor and indoor using UNSCEAR factors are found to be 121.95 $\mu Sv.y^{-1}$, 40.06 $\mu Sv.y^{-1}$ and 183.01 $\mu Sv.y^{-1}$ respectively, and 487.79 $\mu Sv.y^{-1}$, 160.24 $\mu Sv.y^{-1}$ and 732.05 $\mu Sv.y^{-1}$ respectively. Using our model, the occupancy factor for the modelled current study has mean, minimum and maximum value for outdoor and indoor to be 292.60 $\mu Sv.y^{-1}$, 96.14 $\mu Sv.y^{-1}$ and 439.23 $\mu Sv.y^{-1}$ respectively and 317.06 $\mu Sv.y^{-1}$, 104.15 $\mu Sv.y^{-1}$, and 475.83 $\mu Sv.y^{-1}$, respectively. The mean values obtained for AEDE in Walvis Bay beach showed that the present values of indoor and outdoor AEDE (using UNSCEAR factor) is higher than the world average values of 70 $\mu Sv.y^{-1}$ for outdoor and 450 $\mu Sv.y^{-1}$ for indoor (Orgun *et al*., 2007). On the other hand, the modelled factor for indoor and outdoor AEDE was calculated and the mean values indicated the outdoor occupancy factor had higher values than the world average but the mean value for indoor occupancy is lower than the 450 $\mu Sv.y^{-1}$ accepted world average value.

The excess lifetime cancer risk (ELCR) is calculated using Equation 5.18.

$$ELCR = AEDE \times DL \times RF$$

Where $AEDE$ **,** DL and RF is the annual effective dose equivalent, duration of life taken to be 70 years and the risk factor (Sv^{-1}), fatal cancer risk per Sievert. The International Commission on Radiological Protection (ICRP 60) employed the values of 0.05 as the risk for the general public for stochastic effects (Taskin *et al*., 2009). The calculated values for ELCR using AEDE (UNSCEAR factors) and AEDE (Modelled factors) are quoted in Tables 8.3 and a comparison between ELCR (UNSCEAR) and ELCR (Present modelled values) shown in Figure 8.6. The mean ELCR values calculated are above the world average of 0.29×10^{-3} (Taskin *et al*., 2009). This finding did not compare favourably with a similar study by Ramasamy *et al*., (2009) where the average ELCR for all samples is less than the world average.

Table 8.3: Absorbed dose rate (ADR), Radium equivalent activity (Ra_{eq}), external hazard index (H_{ex}), internal hazard index (H_{in}) and excess lifetime cancer risk (ELCR) of studied shore sediment samples from Walvis Bay (WB) beach

Location	ADR (nGy h^{-1})	Ra_{eq} (Bq.kg^{-1})	H_{ex}	H_{in}	ELCR x 10^{-3}	
WB-1	94.25	203.14	0.55	0.93	*0.40	**1.05
WB-2	116.76	253.34	0.68	1.15	*0.50	**1.30
WB-3	97.22	208.95	0.56	0.91	*0.42	**1.09
WB-4	105.31	226.52	0.61	1.03	*0.45	**1.78
WB-5	97.64	209.53	0.57	0.94	*0.42	**1.09
WB-6	94.76	203.57	0.55	0.94	*0.41	**1.06
WB-7	91.13	195.66	0.53	0.89	*0.39	**1.02
WB-8	112.32	242.64	0.66	1.12	*0.48	**1.25
WB-9	42.30	92.80	0.25	0.25	*0.18	**0.47
WB-10	114.08	246.72	0.67	1.13	*0.49	**1.27
WB-11	115.80	250.71	0.68	1.14	*0.50	**1.29
WB-12	82.29	177.40	0.48	0.75	*0.35	**0.92
WB-13	32.66	69.31	0.19	0.19	*0.14	**0.36
WB-14	105.41	225.87	0.61	1.06	*0.45	**1.18
WB-15	78.53	170.15	0.46	0.69	*0.34	**0.88
WB-16	88.73	192.07	0.52	0.81	*0.38	**0.99
WB-17	79.18	170.63	0.46	0.73	*0.34	**0.88
WB-18	130.36	280.68	0.78	1.31	*0.56	**1.45
WB-19	146.40	316.41	0.85	1.47	*0.62	**1.63
WB-20	129.74	279.39	0.75	1.29	*0.56	**1.45
WB-21	107.56	232.22	0.63	1.04	*0.46	**1.20
WB-22	82.74	177.12	0.48	0.79	*0.36	**0.92
WB-23	100.67	216.13	0.58	0.99	*0.43	**1.12
WB-24	76.75	161.48	0.44	0.80	*0.33	**0.86
WB-25	113.45	244.59	0.66	1.12	*0.49	**1.27
WB-26	149.23	316.16	0.85	1.60	*0.64	**1.67
Mean	93.27	213.93	0.58	0.96	*0.43	**1.13
Maximum	149.23	316.16	0.85	1.60	*0.64	**1.67
Minimum	32.66	69.31	0.19	0.19	*0.14	**0.36

*calculation based on UNSCEAR values

**calculation based on present modelled factor

Table 8.4: Comparison of effective dose (μSv.y $^{-1}$) calculated using UNSCEAR and the Current modelled factor in WB beach

Location	Effective dose (μSv y $^{-1}$)			
	UNSCEAR factor		Present factor	
	Outdoor	indoor	Outdoor	indoor
WB-1	115.64	462.58	277.55	300.68
WB-2	153.20	572.80	343.68	372.32
WB-3	119.24	476.94	286.16	310.01
WB-4	129.15	516.61	308.00	335.80
WB-5	119.75	478.98	287.39	311.34
WB-6	116.21	464.85	278.91	302.15
WB-7	111.76	447.03	268.22	290.57
WB-8	137.75	551.01	330.61	358.16
WB-9	51.87	207.49	124.50	134.87
WB-10	139.91	559.63	335.78	363.76
WB-11	142.01	568.06	340.84	369.24
WB-12	100.92	403.68	242.21	262.39
WB-13	40.06	160.24	96.14	104.15
WB-14	129.28	517.12	310.27	336.13
WB-15	96.31	385.23	231.14	250.40
WB-16	108.82	435.27	261.16	282.92
WB-17	97.10	388.42	233.05	252.47
WB-18	159.87	639.48	383.69	415.66
WB-19	179.54	718.18	430.91	466.82
WB-20	159.11	636.45	381.87	413.69
WB-21	131.91	527.65	316.59	342.97
WB-22	101.47	405.88	243.53	263.82
WB-23	123.46	493.85	296.31	321.00
WB-24	94.13	376.52	225.91	244.74
WB-25	139.13	556.53	333.92	361.74
WB-26	183.01	732.05	439.23	475.83
Mean	121.95	487.79	292.60	317.06
Maximum	183.01	732.05	439.23	475.83
Minimum	40.06	160.24	96.14	104.15

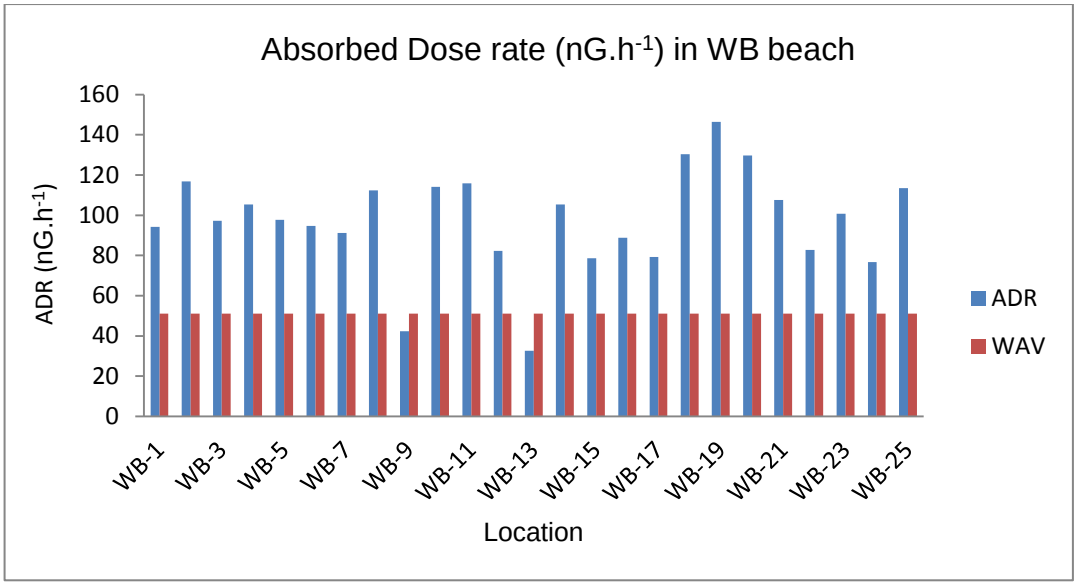

Figure 8.2: Comparison of absorbed dose rate with world average value in Walvis Bay beach.

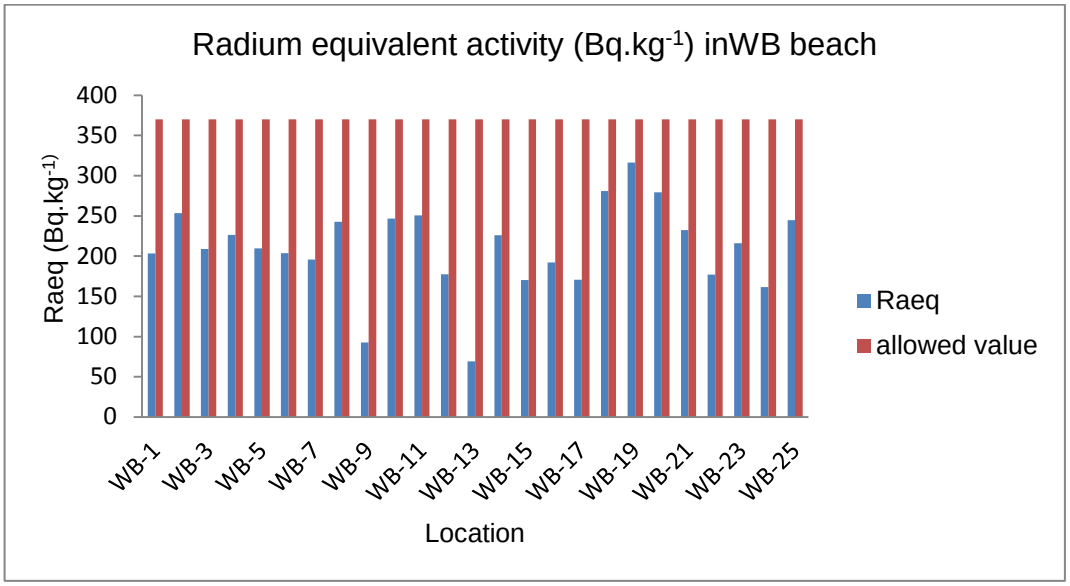

Figure 8.3: Comparison of radium equivalent activity with allowed value in Walvis Bay beach.

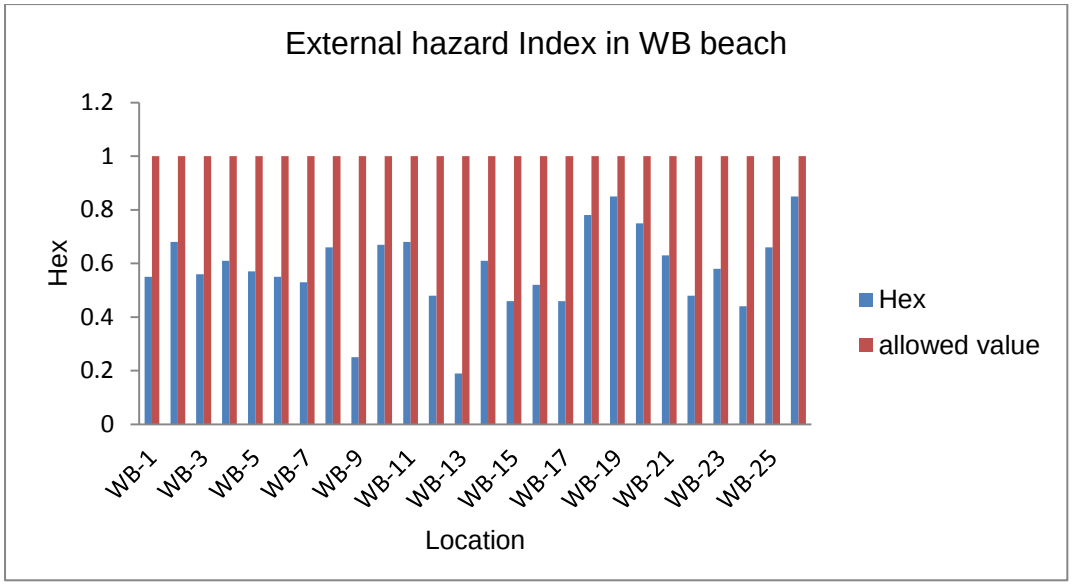

Figure 8.4: Comparison of external hazard Index with allowed value in Walvis Bay beach.

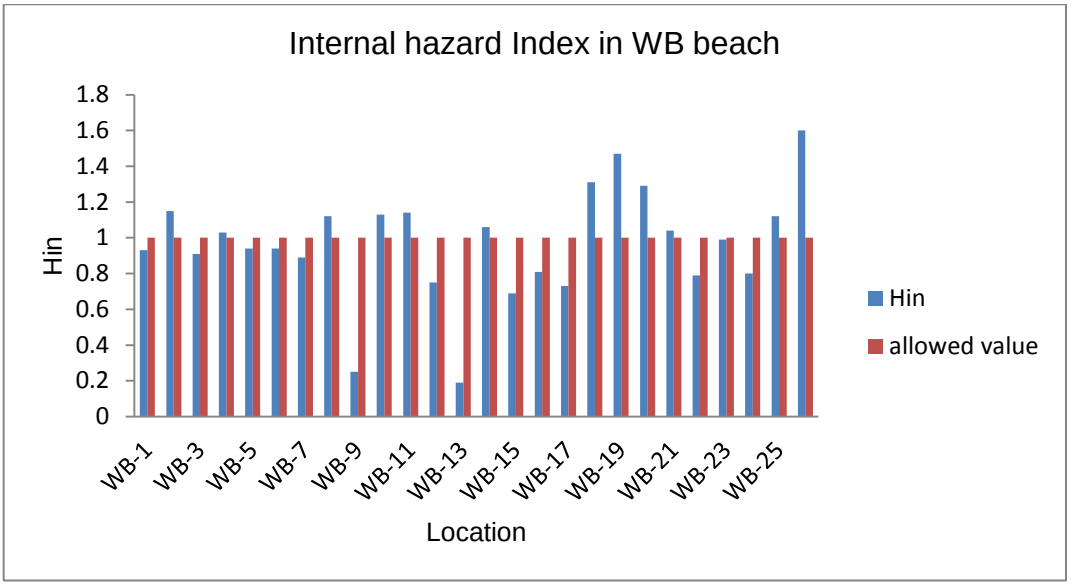

Figure 8.5: Comparison of internal hazard Index with allowed value in Walvis Bay beach.

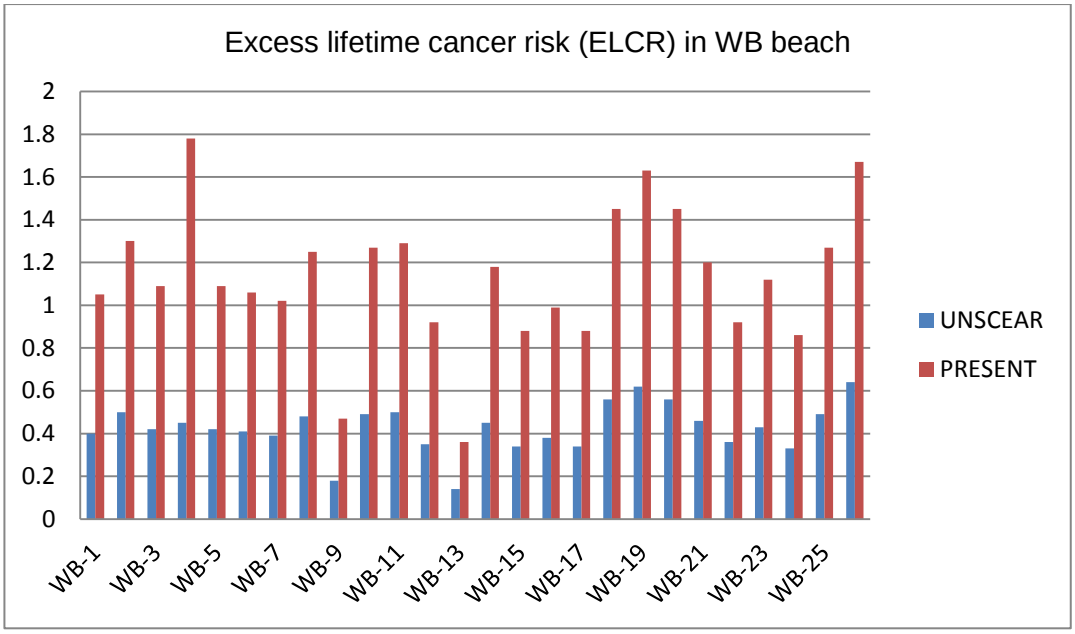

Figure 8.6: Comparison of Excess lifetime cancer risk using UNSCEAR values and the present modelled factor in Walvis Bay beach.

8.4 Activity concentration of ^{238}U, ^{232}Th, and ^{40}K in shore sediments in Swakopmund (SWK) beach

The concentrations of radionuclides in the Swakopmund beach follow a trend similar to that of the activity concentration in Walvis Bay beach. In all the sampling points in the beach of SWK, the mean specific activity concentration is in the order ^{232}Th < ^{238}U < ^{40}K (Figure 8.7).

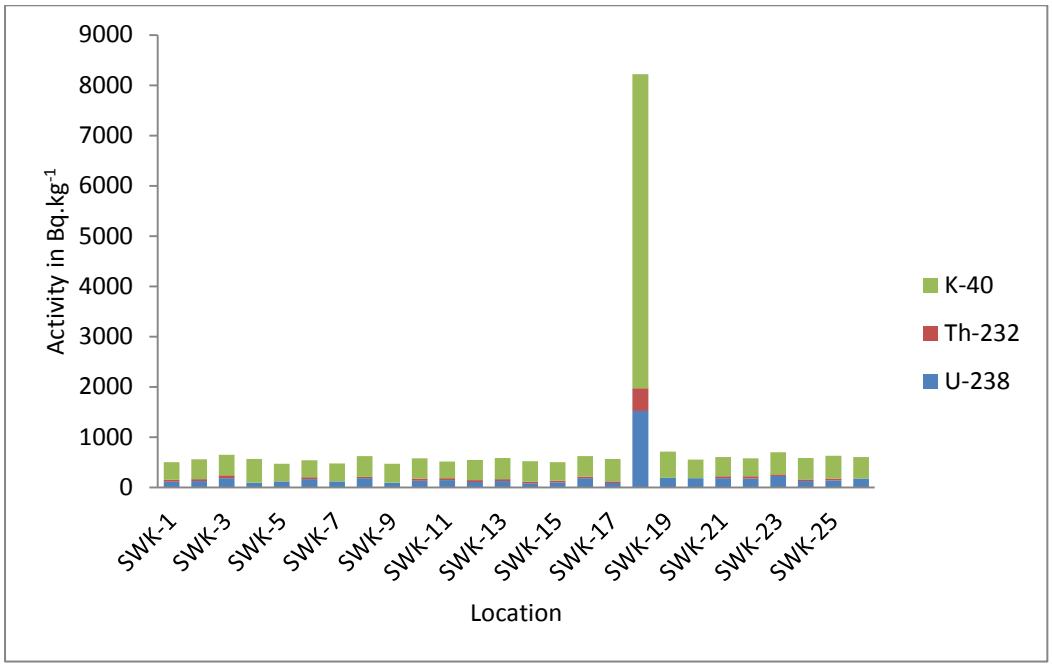

Figure 8.7: Comparison of the mean activity concentrations of ^{238}U, ^{232}Th and ^{40}K for shore sediment samples in Swakopmund beach.

^{238}U activity concentrations ranged from 88.43-1524.73 Bq.kg $^{-1}$ with a mean of 199.76 Bq.kg $^{-1}$ which is significantly higher than the world average value (50 Bq.kg $^{-1}$) (UNSCEAR, 2000). The activity concentrations of ^{238}U, ^{232}Th and ^{40}K are given in Table 8.5. The activity concentrations vary from site to site, because river and sea bottoms can exhibit large variation in chemical and mineralogical properties (Krmar *et al*., 2009). Specifically, SWK-18 has a high concentration of ^{238}U which may have been caused by the solubility and mobility of U (VI) O_2^{2+} (Powell *et al*., 2007). SWK 9, 14 and 17 recorded a low concentration of ^{238}U which may have been caused by low mineralisation and mobility of U (VI) O_2^{2+} (Powell *et al*., 2007).

^{232}Th activity concentrations ranged from BDL - 451.43 Bq.kg $^{-1}$ with a mean concentration value of 42.47 Bq.kg $^{-1}$ (Table 8.5).

Table 8.5: Mean specific activity concentration due to ^{238}U, ^{232}Th and ^{40}K in the various shore sediment samples in Swakopmund (SWK) beach

Location	^{238}U (Bq.kg $^{-1}$)	^{232}Th (Bq.kg $^{-1}$)	^{40}K (Bq.kg $^{-1}$)
SWK-1	115.84	39.31	350.56
SWK-2	133.13	33.98	394.38
SWK-3	186.73	55.99	406.90
SWK-4	100.78	BDL	466.37
SWK-5	125.35	BDL	347.43
SWK-6	169.94	38.94	331.78
SWK-7	120.78	BDL	356.82
SWK-8	185.50	28.38	410.03
SWK-9	97.69	BDL	375.60
SWK-10	138.44	41.17	400.64
SWK-11	145.98	38.20	334.91
SWK-12	111.77	36.46	400.64
SWK-13	132.76	36.70	419.42
SWK-14	88.43	29.48	406.90
SWK-15	105.84	28.22	369.34
SWK-16	188.83	28.18	406.90
SWK-17	90.65	30.65	450.72
SWK-18	1524.73	451.43	6244.35
SWK-19	191.67	BDL	525.84
SWK-20	184.26	BDL	369.34
SWK-21	187.47	40.56	381.86
SWK-22	180.31	45.88	356.82
SWK-23	233.29	31.67	438.20
SWK-24	129.06	33.01	425.68
SWK-25	142.64	36.01	453.85
SWK-26	181.92	BDL	425.68
Mean	199.76	42.47	611.19
Maximum	1524.73	451.43	6244.35
Minimum	88.43	BDL	331.78

This clearly suggests that the mean activity concentration of ^{232}Th is below the world average value of 50 Bq.kg $^{-1}$ (UNSCEAR, 2000). However, some sampling points, SWK-18, SWK-3 indicated elevated concentrations of ^{232}Th which may be indicative of the presence of monazite (Ramasamy *et al*., 2009).

^{40}K activity concentrations ranged from 331.78-6244.35 Bq.kg $^{-1}$ with a mean of 611.19 Bq.kg $^{-1}$. From Table 8.5 it is seen that all the sampling points SWK-1 to SWK-17 and SWK-19 to SWK-26 have measured values below the world average (500 Bq.kg $^{-1}$); their average was 385.86 Bq.kg $^{-1}$. The increased concentrations of SWK-18 may be due to the high content of monazite and the heterogeneous sediment characteristics (Ramasamy *et al*., 2009; Kinyua *et al*., 2011). The activity concentration of ^{238}U in this study was higher than the value (53 Bq.kg $^{-1}$) obtained by Florou and Kritidis, (1992) in similar studies in Greece. However, the concentration of ^{232}Th compare favourably with their findings (Table 8.2).

8.5 Radiological hazards in Swakopmund beach

Radiation hazard arising from exposure to radionuclides of ^{238}U, ^{232}Th and ^{40}K were employed in the estimation of the dose assessment and human radiological risk. These were done by calculating the absorbed dose rate (ADR), the annual effective dose equivalent (AEDE), the radium equivalent activity (Ra_{eq}), external (H_{ex}) and internal hazard index (H_{in}) and excess lifetime cancer risk (ELCR). The results are presented in Tables 8.6 and 8.7.

Table 8.6: Absorbed dose rate (ADR), Radium equivalent activity (Ra_{eq}), external hazard index (H_{ex}), internal hazard index (H_{in}) and excess lifetime cancer risk (ELCR) of studied shore sediment samples from Swakopmund (SWK) beach

Location	ADR (nGy h^{-1})	Ra_{eq} (Bq.kg^{-1})	H_{ex}	H_{in}	ELCR x 10^{-3}	
SWK-1	91.88	199.05	0.54	0.85	*1.58	**1.03
SWK-2	98.48	212.09	0.57	0.93	*1.69	**1.10
SWK-3	137.06	298.13	0.81	1.31	*2.35	**1.53
SWK-4	66.01	136.69	0.37	0.64	*1.13	**0.74
SWK-5	72.40	152.10	0.41	0.75	*1.24	**0.81
SWK-6	115.87	251.17	0.68	1.14	*1.99	**1.29
SWK-7	70.68	148.26	0.40	0.73	*1.21	**0.79
SWK-8	119.94	257.66	0.70	1.20	*2.06	**1.34
SWK-9	60.80	126.61	0.34	0.61	*1.04	**0.68
SWK-10	105.53	228.16	0.62	0.99	*1.81	**1.18
SWK-11	104.48	226.39	0.61	1.01	*1.80	**1.17
SWK-12	90.37	194.76	0.53	0.83	*1.55	**1.01
SWK-13	100.99	217.54	0.59	0.95	*1.73	**1.13
SWK-14	75.63	161.92	0.44	0.68	*1.30	**0.84
SWK-15	81.34	174.63	0.47	0.76	*1.40	**0.91
SWK-16	121.23	260.46	0.70	1.21	*2.08	**1.35
SWK-17	79.19	169.18	0.46	0.70	*1.36	**0.88
SWK-18	1237.49	2651.12	7.16	11.28	*21.45	**13.81
SWK-19	110.48	2.32.16	0.63	1.15	*1.90	**1.23
SWK-20	100.53	212.70	0.57	1.07	*1.73	**1.12
SWK-21	127.03	274.87	0.74	1.25	*2.18	**1.42
SWK-22	125.89	273.39	0.74	1.23	*2.16	**1.41
SWK-23	145.18	312.32	0.84	1.47	*2.49	**1.62
SWK-24	97.31	209.04	0.56	0.91	*1.67	**1.09
SWK-25	106.58	229.08	0.62	1.00	*1.83	**1.19
SWK-26	101.80	214.70	0.85	1.07	*1.75	**1.14
Mean	144.01	308.62	0.83	1.37	*2.48	**1.61
Maximum	1237.49	2651.12	7.16	11.28	*21.45	**13.81
Minimum	60.80	126.61	0.34	0.61	*1.04	**0.68

*calculation based on UNSCEAR values

**calculation based on modelled factor

Table 8.7: Comparison of effective dose (μSv.y $^{-1}$) calculated using UNSCEAR and the current modelled factor in SWK beach

Location	UNSCEAR Outdoor	UNSCEAR Indoor	Modelled Outdoor	Modelled Indoor
SWK-1	112.68	450.72	270.44	292.97
SWK-2	120.77	483.08	289.85	314.00
SWK-3	168.08	672.34	403.40	437.02
SWK-4	80.95	323.81	194.29	210.48
SWK-5	88.79	355.16	213.10	230.86
SWK-6	142.10	568.40	341.04	369.46
SWK-7	86.68	346.73	208.04	225.37
SWK-8	147.10	588.38	353.03	382.45
SWK-9	74.56	298.24	178.94	193.85
SWK-10	129.43	517.70	310.62	336.51
SWK-11	128.14	512.54	307.53	333.15
SWK-12	110.83	443.30	265.98	288.15
SWK-13	123.86	495.43	297.26	322.03
SWK-14	92.75	371.00	222.60	241.15
SWK-15	99.76	399.04	239.43	259.38
SWK-16	148.67	594.70	356.82	386.55
SWK-17	97.12	388.46	233.08	252.50
SWK-18	1517.66	6070.63	3642.38	2945.91
SWK-19	135.49	541.97	325.18	352.28
SWK-20	123.29	493.16	295.89	320.55
SWK-21	155.79	623.17	373.90	405.06
SWK-22	154.40	617.59	370.55	401.43
SWK-23	178.05	712.20	427.32	462.93
SWK-24	119.35	477.39	286.43	310.30
SWK-25	130.70	522.82	313.69	339.83
SWK-26	124.84	499.38	299.63	324.60
Mean	176.61	706.44	413.63	420.72
Maximum	1517.66	6070.63	3642.38	2945.91
Minimum	74.56	298.24	178.94	193.51

The absorbed dose rate (nGy h $^{-1}$) depends on the activity concentrations of ^{238}U, ^{232}Th and ^{40}K natural radioisotopes. The absorbed dose rates were calculated using $(Eq.5.6)$ on the basis of UNSCEAR (2000) guidelines and are given in Table 8.6. Figure 8.8 gives a comparison with world recommended limit.

The absorbed dose rate for Swakopmund beach ranged from 60.80 to 1237.49 nGy. h $^{-1}$ with a mean of 144.01 nGy.h $^{-1}$. The mean absorbed dose rate is found to be 2.82 times the world average value of 51 nGy.h $^{-1}$ (UNSCEAR, 2000). The results from this study are not comparable to those of similar studies undertaken by Ramasamy *et al*., (2009) in which

absorbed dose rates from Tamilnadu beach sediments were found to be 0.59 times the world average.

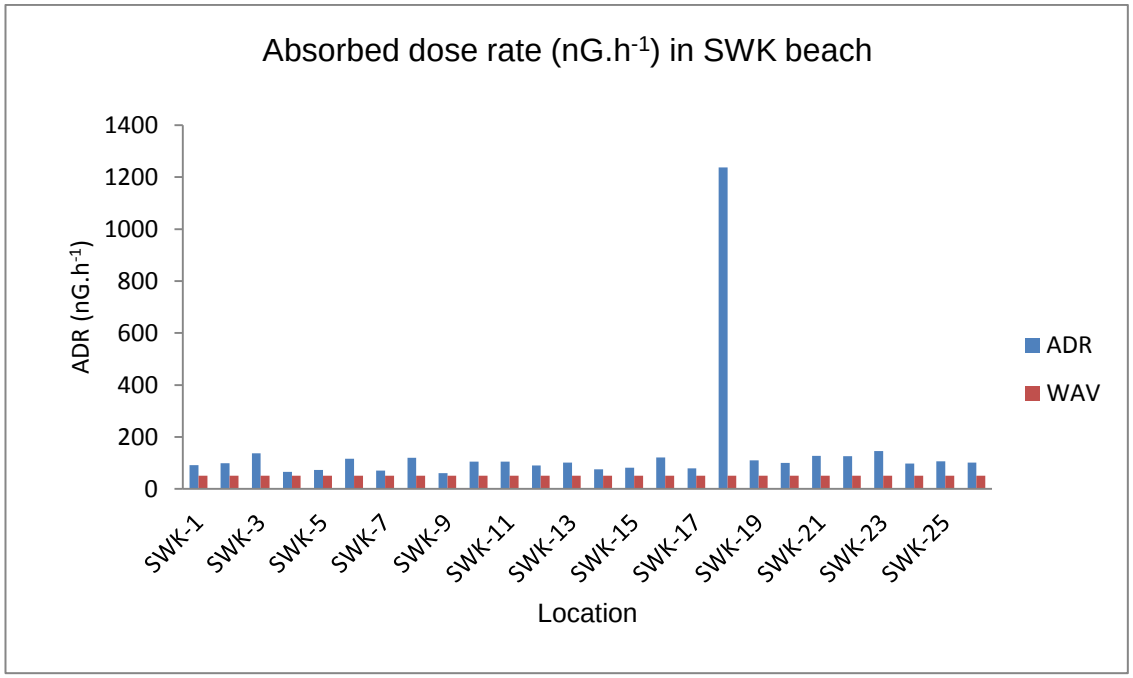

Figure 8.8: Comparison of absorbed dose rate with world average value in Swakopmund beach.

The calculated values of radium equivalent activity (Ra_{eq}) showed radiation hazards from the all sediment samples collected from Swakopmund beach. These values are presented in Table 8.6. The maximum, minimum and mean values obtained are 2651 Bq.kg $^{-1}$, 126 Bq.kg $^{-1}$ and 308.62 Bq.kg $^{-1}$. This study shows that the mean values of Ra_{eq} are below the world allowed value of 370 Bq.kg $^{-1}$ (Figure 8.9). This finding is in agreement with the study by Amekudzie *et al*., (2011) in the assessment of natural radionuclides and dose assessment arising from shore sediments collected from the coast of Greater Accra, Ghana.

The external hazard index (H_{ex}) value ranged from 0.34 to 7.16 with an average value of 0.83 (Table 8.6). The values at all the sampling points are less than unity (Figure 8.10). However, SWK-18 had an elevated H_{ex} (7.16). This finding is in agreement with a similar study carried out by Oyebanjo *et al*., (2012) where the H_{ex} values calculated are less than the recommended value of unity. Hence, sediment samples do not pose any significant radiation hazard when used as building component. On the other hand, H_{in} has values ranging from 0.61 to 11.28 with an average value of 1.37. This study reveals that most of the sampling points in the Swakopmund beach exceeded unity with respect to H_{in} (Table 8.6). This implies that activities involving the use of Swakopmund beach sediments are not safe

when compared with acceptable limit (Figure 8.11) and may result in internal radiation exposure.

The calculated indoor and outdoor annual effective dose equivalent (AEDE) values using both UNSCEAR and the modelled current study are listed in Table 8.7. The mean, minimum and maximum values for outdoor and indoor using UNSCEAR factors are found to be 176.61 $\mu Sv.y^{-1}$, 74.56 $\mu Sv.y^{-1}$ and 1517.66 $\mu Sv.y^{-1}$ respectively for outdoor and 706.44 $\mu Sv.y^{-1}$, 298.24 $\mu Sv.y^{-1}$ and 6070.63 $\mu Sv.y^{-1}$ respectively for indoor. The occupancy factor for the modelled current study has mean, minimum and maximum values for outdoor and indoor to be 413.63 $\mu Sv.y^{-1}$, 178.94 $\mu Sv.y^{-1}$ and 3642.38 $\mu Sv.y^{-1}$ respectively and 420.72 $\mu Sv.y^{-1}$, 193.51 $\mu Sv.y^{-1}$, and 2945.91 $\mu Sv.y^{-1}$ respectively. The mean values obtained for AEDE in Swakopmund beach showed that the present values of indoor and outdoor AEDE (using UNSCEAR factor) is higher than the world average values (70 $\mu Sv.y^{-1}$ for outdoor, 450 $\mu Sv.y^{-1}$ for indoor) (Orgun *et al*., 2007). On the other hand, the modelled factor for indoor and outdoor AEDE was calculated and the mean values indicated the outdoor occupancy factor had higher values than the world average but the mean value for indoor occupancy is lower than the 450 $\mu Sv.y^{-1}$ acceptable world average value.

The calculated values for ELCR using AEDE (UNSCEAR factors) and AEDE (Modelled factors) are listed in Tables 8.7 and a comparison between ELCR (UNSCEAR) and ELCR (Present modelled value) is in Figure 8.14. The mean ELCR values calculated are above the world average of 0.29×10^{-3} (Taskin *et al*., 2009). This finding did not compare favourably with a similar study by Ramasamy *et al*., (2009) where the average ELCR for all samples is less than the world average.

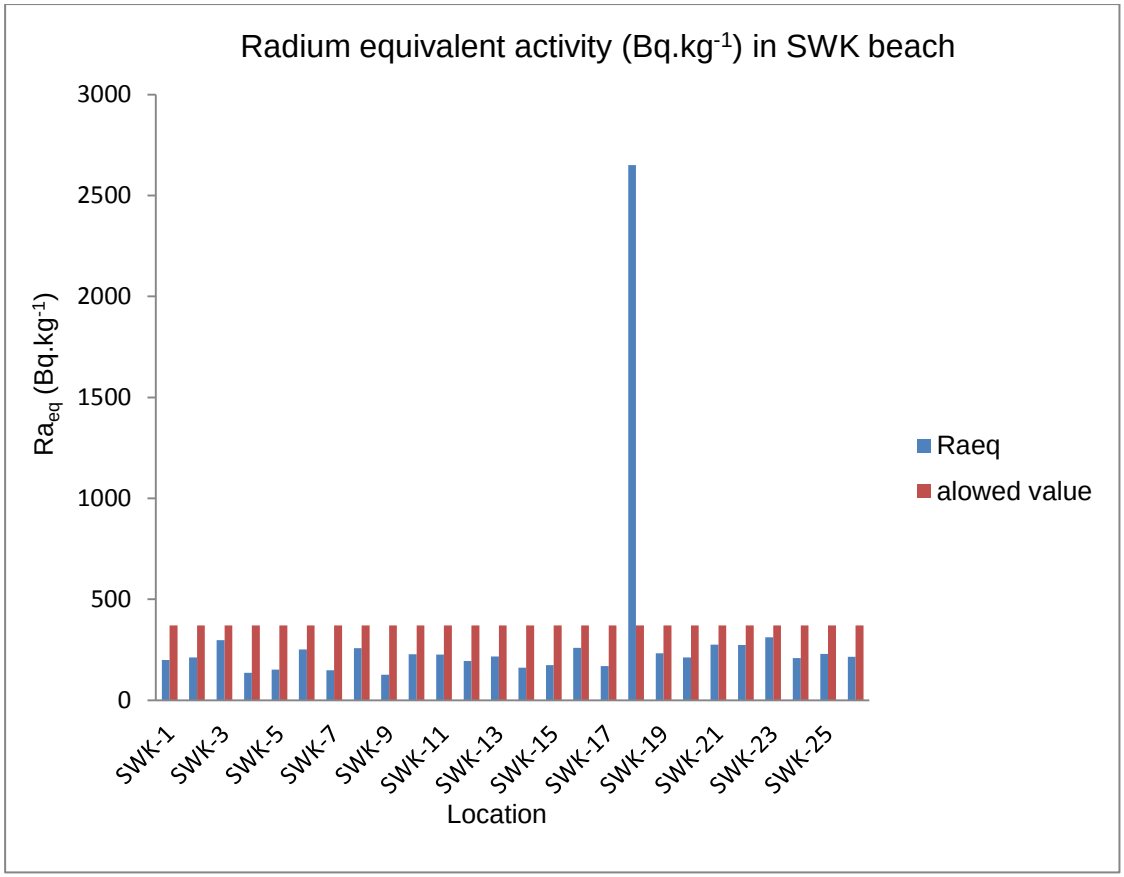

Figure 8.9: Comparison of radium equivalent activity with world allowed value in Swakopmund beach.

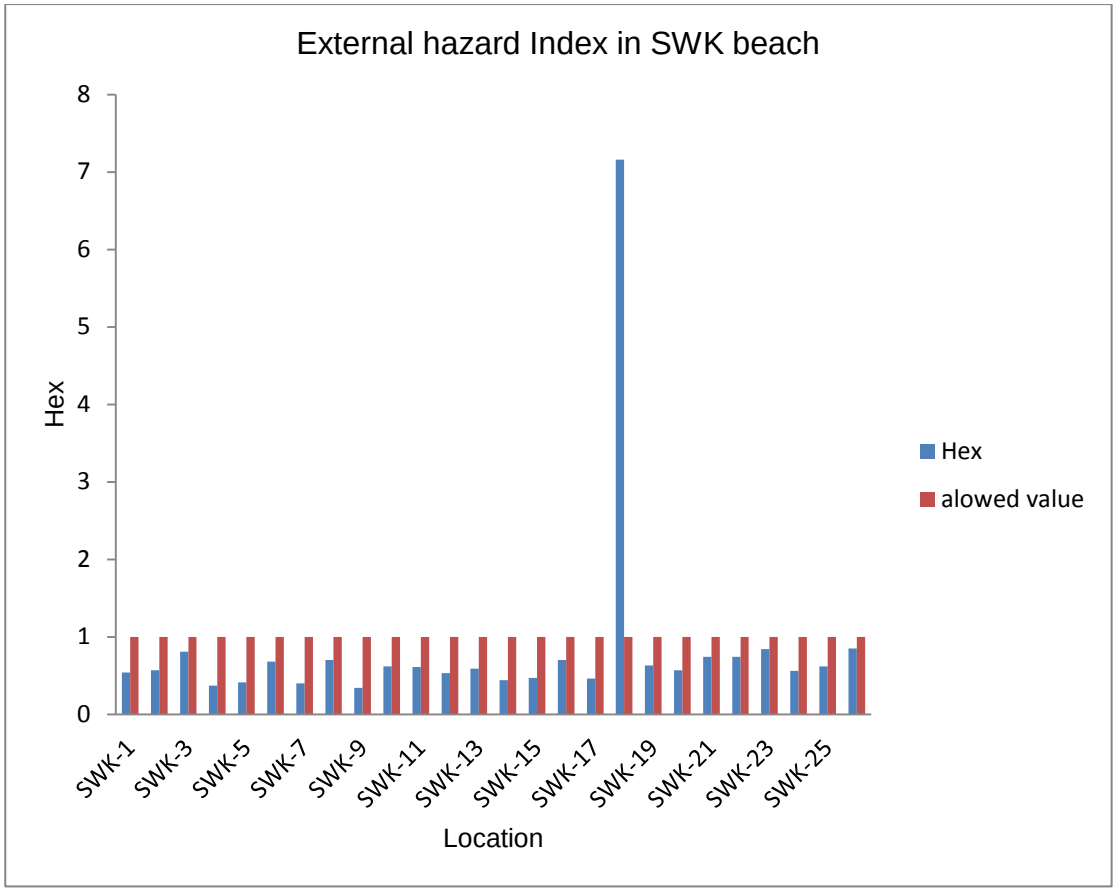

Figure 8.10: Comparison of external hazard Index with allowed value in Swakopmund beach.

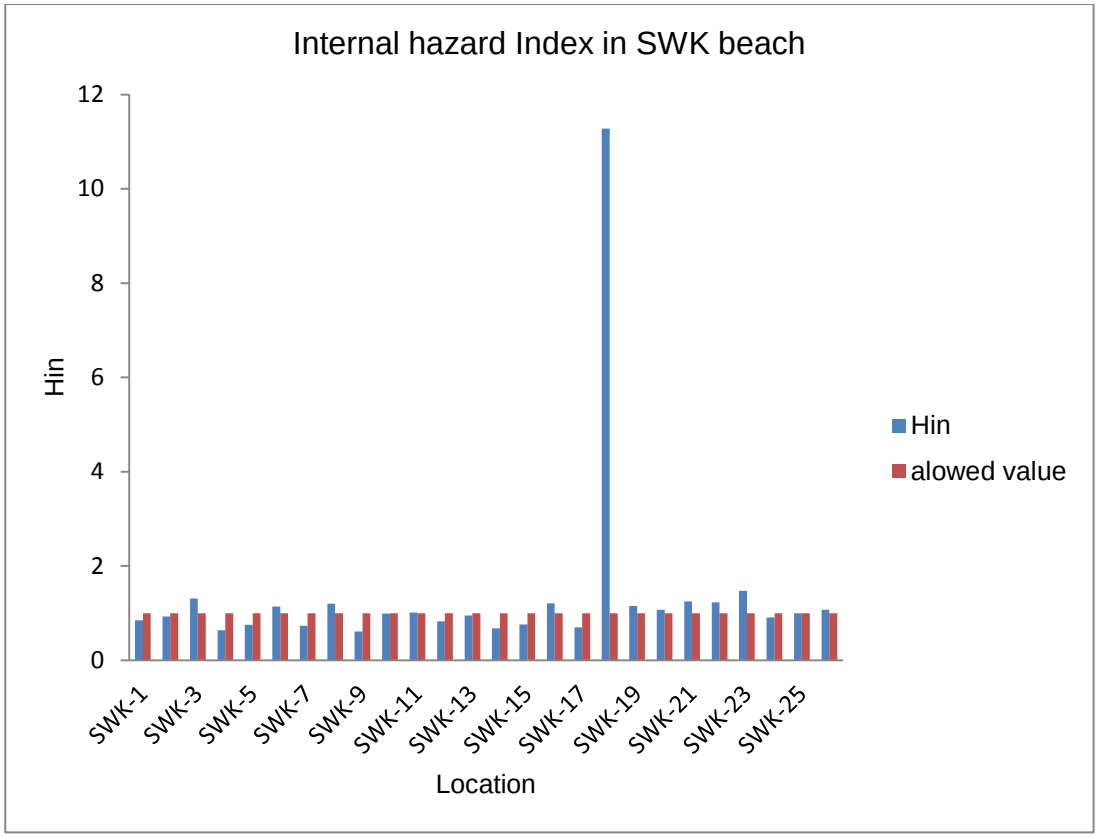

Figure 8.11: Comparison of internal hazard Index with allowed value in Swakopmund beach.

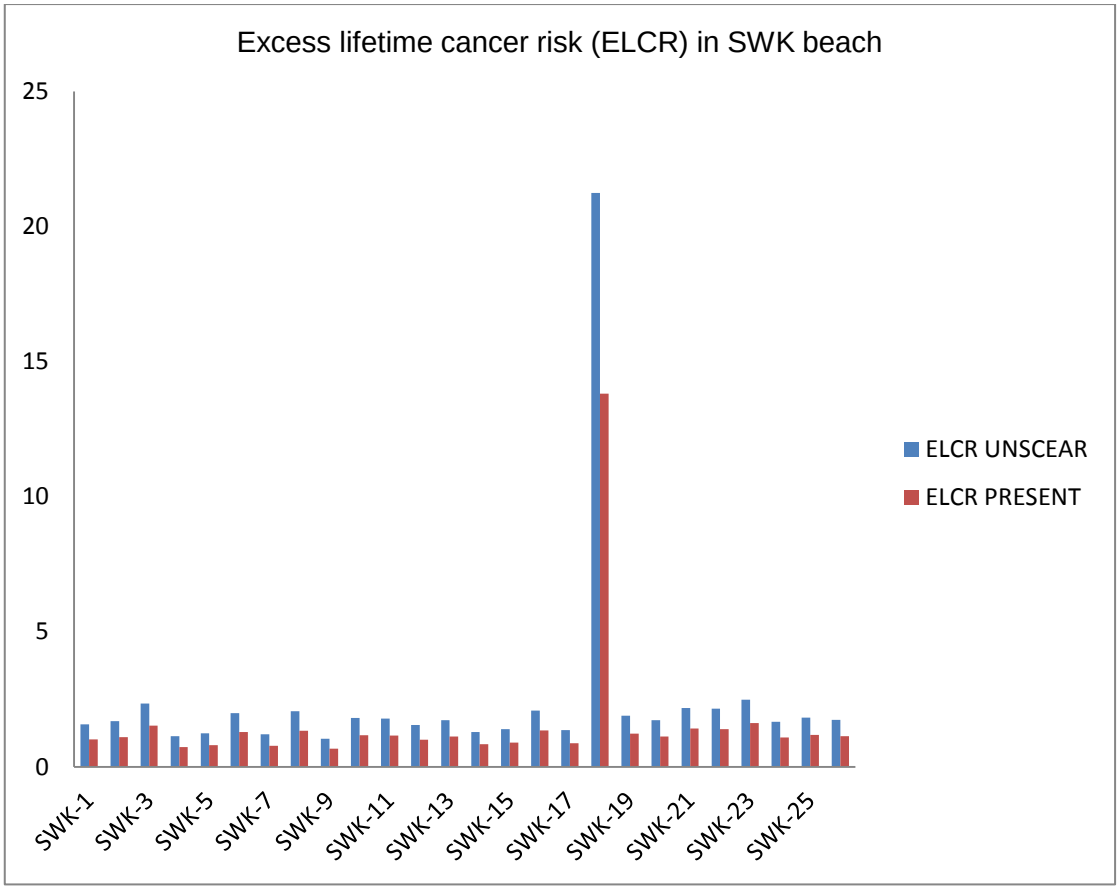

Figure 8.12: Comparison of Excess lifetime cancer risk using UNSCEAR values and the Present modelled values from Swakopmund beach.

8.6 Activity concentration of ^{238}U, ^{232}Th, and ^{40}K in shore sediments in Henties Bay (HB) beach

The results of the specific activity concentration of ^{238}U, ^{232}Th and ^{40}K radionuclides in the beach shore sediment samples for 26 sampling points in Henties Bay are presented in Table 8.8. The mean activity concentration is in the order ^{232}Th < ^{238}U < ^{40}K (Figure 8.13). The measured activity concentrations range from 25.32 - 232.43 Bq.kg $^{-1}$ for ^{238}U with a mean of 176.44 Bq.kg $^{-1}$, BDL – 77.99 Bq.kg $^{-1}$ for ^{232}Th with a mean of 41.16 Bq.kg $^{-1}$ and 247.25 – 482.02 Bq.kg $^{-1}$ for ^{40}K with a mean of 354.38 Bq.kg $^{-1}$. The mean activity concentration for ^{232}Th and ^{40}K are below the world average values (50 Bq.kg $^{-1}$ and 500 Bq.kg $^{-1}$). However, at some sampling points, the concentration of ^{232}Th is higher than the world average value, which is indicative of the presence of monazite (Ramasamy *et al*., 2009). The mean activity concentration of ^{238}U was found to be 3.53 times the world average value (500 Bq.kg $^{-1}$).

Table 8.8: Mean specific activity concentration due to ^{238}U, ^{232}Th and ^{40}K in the various shore sediment samples in Henties Bay (HB) beach

Location	^{238}U (Bq.kg $^{-1}$)	^{232}Th (Bq.kg $^{-1}$)	^{40}K (Bq.kg $^{-1}$)
HB-1	112.63	45.80	334.91
HB-2	229.46	77.99	294.22
HB-3	211.19	52.74	294.22
HB-4	175.12	40.44	350.56
HB-5	199.58	35.81	384.99
HB-6	206.86	69.55	341.17
HB-7	184.76	22.74	353.69
HB-8	169.81	27.20	359.95
HB-9	147.34	25.25	338.04
HB-10	25.32	29.92	353.69
HB-11	197.48	53.06	325.52
HB-12	232.55	56.72	344.30
HB-13	123.38	BDL	391.25
HB-14	143.51	33.86	400.64
HB-15	214.15	66.54	247.27
HB-16	150.92	39.14	334.19
HB-17	232.43	63.42	322.39
HB-18	154.25	34.10	425.68
HB-19	218.10	BDL	482.02
HB-20	183.03	29.07	413.16
HB-21	197.35	56.68	322.39
HB-22	115.47	29.92	363.08
HB-23	152.15	35.93	359.95
HB-24	222.67	50.91	331.78
HB-25	206.12	59.89	363.08
HB-26	155.86	33.41	381.86
Mean	176.44	41.16	354.38
Maximum	232.43	77.99	482.02
Minimum	25.32	BDL	247.25

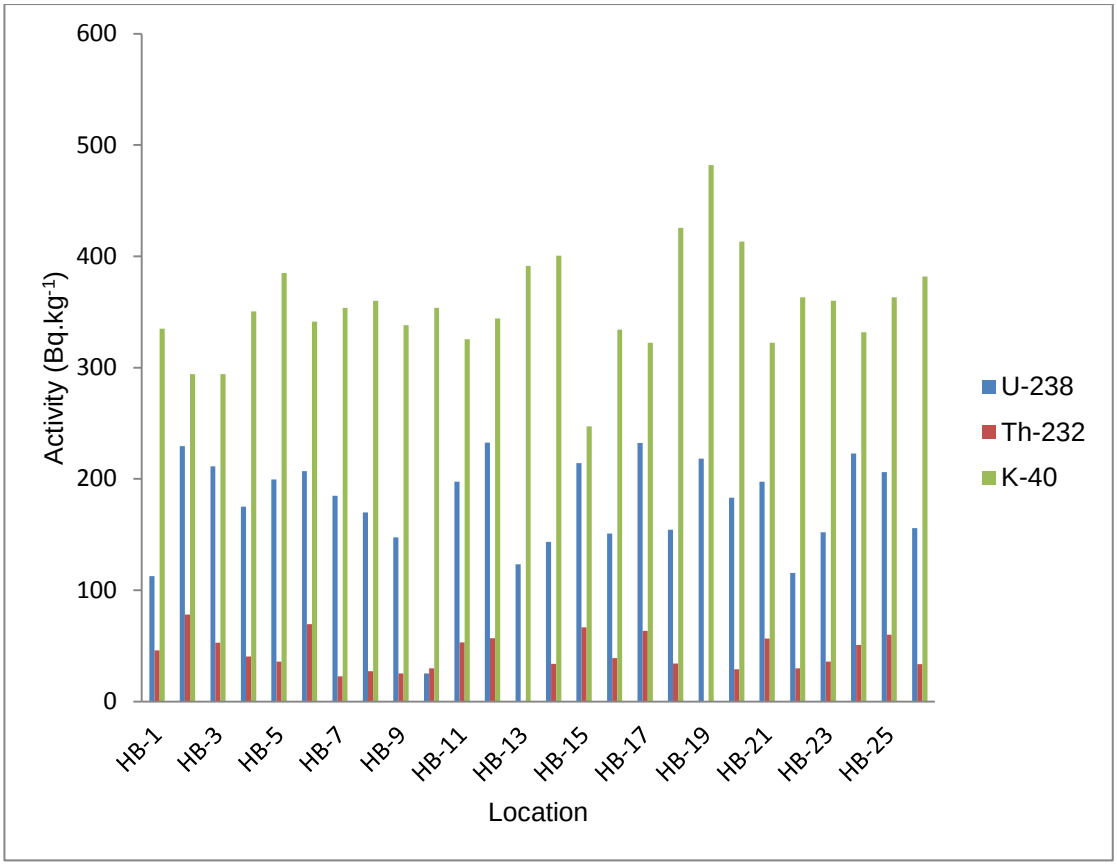

Figure 8.13: Comparison of the mean activity concentrations of ^{238}U, ^{232}Th and ^{40}K for shore sediment samples in Henties Bay beach.

8.7 Radiological Hazards in Henties Bay beach

The absorbed dose rate for HB beach ranges from 29 – 155.16 nGy.h $^{-1}$ with the highest dose rate corresponding to HB-10 and the lowest dose rate associated with HB-2 (Table 8.9). The calculated mean absorbed dose of 105.95 nGy.h $^{-1}$ is higher than the world average value (51 nGy.h $^{-1}$) (Figure 8.14) (UNSCEAR, 2000). A study by Taskin *et al*., (2009) indicated an average outdoor terrestrial gamma dose rate of 60 nGy.h $^{-1}$ in the world with a range from 10 – 200 nGy.h $^{-1}$. This present study therefore has a dose rate 2.08 times the world safe values.

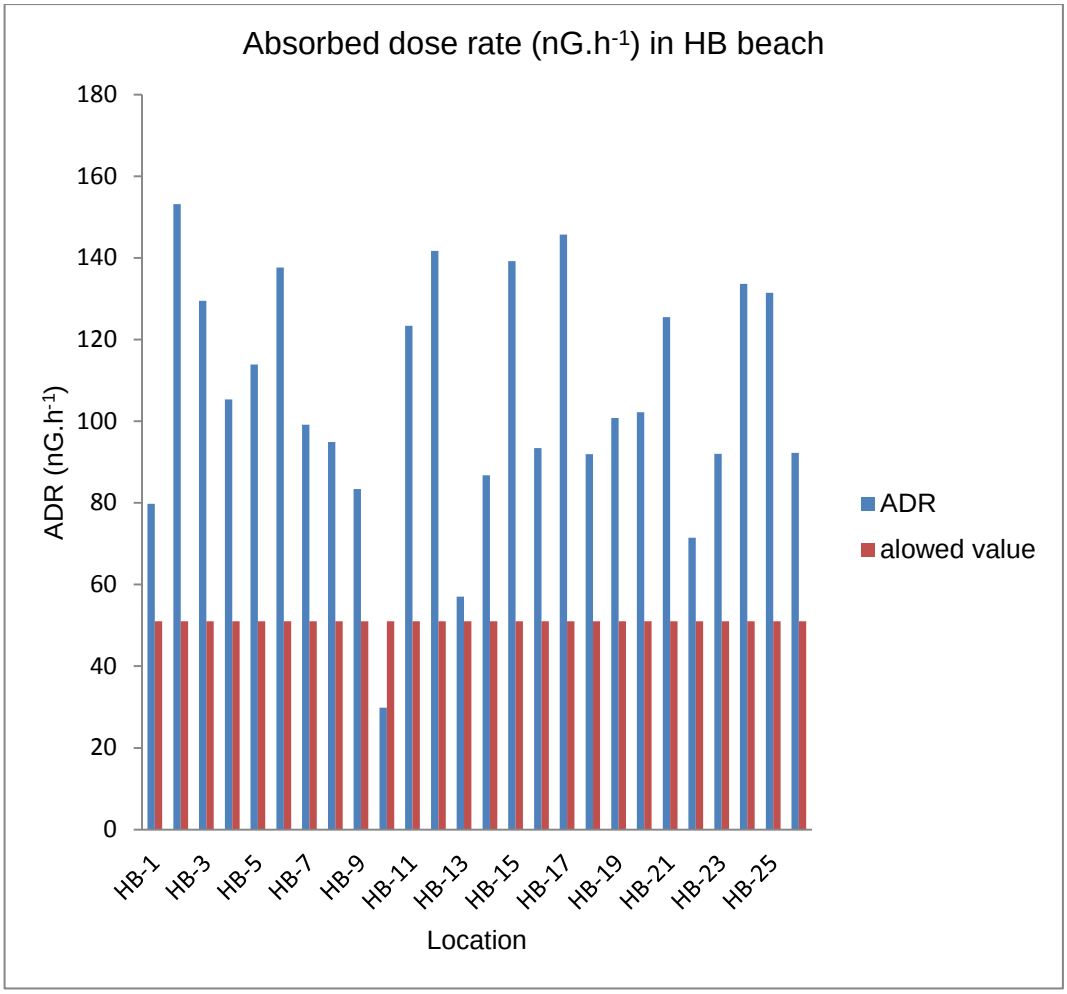

Figure 8.14: Comparison of absorbed dose rate with world allowed value in Henties Bay beach.

The radium equivalent activities (Ra_{eq}) of the shore sediment samples from HB beach were calculated on the basis of $(Eq.5.15)$ and are presented in Table 8.9 and the values obtained were compared with world recommended value presented as Figure 8.15.

Table 8.9: Absorbed dose rate (ADR), Radium equivalent activity (Ra_{eq}), external hazard index (H_{ex}), internal hazard index (H_{in}) and excess lifetime cancer risk (ELCR) of studied shore sediment samples from Henties Bay (HB) beach

Location	ADR (nGy h^{-1})	Ra_{eq} (Bq.kg^{-1})	H_{ex}	H_{in}	ELCR x 10^{-3}	
HB-1	79.74	203.91	0.55	0.86	*0.34	**0.82
HB-2	153.16	363.64	0.98	1.60	*0.66	**1.58
HB-3	129.47	309.26	0.84	1.41	*0.56	**1.33
HB-4	105.37	259.94	0.70	1.18	*0.45	**1.09
HB-5	113.88	280.43	0.76	1.30	*0.49	**1.17
HB-6	137.62	332.59	0.90	1.46	*0.59	**1.42
HB-7	99.14	244.51	0.66	1.16	*0.43	**1.02
HB-8	94.92	236.42	0.64	1.10	*0.41	**0.98
HB-9	83.36	209.48	0.57	0.96	*0.36	**0.56
HB-10	29.81	95.34	0.26	0.33	*0.13	**0.31
HB-11	123.33	298.42	0.81	1.34	*0.53	**1.27
HB-12	141.74	340.17	0.92	1.55	*0.61	**1.46
HB-13	57.04	153.51	0.41	0.75	*0.24	**0.59
HB-14	86.79	222.78	0.60	0.99	*0.37	**0.84
HB-15	139.17	238.34	0.89	1.47	*0.60	**1.43
HB-16	93.41	232.62	0.63	1.04	*0.40	**0.96
HB-17	145.73	347.94	0.94	1.57	*0.63	**1.50
HB-18	91.90	235.79	0.64	1.05	*0.39	**0.95
HB-19	100.80	255.22	0.69	1.28	*0.43	**1.04
HB-20	102.16	256.41	0.69	1.19	*0.44	**1.05
HB-21	125.45	303.23	0.82	1.35	*0.54	**1.29
HB-22	71.46	186.21	0.50	0.82	*0.31	**0.74
HB-23	92.04	231.24	0.62	1.04	*0.40	**0.95
HB-24	133.66	321.02	0.67	1.47	*0.57	**1.38
HB-25	131.44	319.72	0.86	1.42	*0.56	**1.35
HB-26	92.23	233.04	0.63	1.05	*0.40	**0.95
Mean	105.95	261.58	0.70	1.18	*0.44	**1.08
Maximum	153.16	363.64	0.98	1.60	*0.66	**1.58
Minimum	29.81	95.34	0.26	0.33	*0.13	**0.31

*calculation based on UNSCEAR values

**calculation based on modelled factor

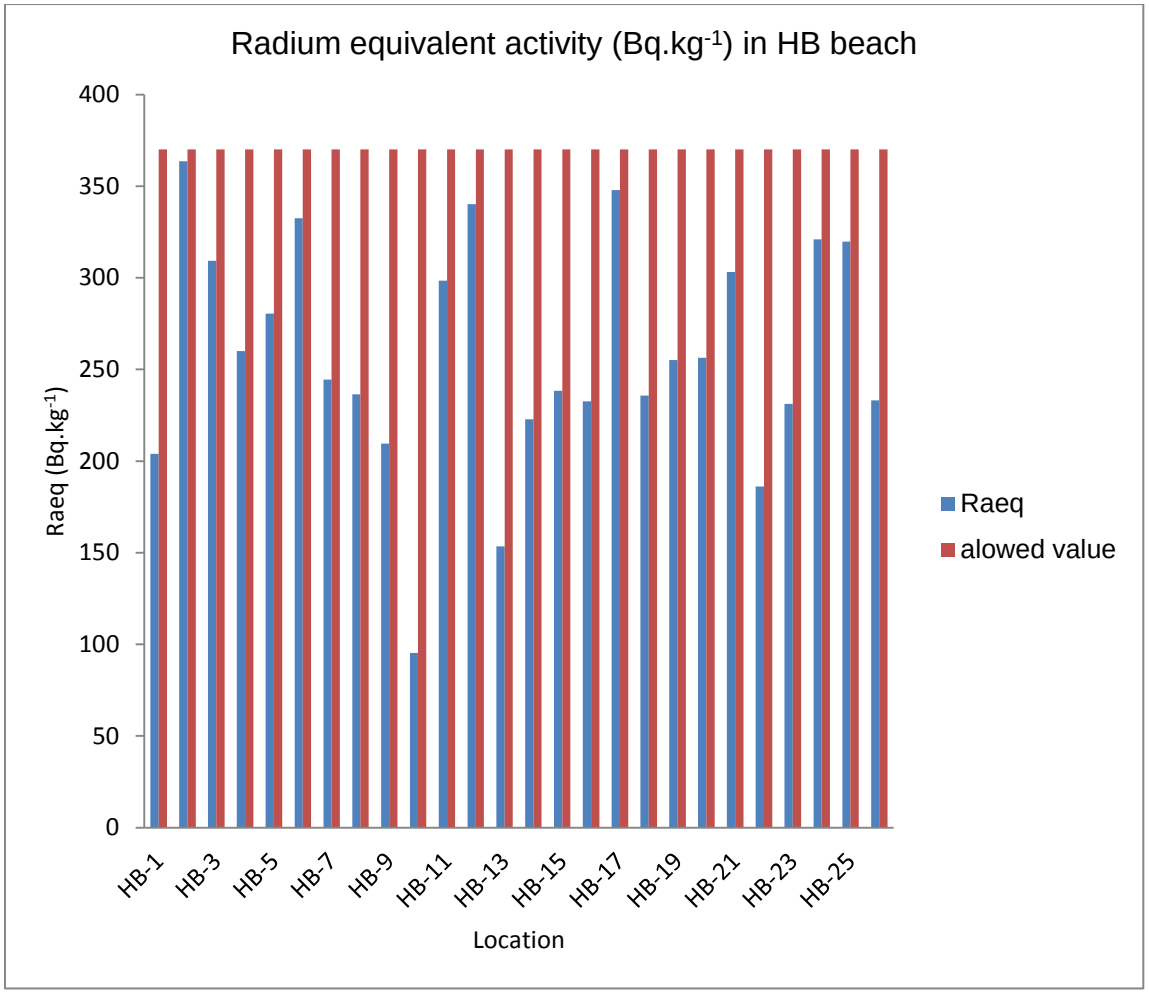

Figure 8.15: Comparison of radium equivalent activity with world allowed value in Henties Bay.

For all the shore sediment samples under investigation, the radium equivalent values are lower than the world acceptable value 370 Bq.kg $^{-1}$ ranging from 95.34 – 363.64 Bq.kg $^{-1}$.

The external hazard index (H_{ex}) value ranged from 0.26 to 0.98 with an average value of 0.0.70 (Table 8.9) which indicated that all the sampling point are less than unity (Figure 8.16).

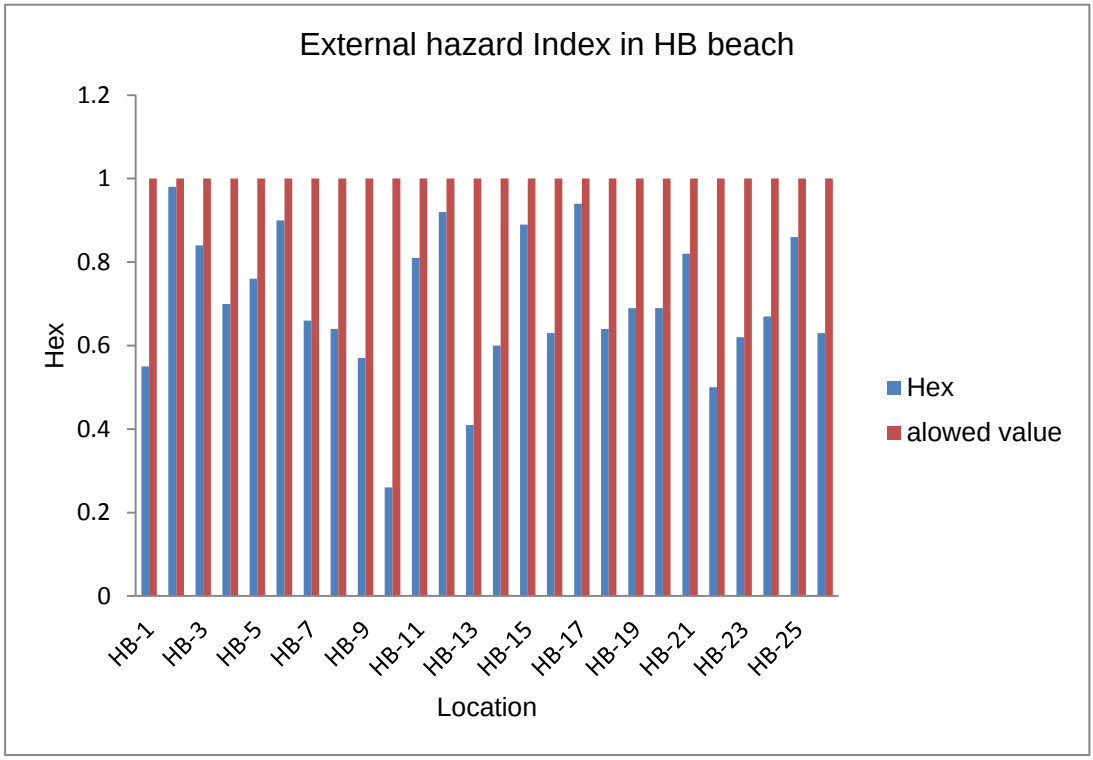

Figure 8.16: Comparison of external hazard Index with allowed value in Henties Bay.

This finding is in agreement with the findings in SWK beach, and also from similar studies undertaken by Oyebanjo *et al*., (2012) in Osun, Nigeria, where the H_{ex} values calculated are less than the recommended value of unity. Hence, like the sediment samples from SWK beach, the HB beach do not pose any significant radiation hazard when used as building component. On the other hand, H_{in} has value ranging from 0.33 to 1.60 with an average value of 1.18. This study reveals that most of the sampling points in the Henties Bay beach exceeded unity with respect to H_{in} (Table 8.9). This implies that activities involving the use of shore sediments are not safe and may result to internal radiation exposure.

The calculated indoor and outdoor annual effective dose equivalent (AEDE) values using both UNSCEAR and the modelled current study are listed in Table 8.10. The mean, minimum and maximum value for outdoor and indoor using UNSCEAR factors are found to be 129.94 $\mu Sv.y^{-1}$, 36.56 $\mu Sv.y^{-1}$ and 187.83 $\mu Sv.y^{-1}$, respectively and 519.77 $\mu Sv.y^{-1}$, 146.24 $\mu Sv.y^{-1}$ and 751.33 $\mu Sv.y^{-1}$, respectively. Using our model, the occupancy factor for the modelled current study has mean, minimum and maximum values of 311.80 $\mu Sv.y^{-1}$, 87.75 $\mu Sv.y^{-1}$ and 450.80 $\mu Sv.y^{-1}$ respectively for outdoor and 337.85 $\mu Sv.y^{-1}$, 95.06 $\mu Sv.y^{-1}$, and 488.37 $\mu Sv.y^{-1}$, respectively for indoor. The mean values obtained for AEDE in Swakopmund beach showed that the present values of indoor and outdoor AEDE (using

UNSCEAR factor) is higher than the world average values (70 μSv.y^{-1} for outdoor, 450 μSv.y^{-1} for indoor) (Orgun *et al*., 2007). On the other hand, the modelled factor for indoor and outdoor AEDE was calculated and the mean values indicated the outdoor occupancy factor had higher values than the world average but the mean value for indoor occupancy is lower than the 450 μSv.y^{-1} acceptable world average value.

The calculated values for ELCR using AEDE (UNSCEAR factors) and AEDE (Modelled factors) are listed in Tables 8.9 and a comparison between ELCR (UNSCEAR) and ELCR (Present modelled value) presented in Figure 8.18. The mean ELCR values calculated are above the world average of 0.29 x 10^{-3} (Taskin *et al*., 2009). This finding did not compare favourably with a similar study by Ramasamy *et al*., (2009) where the average ELCR for all samples is less than the world average.

Table 8.10: Comparison of effective dose (μSv.y $^{-1}$) calculate using UNSCEAR and the current modelled factor in HB beach.

Location	UNSCEAR Outdoor	UNSCEAR Indoor	modelled Outdoor	modelled Indoor
HB-1	97.79	391.17	234.70	254.26
HB-2	187.83	751.33	450.80	488.37
HB-3	158.78	635.11	381.07	412.82
HB-4	129.23	516.92	310.15	336.00
HB-5	139.66	558.63	335.18	363.11
HB-6	168.78	675.10	405.06	438.82
HB-7	121.58	486.32	291.79	316.11
HB-8	116.41	465.65	279.39	302.67
HB-9	102.24	408.95	245.37	265.82
HB-10	36.56	146.24	87.75	95.06
HB-11	151.25	604.99	362.99	393.24
HB-12	173.83	695.31	417.19	451.95
HB-13	69.96	279.83	167.90	181.89
HB-14	106.45	425.78	255.47	276.76
HB-15	170.68	682.71	409.62	443.76
HB-16	114.55	458.22	274.93	297.84
HB-17	178.72	714.89	428.94	464.68
HB-18	112.71	450.83	270.50	293.04
HB-19	123.63	494.50	296.70	321.43
HB-20	125.29	501.16	300.69	325.75
HB-21	153.85	615.42	369.25	400.02
HB-22	87.64	350.56	210.33	227.86
HB-23	112.87	451.50	270.90	293.47
HB-24	163.93	655.71	393.42	426.21
HB-25	161.20	644.81	386.88	419.12
HB-26	113.11	452.44	271.46	294.08
Mean	129.94	519.77	311.86	337.85
Maximum	187.83	751.33	450.80	488.37
Minimum	36.56	146.24	87.75	95.06

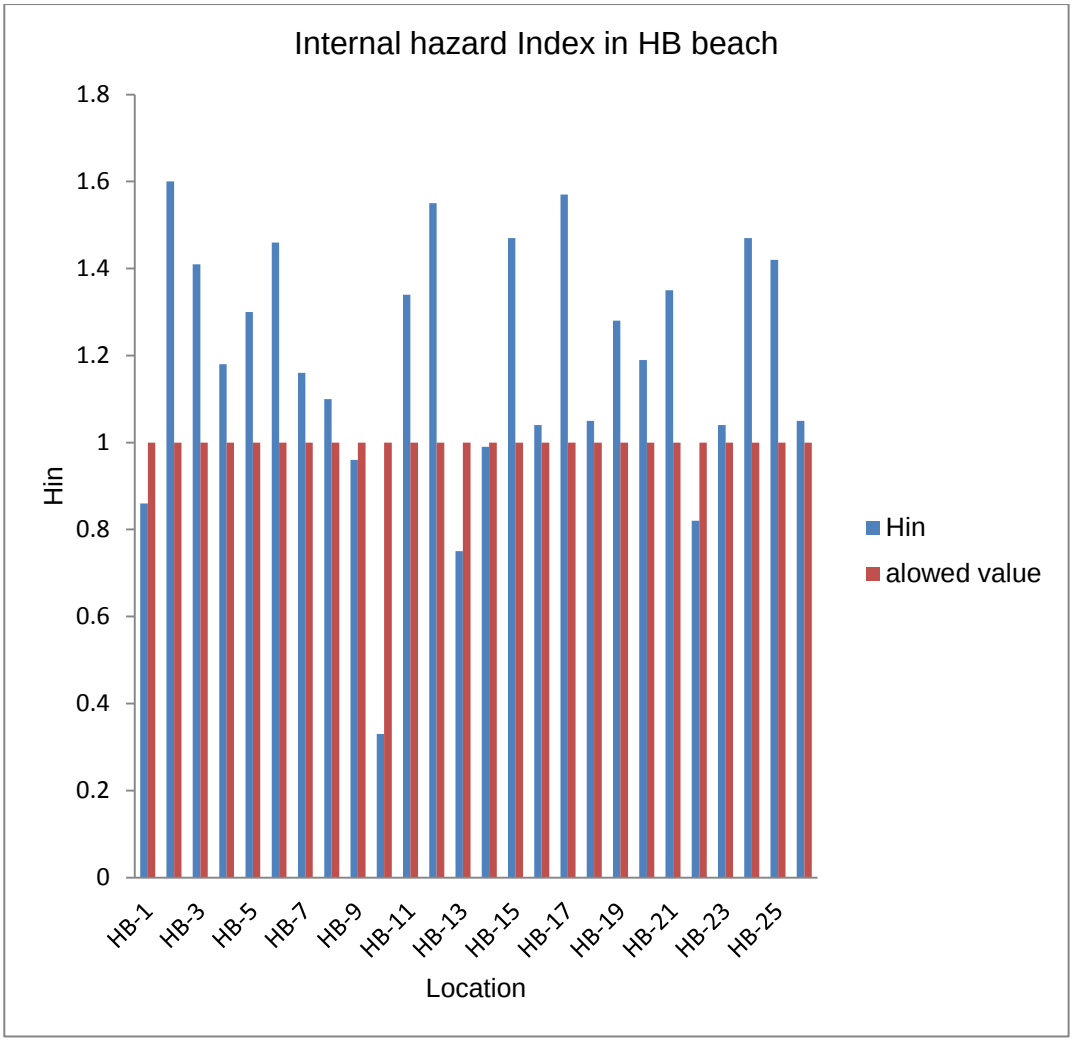

Figure 8.17: Comparison of internal hazard Index with allowed value in Henties Bay.

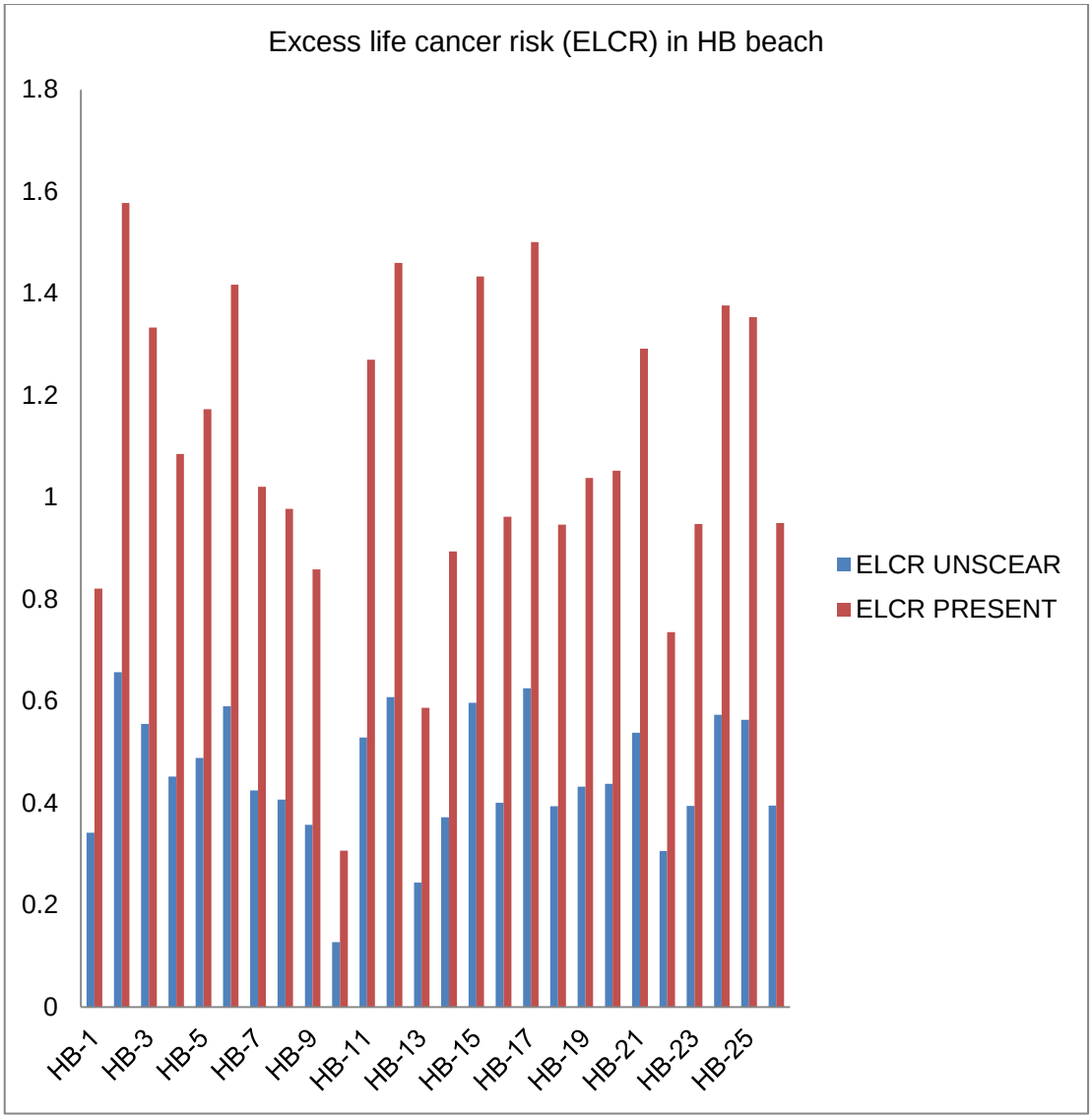

Figure 8.18: Comparison of Excess lifetime cancer risk using UNSCEAR values and the Present modelled values from Henties Bay beach.

8.8 Comparison of activity concentrations from sediments samples from Walvis Bay, Swakopmund and Henties Bay beaches with those in other countries

The mean activity concentrations of ^{238}U, ^{232}Th and ^{40}K in the shore sediment samples from beaches of Walvis Bay, Swakopmund and Henties Bay were compared with those from similar investigations in other countries and a summary of the results are presented in Table 8.11. This study showed that the activity concentration trend of ^{238}U and ^{232}Th along the coast line of the Erongo region is in the order WB < HB < SWK and the trend of ^{40}K follows the order HB < WB < SWK. The values of ^{232}Th and ^{40}K obtained from this study are comparable with most reported values from other countries except in the case of Brazil and Bangladesh. In contrast, values of ^{238}U fall within the highest of all reported values from other countries. This high activity concentration of ^{238}U in the coastline of the Erongo region may have been caused by uranium mining activities in the region which are only a few kilometre from the coastline.

Table 8.11: Comparison of mean activity concentrations of Walvis Bay, Swakopmund and Henties Bay beaches with similar studies in other countries

Mean activity concentration Bq.kg $^{-1}$			Country/References
^{238}U	^{232}Th	^{40}K	
142.79	29.69	359.78	Walvis Bay Beach, Namibia **(present)**
199.76	42.47	611.19	Swakopmund beach, Namibia **(present)**
176.44	41.16	354.38	Henties Bay beach, Namibia **(present)**
50.0	50.0	500.0	World average value, UNSCEAR, 2000
7.31	46.85	384.03	Ponnaiyar river, India, Ramasamy *et al*., 2010
7.82	24.52	274.87	Tamilnadu beach, India, Ramasamy *et al*., 2009
1.42	1.49	21.31	Coast of Accra, Ghana, Amekudzie *et al*., 2011
28.67	27.96	302.4	Hungary, UNSCEAR, 2000
54-180	128-349	47-283	Brazil, Freitas and Alencar, 2004
5-19	5-44	136-1087	Spain, Rosell et al., 1991
64.39	13.24	47.2	Zircon, Bangladesh, Alam *et al*., 1999
24.0	35.7	423.67	Osun river, Nigeria, Oyebanjo *et al*., 2012

8.9 Comparison of absorbed dose rate, annual effective dose rate, radium activity, external/internal hazard index and excess lifetime cancer risk from Walvis Bay, Swakopmund and Henties Bay beach sediment

The results of the comparisons of absorbed dose rate, annual effective dose rate, radium equivalent activity, hazard index and excess lifetime cancer risk from all the three sampled beaches along the coastline of the Erongo region are presented in Table 8.12.

The mean absorbed dose rate due to the presence of the activity concentration of ^{238}U, ^{232}Th and ^{40}K in the shore sediment samples along the coastline of the Erongo region of Namibia was found to range between 93.27 $nGyh^{-1}$ and 144.01 $nGyh^{-1}$ with an average of 114.41 $nGyh^{-1}$. The highest dose rate was found in SWK and the least dose rate was associated with the WB beach. All the sampled locations have dose rates higher than the world average value.

The mean annual effective dose rate using UNSCEAR outdoor occupancy factor* and the Present modelled factor** was found to range between 121.01 $\mu Sv.y^{-1}$ and 176.61 $\mu Sv.y^{-1}$ with an average of 142.52 for UNSCEAR and 292.66 $\mu Sv.y^{-1}$ and 413.63 $\mu Sv.y^{-1}$ with an average of 339.36 $\mu Sv.y^{-1}$ for our Present modelled factor. This study reveals that both the UNSCEAR factor and the present modelled factor have higher values than world accepted values. However, the study has also shown that the use of the UNSCEAR factor might underestimate the annual effective dose rate to the population.

The radium equivalent activity was ranging between 213.93 $Bq.kg^{-1}$ and 308.62 $Bq.kg^{-1}$ with an average of 261.38. Clearly, all beaches have values below the international acceptable limit. The external and internal hazard index also ranged from 0.58 to 0.83 (H_{ex}) with an average of 0.70 and 0.96 to 1.37 (H_{in}) with an average of 1.17. Comparing with the world standards, the H_{ex} poses less risk since the values are less than unity. However, the use of shore sediments for construction material poses a great risk to internal exposure since the internal hazard index is greater than the world safe standard. The average values of ELCR for both UNSCEAR factor and the present modelled factor for all locations are more than the world average value (0.29×10^{-3}) (Figure 8.19) (Taskin *et al*., 2009).

Table 8.12: Comparison of absorbed dose rate, annual effective dose rate, radium equivalent activity, external/internal hazard index and excess lifetime cancer risk from Walvis Bay, Swakopmund and Henties Bay beaches.

Site	Absorbed dose rate ($nGyh^{-1}$)	Annual effective dose rate ($\mu Sv.y^{-1}$)		Ra_{eq} ($Bq.kg^{-1}$)	Hazard index (H_{ex})	(H_{in})	Excess lifetime cancer risk $x10^{-3}$	
WB	93.27	121.01*	292.60**	213.93	0.58	0.96	0.43*	1.13**
SWK	144.01	176.61*	413.63**	308.62	0.83	1.37	2.48*	1.61**
HB	105.95	129.94*	311.86**	261.58	0.70	1.18	0.44*	1.08**
Average	114.41	142.52*	339.36**	261.38	0.70	1.17	1.12*	1.27**
WAV	51	70 (outdoor)		370	≤ 1	< 1	0.29	

WAV world average value (UNSCEAR)

*UNSCEAR factor

**Present modelled factor

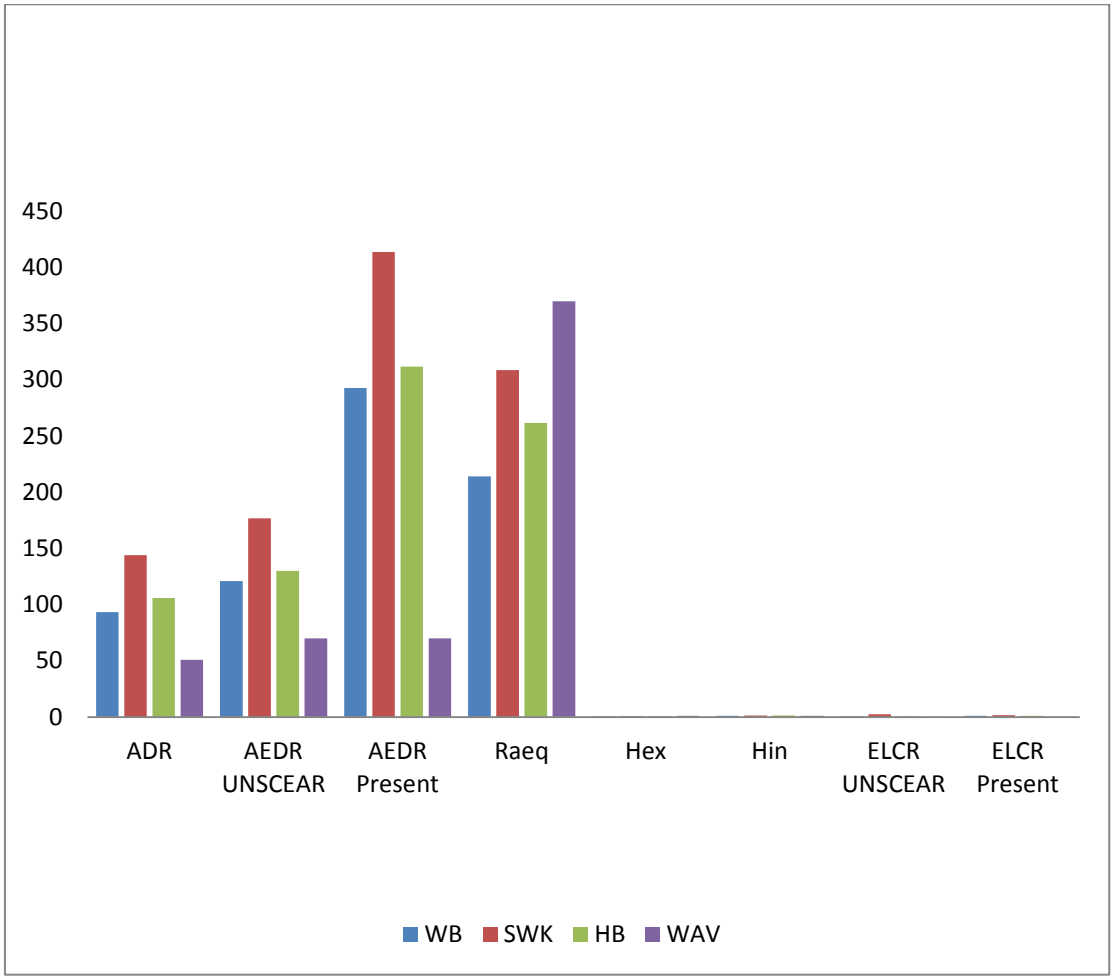

Figure 8.19: Comparison of ADR, AEDR, Raeq, Hex, Hin and ELCR from WB, SWK and HB

8.10 Summary

This chapter has reported the concentration of natural radionuclides in shore sediment samples collected from the beaches of Walvis Bay, Swakopmund and Henties Bay. Objectives set in chapter 1 have been achieved. The results of the analysis were used in evaluating effective dose rate and hazard index due to natural radionuclides and their decay products from sediment samples. The results have shown that the present modelled factors were 2.4 times the UNSCEAR outdoor occupancy.

CHAPTER 9

FUTURE DIRECTIONS AND CONCLUSION

9.1 Project outcomes

From the study of literatures, sediments have been widely used as environmental indicator and their ability to trace contamination sources and monitor contaminants is widely recognized (Lazano *et al*., 2002; Seddeek *et al*., 2005; 1994; Kurnaz *et al*., 2007).

In chapter 1 a general background for the common radionuclides and their origin were looked at. Overviews of studies on NORMs from different parts of the world were reviewed. This chapter also looked at heavy metals as useful indicator for contamination in surface soil and sediment.

The objectives outlined in this chapter have been met and a number of additional objectives were achieved. Primarily, the major project outcomes were:

(i) The measurement of the levels of natural radionuclide concentration in the shore sediments.

(ii) The evaluation of the baseline activity concentration trend along the coastline shore sediments.

(iii) The re-evaluation of the occupancy factor for effective dose estimation for the coastline.

(iv) The ascertainment of the absorbed dose rate and annual effective dose from the shore sediments that may accrue to the human along the coastline.

(v) The evaluation of the hazard index due to natural radionuclides and their decay products from sediments samples along the coastline.

(vi) The determination of the baseline data of the level of some heavy metals of environmental and human impacts along the coastline shore sediments.

Additionally the following outcomes were also achieved:

(i) The evaluation of the seasonal variations of metal concentrations

(ii) The determination of the excess lifetime cancer risk (ELCR) as a result of the use of shore sediments for building materials

(iii) The assessment of the internal hazard index of the shore sediments to see if the sediments contribute significantly to internal irradiation from sediments that are used as building material.

In chapter two the structure of the atom was looked at and the principles of radioactivity and radioactive decay was explained as a statistical phenomenon.

Chapter three described the principle of gamma-ray spectrometry instruments. Although there are various possible interaction mechanisms for gamma rays in matter, only the three most important mechanisms that play a significant role in radiation measurement were described. That is, photoelectric absorption, Compton scattering and pair production. This chapter also looked at different detection instrument and we gave reasons for our choice of high energy resolution semiconductor detector in this present study.

In chapter four biological effects of ionising radiation and toxicology of some heavy metals were looked at. The basic radiation quantities and units were also discussed in this chapter.

In chapter five the research methodology were explained and a detailed description of the study areas was given. This chapter also outlined the method of sample preparation and analysis.

In chapter six, the possible exposure to NORMs based on a survey using a well-designed questionnaire was explained. The findings showed that on average the studied population spends (1.00-15.40, 0.00-10.33 and 8.60-15.07) number of hours in leisure, occupation and other activities respectively in the beach of Walvis Bay. The mean time spent for different activities at the beach in Swakopmund showed that more hours were allocated to other activities. The values of the time spent ranged from 1.00-17.00 (leisure), 0.00-10.20 (occupation) and 7.00-17.84 (Other). In this chapter it was also revealed that high proportion of hours is spent in leisure activities at the beach of Henties Bay. Furthermore, the results obtained from the questionnaire was used in MATLAB to model the occupancy factor for the evaluation of the annual effective dose rate to the public who are engaged in one activity or the other along the coastline. The results were found to be outdoor (0.48) and indoor (0.52).The difference between the present outdoor modelled values and the one given by UNSCEAR has been estimated to be 2.4 times the values of UNSCEAR. On the other hand, the indoor modelled value is estimated to be 0.65 times less than the UNSCEAR factors. Hence, findings from this present study have shown that the use of the UNSCEAR factors in the coastline of the Erongo region would introduce large errors.

In chapter seven we discussed the elemental composition of the shore sediments was discussed. Furthermore, an assessment on the contamination status of heavy metals was done and results showed high enrichment for cadmium (Cd) in both seasons of summer and winter, moderate degree of contamination of arsenic (As) in summer seasons in the beach of Walvis Bay. The geo-accumulation index found that the beach of Walvis Bay (summer) showed moderate pollution with Cd, unpolluted beach of Swakopmund with Cd and polluted to moderately polluted beach of Henties Bay with Cd in the winter seasons. However, the results of pollution load index (PLI) from this present study revealed PLI values < 1 which clearly indicated that all the beaches are not polluted with heavy metals.

In chapter eight we looked at the mean specific activity concentrations of ^{238}U, ^{232}Th and ^{40}K were looked at and compared the concentration with the world average values. Results of the comparison of absorbed dose rate from all sampled locations were found to be higher than the world average values.

9.2 Future directions

This study has drawn to a close but has opened up a number of potential future research projects.

In order to obtain a more statistically significant picture of the complete information on NORMs and heavy metal concentrations with high geographical resolution, future work should involve the analysis of more samples on a more geographical coverage of about 120 km^2 which have already been collected but postponed due to time limitation in this present study. The total number of shore sediment samples would therefore be around three times more of the investigated samples in the current work. Also, more study is suggested for bottom sediment from the sea and surrounding catchment.

Further study is also suggested in the area of developing an experimental laboratory procedure to investigate evaporative effect given rise to radon exhalation rate in the coastline. Equally, we suggest chemical speciation studies on the geochemistry of ^{238}U in the coastline of the Erongo region.

A further study that can be done is to investigate seasonal changes in the concentration of NORMs in the shore sediment and the application of more advanced instrumentation for the detection of mercury concentration levels in the beaches.

9.3 Conclusions

At the onset of the present study, it was noted that there was limited information regarding the levels of natural radioactivity and heavy metals along the coastline of the Erongo region. The results of this study have added to the body of knowledge of NORMs and heavy metals in Namibia.

To the best of the knowledge of the researcher, all studies on natural radioactivity from shore sediment from coastal areas have employed the outdoor and indoor occupancy factors recommended by United Nations Scientific Committee on the Effects of Atomic Radiation (UNSCEAR). This assumption, however, may not adequately represent the actual situation in the study area. The modelled occupancy factor in this present study will provide baseline information for future studies to be developed from the finding.

REFERENCES

Abah, J., Mashebe, P., Onjefu, S.A. (2014), Survey of the Level of Heavy Metals in Roadside Dust along Katima Mulilo Urban Road Construction, Namibia, *American Journal of Environmental Protection* 3 (1), 19-27.

Abah, J., Mashebe, P., Onjefu, S.A., Malu, S.P. (2015), Assessment of the In-Situ Concentrations of Some Heavy Metals in Surface Soil Dust at the Katima Mulilo Urban Waste Dumpsite, Namibia, *International Journal of Advanced Scientific and Technical Research* 5 (4), 88-100.

Abbasi, S.A., Abbasi, N., Soni, R. (1998), Heavy Metals in the Environment (1st edition), Mittal Publication.

Abdi, M.R., Kamali, M., Vaezifa, S. (2008), Distribution of Radioactivity Pollution of ^{238}U, ^{232}Th, ^{40}K and ^{137}Cs in North Western Coasts of Persian Gulf Iran, *Marine Pollution Bulletin* 56, 751-757.

Aboud, S.J., Nandini, N. (2009), Heavy Metal Analysis and Sediment Quality Values in Urban Lakes, *American Journal of Environmental Science* 5 (6), 678-687.

Abusini, M. (2007), Determination of Uranium, Thorium and Potassium Activity Concentration in Soil Cores in Araba Valley, Jordan, *Radiation Protection Dosimetry* 43, 103-107.

Adaikpo, E.O. (2013), Distribution and Enrichment of Heavy Metals in Soils from Waste Dump Sites Within Imoru and Environs, Southwest Nigeria, *Journal of Environment and Earth Science* 3(4), 45-54.

Ademoroti, C.M.A. (1996), Environmental Chemistry and Toxicology, Ibadan Foludex Press Inc.

Adloff, J.P., Guillaumont, R. (1993), *Fundamentals of Radiochemistry*, London: CRC Press Inc.

Ajayi, O.S. (2009), Measurement of Activity Concentration of ^{40}K, ^{226}Ra and ^{232}Th for Assessment of Radiation Hazards from Soils of South West Region of Nigeria, *Radon and Environmental Biophysics* 48, 323-332.

Akram, M., Riffat, M., Qureshi, N., Solaija, T.J. (2006), Gamma-Emitting Radionuclides in the Shallow Marine Sediments off the Sindh Coast, Arabian Sea, *Radiation Protection Dosimetry* 118, 440-447.

Akram, M., Qureshi, M., Riffat, M., Ahmad, N., Solaija, T.J. (2007), Determination of Gamma- Emitting Radionuclides in the Inter-tidal Sediments of Balochistan (Pakistan) Coast, Arabian Sea, *Radiation Protection Dosimetry* 123, 268-273.

Alam, M.N., Chowdhury, M.I., Kamal, M., Ghose, S., Islam, M.N., Mustafa, M.N. (1999), The ^{226}Ra, ^{232}Th and ^{40}K Activities in Beach Sand minerals and Beach Soils of Cox's Bazar, Bangladesh, *Journal of Environmental Radioactivity* 46, 243-250.

Alenikov, V.A. (1989), Health and Environment Consequences of Chernobyl Accident, *High Technology and Development* 2, 35-108.

Al- Hamarneh, I.F., Awadallah, M.I. (2009), Soil Radioactivity Levels and Radiation Hazard Assessment in the Highland of Northern Jordan, *Radiation Measurements* 44, 102 110.

Alloway, B.J. (1995), Soil Processes and the Behavior of Heavy Metals. In: Heavy metals in soils (2nd edition) (B.J. Alloway ed). New York: Blackie.

Amadi, A.N., Olasehinde, P.I., Okosun, E.A., Okoye, N.O., Okunlola, I.A., Alkali, Y.B., Dan Hansan, M.A. (2012), A Comparative Study on the Impact of AVU and Ihie Dumpsite on Soil Quality in Southeastern Nigeria, *American Journal of Chemistry* 2 (1), 17-23.

Amdur, M.O., Doull, J., Classen, C.D. (1991), The Basic Science of Poisons, *Journal of Soil Science* 49, 639-643.

Amekudzie, A., Emi-Reynolds, G., Faanu, A., Darko, E.O., Awudu, A.R., Adukpo, O., Quaye, L.A.N., Kpordzro, R., Agyemang, B., Ibrahim, A. (2011), Natural Radioactivity Concentrations and Dose Assessment in Shore Sediments along the Coast of Greater Accra, Ghana, *World Applied Science Journal* 13 (11), 2338-2343.

Ana, C., Zoran K. (2010) Heavy Metals Distribution in Marine Sediments of East Adriatic Sea, *Rapp. Comm. Int. Mer Medit.* 39.

Anjos, R.M., Veiga, R., Soares, T., Santos, A.M., Aguiar, J.G., Frasca, M.H.B.O., Brage, J.A.P., Uzeda, D., Mangia, L., Facure, A., Mosquera, B., Carvailo, C., Gomes, P.R.S. (2005), Natural Radionuclide Distribution in Brazilian Commercial Granites, *Journal of Radiation Measurement* 75, 315-327.

Arogunjo, A.M., Adekola, A.S. (2007), Occupancy Factor Model for Exposure to Atmospheric Radiation by Urban and Rural Dwellers in Nigeria, *Journal of Applied Sciences* 7, 1343-1346.

Arogunjo, A.M., Ohenhen, H.O., Olowookere, S.P. (2004), A Re-Evaluation of the Occupancy Factors for Effective Dose Estimation in Tropical Environment, *Radiation Protection Dosimetry* 1-7.

Attia, T.E., Shendi, E.H., Shehata, M.A. (2014), Assessment of Natural and Artificial Radioactivity levels and Radiation Hazards and their Relation to Heavy Metals in the Industrial area of Port Said City, Egypt *Journal of Earth Science and Climatic Change* 5 (4), 1-11.

Agency for Toxic Substances and Disease Registry, (1994), Toxicological profile for Zinc, ATSDR, US Dept. of Health and Human Service, Atlanta 205-88-0606.

Azu, O.S., Ike, E.E. (1998), Health Implication of Nuclear Radiation Levels in Mining Processing Plants in Jos metropolis, *American Journal of Applied Science and Measurement* 2, 84-86.

Baldwin D.R., Marshall, W.J. (1999), Heavy Metal Poisoning and its Laboratory Investigation, *Ann Clin Biochem* 36, 267-300.

Benamar, M.A., Zenouki, A., Idiri, Z., Tobbeche, S. (1997), Natural and Artificial Radioactivity Levels in Sediments in Algiers Bay, *Applied Radiation and Isotopes* 48, 1161-1164.

Beretka, J., Mathew, P.J. (1985), Natural Radioactivity of Australian Building Material, Industrial Waste and By-Products, *Health physics* 48, 87-95.

Biological Effects of Ionizing Radiations. (2006), "Health Risks from Exposure to Low levels of Ionizing Radiation", BEIR Vll Phase 2, 2006 report, National Academics Press, Washington, DC.

Browne, E., Firestone, R.B., Shirley, V.S. (1986), Table of Radioactive Isotopes, New York: John Wiley and Sons Inc.

Cember, H. (1996), *Introduction to Health Physics* (3rd edition), New York: McGraw-Hill Companies Inc.

Cember, H., Johnson, T.E. (2009), *Introduction to Health Physics* (4th edition), New York: McGraw-Hill Companies, Inc.

Centeno, J.A., Mullick, F.G., Isbak, K.G., Franks, T.J., Burke, A.P., Koss, M.N., Perl, D.P., Tchounwou, P.B., Pestaner, J.P. (2005), Environmental Pathology. In: Selinus, O. (Ed), The Essentials of Medical Geology: Impacts of the Natural Environment on Public Health. Elsevier Academic Press.

Chakravarty, M., Patgiri, A.D. (2009), Metal Pollution Assessments of Dikrong River, N.E. India, *Journal of Human Ecology*, 27 (1), 63-67.

Chowdhury, M.I., Alam, M.N., Hazari, S.K.S. (1999), Distribution of Radionuclides in River Sediments and Coastal Soils of Chittagong, Bangladesh and Evaluation of the Radiation Hazard, *Applied Radiation and Isotope* 51, 747-755.

Chiroma, T.M., Ebewele, R.O., F.K. Hymore, F.K. (2014), Comparative Assessment of Heavy Metal Levels in Soil, Vegetables and Urban Grey Waste Water Used for Irrigation in Yola and Kano, *International Refereed Journal of Engineering and Science (IRJES)* 3, 1-9.

Christophoridis, C., Dedepsidis, D., Fytianos, K. (2009), Occurrence and Distribution of Selected Heavy metals in the Surface Sediments of Thermaikos Gulf, N. Greece. Assessment using Pollution indicators *J. Hazardous Mat.* 168, 1082-1091.

Clarkson, E. (2001), Toxic Effect of Metals. In: Casarett and Doullis Toxicology: Basic Science of Poisons. (6th edition) (C.D. Klassen, ed.). New York: Mc-Graw-Hill Companies, Inc.

Cothern, C.R., Lappenbusch, W.L. (1986), Occurrence of Uranium in Drinking Water in the US, *Health Physics* 45, 89-99.

Dahlgaard, H. (1996), Polonium-210 in Mussels and Fish from the Baltic-North Sea Estuary, *Journal of Environmental Radioactivity* 32 (1), 91-96.

Davies, B.E. (1995), Lead, In Heavy metals in soil (2nd edition), (B.J. Alloway, ed), New York: Blackie.

Defew, L.H., Mair, J.M., Guzman, H.M. (2005), An Assessment of Metal Contamination in Mangrove Sediments and Leaves from Punta Mala Bay, Pacific Panama. *Marine Pollution Bulletin* 50, 547-552.

Denagbe, S.J. (2000), Radon-222 Concentration in Sub Soils and its Exhalation Rate from Soil Samples, *Journal of Radiation Measurements* 32, 27-34.

Deneley, D., Hawkes, D., Hancock, P., Williams, B. (1976), Earth Resource – A Dictionary of Terms and Concepts Arrow Books, London.

Dissanayake, C.B., Chandrajith, R. (2009), Introduction to Medical Geology (Erlangen Earth Conference Series). Springer, Dordrecht / Heidelberg.

Duffus, J.H. (2002), Heavy Metals: A Meaningless Term? (IUPAC Technical Report), Pure and Applied Chemistry 74 (5), 793-807.

Edokpay, J.N. Odiyo, J.O., Olasoji, S.O. (2014), Assessment of Heavy Metal Contamination of Dzindi River, In Limpopo Provine, South Africa, *International Journal of Natural Sciences Research* 2 (10), 185-194.

Eisenbud, M., Gesell, T. (1997), Environmental Radioactivity from Natural, Industrial and Military source (4th edition), London: Academic Press.

El-Amri, E.A., Al Jarallah, M., Abu- Jarad, F., Fazal-ur, R. (2003), Uniformity in Radon Exhalation from Construction Materials using a Technique, *Journal of Radiation Measurements* 36 (1-6), 453-456.

El-Dine, N., El- Shershaby, A., Ahmed, F., Abdel-Haleem, A.S. (2001), Measurement of Radioactivity and Radon Exhalation Rate in Different Kinds of Marbles and Granites. *Journal of Applies Radiation and Isotopes* 55, 853-860.

El- Fawal, M.M. (2011), Mathematical Modelling for Radon Prediction and Ventilation Air Cleaning System Requirements in Underground Mines, *Journal of American Science* 7 (2), 389-402.

El- Gamal, A., Nasr, S., El- Taher, A. (2007), Study of the Spatial Distribution of Natural Radioactivity in Upper Egypt Nile River Sediments, *Radiation Measurement* 42, 457 469.

El-Mamoney, M.H., Khater, A.E.M. (2004), Environmental Characterization and Radio ecological Impacts of Non-Nuclear Industries on the Red Sea Coast. *Journal of Environmental Radioactivity* 73, 151-168.

El-Kameesy, S.U., El-Minyawi, S.M., Miligy, Z., El-Mabrouk, E.M. (2008), Natural Radioactivity of Beach Sand Samples in Tripoli Region, Northwest Libya, *Turkish Journal of Environmental Science* 32, 245-251.

Environmental Protection Agency. (1996), "Method 3050B, Acid Digestion of Sediment, Sludge, and Soils".

Erongo Regional Council. (2013), ERC 2013 Annual Report, Lienette Publications.

Ewan, C., Anagnostopoulou, M.A., Ward, N.I. (2009), Monitoring of Heavy Metal Levels in Roadside Dusts of Thessaloniki, Greece in Relation to Motor Vehicle Traffic Density and Flow. *Epubs. Surrey.ac.uk/…/Monitoring of Heavy Metal Levels in Roadside…, Accessed 11 September 2015*.

Faires, R.A., Boswell, G.G.J. (1981), *Radioisotope Laboratory Techniques* (4 edition), London: Butteworth and Co Publishers Ltd.

Farai, I.P., Sanni, A.O. (1992), Radon-222 in a Groundwater in Nigeria, a Survey. *Journal Health Physics* 62, 96-98.

Florou, H., Kritidis, P. (1992), Gamma Radiation Measurements and Dose Rate in the Coastal Area of a Volcanic Island Aegean Sea, Greece, *Radiation Protection Dosimetry* 45, 277-279.

Foley, R., Bell, T., Liverman, D.G.E. (2011), Urban Geochemical Hazard Mapping of St. John's Newfoundland, Canada, *Atlantic Geology* 47, 138-157.

Forstner G.T., Wittman, G.I.W. (1983), Mining Pollution in Aquatic Environment, *Journal of Natural Environment* 25 (4), 206-208.

Freitas, A.C., Alencar, A.S. (2004), Gamma Dose Rate and Distribution of Natural Radionuclides in Sand Beaches IIha Grande Southeastern Brazil. *Journal of Environmental Radioactivity* 75, 211-223.

Gerrado, C.M. (1974), Radioactive Potassium, *The nucleons* 12, 4-8.

Gilmore, G.R. (2008), Practical Gamma-ray Spectrometry (2nd edition), New York: John Wiley and Sons.

Gregorauskiene, V. (2008), Overview of the Quality Criteria in the Eastern European Countries, Proceedings of the Conference; The Abiotic Environment- Evaluation of Changes and Hazards- Case stud, Polish Geological Institute Special Paper 24, 45 54.

Goyer, R.A., Clarkson, E. (2001), Toxic Effect of Metals. In Casarett and Doullis Toxicology: Basic Science of Poison. (6th edition), (C.D. Klassn, ed.), Mc-Graw Hill, New York. pp 811-867.

Guidotti, T.L. (2005), Toxicology, In: Selinus O. (ed). The Essentials of Medical Geology: Impacts of the Natural Environment on Public Health. Elsevier Academic Press.

Hakanson, L. (1980), An Ecological Risk Index for Aquatic Pollution Control a Sedimentological Approaches, *Water Resources* 14 (8), 975-1001.

Hansen W.L. (1971), High Purity Germanium-Observations on the Nature of Acceptors *Nuclear Instrument and Methods* 94, 377-380.

Harvey, B.G. (1969), *Introduction to Nuclear Physics and Chemistry* (2nd edition), New Jersey: Prentice-Hall Inc.

Hendee, W.R. (1973), Radioactive Isotopes in Biological Research (1st edition), New York: John Wiley and Sons, Publication.

Hu, Q.H., Weng, J.Q., Wang, J.S. (2010), "Sources of Anthropogenic Radionuclides in the Environment: a Review", *Journal of Environmental Radioactivity* 101 (6) 426-437.

Huda, A.A. (2011), A Determination of Natural Radioactivity Levels in the State of Qatar using High-Resolution Gamma-ray Spectrometry. PhD Thesis, University of Surrey, UK.

Huu, H.H., Rudy, S., Damme, A.V. (2010), "Distribution and Concentration Status of Heavy Metals in Estuarine sediment Near Cau Ong Harbor Ha Long Bay, Vietnam", *Geologica Belgica* 13 (1-2), 37-47.

International Atomic Energy Agency. (1986), "Facts About Low Level Radiation Exposure", Technical Report A.N.E 985-06482, IAEA, Vienna.

International Atomic Energy Agency. (1987), "Radiological Accident in Soreq, Brazil", IAEA Publication, Vienna.

International Atomic Energy Agency. (1989), "Measurement of Radionuclides in Food and the Environment", Technical Report No. 295, IAEA, Vienna.

International Atomic Energy Agency. (1998), "Diagnosis and Treatment of Radiation Injuries", Technical Reports Series, No. 2, IAEA, Vienna.

International Atomic Energy Agency. (2005), International Atomic Energy Agency. "IAEA TECDOC-1472", Proceedings of an international Conference on Naturally Occurring Radioactive Materials (NORM IV), Poland: IAEA, Vienna.

International Atomic Energy Agency. (2014), Nuclear Medicine Physics: A hand Book for Students and Teachers. IAEA, Vienna.

International Commission on Radiological Protection (1991), ICRP Publication 60, Recommendations of the International Commission on Radiological Protection, Pergamon Press, Oxford.

International Commission on Radiological Protection (2000), Annals of the ICRP, Risk Estimation for Multifactorial Diseases. ICRP Publication, Pergamon Press, Oxford.

Ike, E.E., (2008), Fundamental Principles of University Physics. Enic Education Consultants and Publishers Ltd.

Jarup, L. (2003), Hazards of Heavy Metal Contamination, *British Medical Bull.* 68, 167-182.

Jibiri, N.N., Mabawonku, A.O., Oridate, A.A., Ujiagbedion, C. (1999), "Natural Radioactivity Concentration Levels in Soil and Water around a Cement Factory at Ewekoro, Ogun State Nigeria", *Nigerian Journal of Physics* 11, 12-16.

Jibiri, N.N., Farai, I.P., Alausa, S.K. (2007), "Estimation of Annual Effective Dose due to Natural Radioactive Elements in Ingestion of Food Stuffs in tin Mining Areas of Jos Plateau, Nigeria", *Journal of Environmental Radioactivity* 94, 31-40.

Joshua, E.O., Oyebanjo, A.O. (2009), "Distribution of Heavy Metals in Sediments of Osun River Basin Southwestern Nigeria", *Research Journal of Earth Science* 1(2), 74-80.

Kaladharan, P., Prema, D., Valsala, K.K., Leelabhai, K.S., Rajagopalan, M. (2005), Trends in Heavy Metal Concentrations in Sediment, Finfishes and Shell fishes in Inshore Water of Cochin, SouthWest Coast of India, *Journal of Marine and Biological Sciences.* 47 (1), 1-7.

Kaplan, I. (1962), Nuclear Physics (2nd edition), USA: Addison-Wesley Publishing Company Inc.

Kathren R.L. (1998), "NORM Sources and Their Origins", *Applied Radiation and Isotopes*, 49 (3), 149-168.

Khandaker, M.U. (2011), "High Purity Detector in Gamma-Ray Spectrometry", *International Journal of Fundamental Physical Sciences*, 1 (2), 42-46.

Kinyua, R., Atambo, V.O., Ongeri, R.M. (2011), "Activity Concentrations of ^{40}K, ^{232}Th, ^{226}Ra and Radiation Exposure Levels in the Tabaka Soapstone Quarries of the Kisii Region, Kenya", *African Journal of Environmental Science and Technology* 5 (9), 682-688.

Klement, A.W. (1982), "Natural Source of Environmental Radiation. In Handbook of Environmental Radiation, Florida: CRC Press, Inc.

Knoll, G.F. (2000), Radiation Detection and Measurement (3rd edition), U.S.A. John Wiley and Sons Inc.

Krane, K.S. (1988), Introductory Nuclear Physics. Chichester: John Wiley and Sons Inc.

Krmar, M., Slivka, J., Varga, E., Bikit, I., Veskovic, M. (2009), Correlations of Natural Radionuclides in Sediment from Danube, *Journal of Geochemical Exploration* 100 (1), 20-24.

Kurnaz, A., Kucukomeroglu, B., Keser, R., Okumusoglu, N.T., Korkmaz, F., Karahan, G., Cevik, U. (2007), "Determination of Radioactivity Levels and Hazards of Soil and Sediment samples in Firtina Valley (Rize, Turkey)", *Applied Radiation and Isotopes* 65, 1281-1289.

Lancaster, N. (1989), The Namib Sand Sea: Dune Forms, Processes and Sediments, A.A. Balkema, Rotterdam.

L'Annunziata, M.F. (2007) Radioactivity: Introduction and History, Amsterdam: Elservier B.V.

Lamarsh, J.R., Bell, G.I. (2009), “Introduction to Nuclear Reactor Theory”, *Physics Today*, 20 (3), 110-111.

Lapp, R.E., Andrews, H.L. (1972), Nuclear Radiation Physics (4 edition), Sir Isaac Pitman and Sons Ltd.

Lars, J. (2003), “Hazards of Heavy Metal Contamination”, *British Medical Bulletin*. 68. 167 182.

Lazano, J.C., Blanco, R.P., Vara, T.F. (2002), “Distribution of Long-Live Radionuclides of ^{238}U Series in the Sediments of a Small River in a Uranium Mineralized Region of Spain’, *Journal of Environmental Radioactivity* 63, 153-171.

Learning and Teaching Scotland (2011), Physics: Semiconductors and Band Theory Support Material, Scotland Qualification Authority, LTS, Scotland.

Li Y., Yetang, H., Duojun, W., Yongxuan, Z. (2007), “Determination of Free Heavy Metal Ion Concentrations in Soils around a Cadmium Rich Zinc Deposit”, *Geochemical Journal* 41, 235-240.

Lilley, J. (2001), Nuclear Physics: Principles and Applications, Chichester: John Wiley and Sons, Inc.

Lorimore, S.A., Philip, J.C., Eric, G.W. (2003), “Radiation-Induce Genomic Instability and Bystander Effect: Inter-Related Non targeted Effects of Exposure to Ionizing Radiation”, *Oncogene* 22, 7058-7069.

MacFarland, H.N. (1979), Pulmonary effects of Cadmium. In: Cadmium toxicity (J.E. Mennea red.) Dekker.

Magill, J., Galy, J. (2004), *Radioactivity Radionuclides Radiation* (Vol. 1): Springer Science and Business Media, 46-49.

Manoli, E., Voutsa, D., Samara, C. (2002), “Chemical Characterization and Source Identification/Apportionment of Fine and Coarse Air particles in Thessaloniki, Greece”, *Atmosphere and Environment* 36, 949-961.

Martin, J.M., Meybeck, M. (1979), “Elemental Mass Balance of Materials Carried by Major World Rivers”, *Marine Chemistry* 7, 173-206.

McGrath, S.P. (1995), Chromium and Nickel. In: Heavy metals in soils (2nd edition) (B.J. Alloway, ed.), New York: Blackie.

Mmolawa, K.B., Likuku, A.S., Gaboutloeloe, G.K. (2011), “Assessment of Heavy Metal Pollution in Soils along Major Roadside Areas in Botswana”, *African Journal of Environment Science and Technology* 5, 186-196.

Moja S.J., Mnisi, J.S. (2013) “Seasonal Variations in Airborne Heavy Metals in Vanderbijlpark, South Africa”, *Journal of Environmental Chemistry and Ecotoxicology* 5 (9), 227-233.

Momont-Ciesla, K., Gwiazdowki, B., Biernacka, M., Zak, A. (1982), Radioactivity of Building Material in Poland Natural Radiation Environment. In: Vohra, G., Pillai, K.C., Sadavisan, S., (ed.), New York: Halsted Press.

Murphy, J.V. (1970), "Intoxication Following Ingestion of Elemental Zinc", *JAMA*, 212 2119 2120.

National Council on Radiation Protection and Measurement. (1975), "Natural Background Radiation in the United State", NCRP Report No. 45. NCRP Washington D.C.

National Council on Radiation Protection and Measurement. (1985), A handbook of Radioactivity Measurements Procedures (2nd edition), NCRP Report No. 58. NCRP, Maryland.

Niemann, E.G. (1983), Radiation Biophysics. Edited by Hopper W. Lohmann, W, Markt. H, Zilgler H, (2ND edition), New York: Springer Verlag Berlin Heidelberg.

Nielson, K.K., Rogers, V.C., Holt, R.B. (1996), "Measurement and Calculations of Soil Radon Flux at 325 Sites throughout Florida", *Environmental International* 22 (suppl 1), S471 S476.

Nikulina, A., Dullo, W.C. (2009), "Eutrophication and Heavy Metal Pollution in the Flensburg Fjord: A Reassessment after 30 Years", *Marine Pollution Bulletin* 58, 905-915.

Nour, K.A. (2004), "Natural Radioactivity of Ground and Drinking Water in some Areas of Upper Egypt", *Turkish Journal of Engineering, Environment and Science* 28, 345 354.

Noz, M.E., Maguire, G.Q. (2007), Radiation Protection in Health Sciences, London: World Scientific Publishing Co. Pte. Ltd.

Namibia 2011 Population and Housing Census Preliminary Results. (2011), NPC www.gov.na/do.cuments/.../0ea026d4-9697-4851-a693-1b97a1317c60, (2012). Acessed; 21 september 2015.

O'Brien, R., Cooper, M. (1998), "Technologically Enhanced Naturally Occuring Radioactivity Material (NORM): Pathway Analysis and Radiological Impact", *Applied Radiation and Isotopes* 49 (3), 227-239.

Ogbeibu, A.E., Omoigberale, O.M., Ezenwa, I.M., Eziza, J.O., Igwe, J.O. (2014), "Using Pollution Load Index and Geoaccumulation Index for the Assessment of Heavy Metal Pollution and Sediment quality of Benin River, Nigeria", *Natural Environment* 1-9.

Ogwuegbu, M.O., Duruibe, J.O. (2005), "Environmental Pollution and Bio-Toxicity of Certain Heavy Metals. Proceeding of a Conference, Nigeria: Chemical Society of Nigeria, pp 285-287.

Olli, G., and Destouni, G. (2008), Long-Term Heavy Metal Loading to near-Shore Lake Sediments, *Water Air Soil Pollution* 192, 105-116.

Omole, O., Akambi, A.S. (1997), “Gamma Ray Emission and the Associated Electric Field”, *Journal of Mining and Geology* 33 (2), 127-134.

O’Neill, P. (1995), Arsenic. In: Heavy metals in soils. (2nd ed) (B.J. Alloway, ed.), New York: Blackie.

Oni, M.O., Farai, I.P., Aodugba, A.O. (2011), Natural Radionuclide Concentrations and Radiological Impact Assessment of River Sediments of the Coastal Areas of Nigeria, *Journal of Environment Protection* 2, 418-423.

Orgun, Y., Altinsoy, N., Sahin, S.Y., Gungor, Y., Gultekin, A.H., Karaham, G., Karaak, Z. (2007), “Natural and Anthropogenic Radionuclides in Rock and Beach Sand from Ezine region (Canakkale). Western Anatolia, Turkey”, *Applied Radiation and Isotopes* 65, 739-747.

Ortec. (2003), High Purity Germanium (HPGe). http://www.ortec-online.com/papers/la ur 03 4020, Accessed, 05/05/2016.

Oyebanjo, O.A., Joshua, E.O., Jibiri, N.N. (2012), “Natural Radionuclides and Hazards of Sediment Samples Collected from Osun River in Southwestern Nigeria” *The Pacific Journal of Science and Technology* 391-396.

Oyedele, J.A., Shimboyo, S., Sitoko, S., Gaoseb, F. (2010), “Assessment of Natural Radioactivity in Soils of Rossing Uranium Mine and its Satellite Town in Western Namibia, Southern Africa”, *Nuclear Instruments and Methods in Physics Research* A 619, 467-469.

Paul, J.E., Mohammed, A.R., Sodee, D.B. (1979), Nuclear Medicine Technology (3rd edition), London: Macmillan Educational Limited.

Pereira, A.J.S.C., Neves, L.J.P.F. (2012), “Estimation of the Radiological Background and Dose Assessment in Areas with Naturally Occurring Uranium Geochemical Anomalies”, *Journal of Environmental Radioactivity* 112, 96-107.

Powell, B.A., Hughes, L.D., Soreefan, M.A., Deborah, F., Michaal, W., Devol, T.A. (2007), “Elevated Concentrations of Primodial Radionuclides in Sediments from the Reedy River and Surrounding Creeks in Simpsonville, South Carolina”, *Journal of Environmental Radioactivity* 94, 121-128.

Prince, J.H. (1979), “Comments on Equilibrium, Transient Equilibrium and Secular Equilibrium in Serial Radioactive Decay”, *Journal of Nuclear Medicine* 20, 162-164.

Radojevic, M., Bashkin, N.V. (1999), “Practical Environmental Analysis” Royal Society of Chemistry and Thoma Graham House, Cambridge, U.K. 356-377.

Ramanibai, R., and Shanthi M. (2012), Heavy Metal Distribution in the Coastal Sediment of Chennai Coast. *Institute of Integrated Omics and Applied Biotechnology Journal* 3(2), 12-18.

Ramasamy, V., Senthil, S., Meenakshisundaram, V., Gajendran, V. (2009), “Measurement of Natural Radioactivity in Beach sediments from North East Coast of Tamilnadu, India”, *Research Journal of Applied Science Engineering and Technology* 1(2), 54-58.

Ramasamy, V., Suresh, G., Meenakshisundaram, V., Ponnusamy, V. (2010), Distribution and Characterization of Minerals and Naturally Occurring Radionuclides in River Sediments”, *Carpathian Journal of Earth and Environmental Sciences* 5 (1), 41-48.

Ramasamy, V., Suresh, G., Meenakshisundaram, V., Ponnusamy, V. (2011), “Horrizontal and Vertical Characterization of Radionuclides and Minerals in River Sediments, *Applied Radiation and Isotopes* 69, 184-195.

Rasheed, M.N., Awalallah, R.M. (1998), “Trace Elements in Faba Bean (Vice Faba L.) Plant and Soil as Determined by AAS and Iron Selective Electrode”, *Journal of Science, Food Agriculture*, 77, 18-24.

Ravichandran, R., Manickam, S. (2012), “Heavy Metal Distribution in Coastal Sediment of Chennai Coast”, *IIOABJ* 3(2), 12-18.

Roesner H., Schreuder, C.R. (1992), Uranium Unpublished Chapter 7.1: In Mineral Resources of Namibia, Geological Survey, Ministry of Mines and Energy, Namibia.

Rosell, J.R., Ortega, X., Dies, X. (1991), “Natural and Artificial Radionuclides on the Northeast Coast of Spain”, *Journal of Health Physics* 60, 709-712.

Saikia, B.J., Goswami, S.R., Borah, R.R. (2014), “Estimation of Heavy Metals Contamination and Silicate Mineral Distributions in Suspended Sediments of Subansiri River”, *International Journal of Physical Sciences* 9 (21), 475-486.

Samara, C., Voutsa, D. (2005), “Size Distribution of Airborne Particulate Matter and Associated Heavy Metals in the Roadside Environment”, *Chemosphere* 59, 1197 1206.

Santos, I.R., Silva-Filho, E.V., Schaefer, C.E., Albuquerque-Filho, Campos, L.S. (2005), “Heavy Metal Contamination in Coastal Sediments and Soil Near the Brazilian Antartic Station, Kin George Island”, *Marine Pollution Bulletin* 50, 185-194.

Scholten, L.C., Timmermans, C.W.M. (1996), “Natural Radioactivity in Phosphate .Fertilizers”, *Fertilizer Research* 43, 103-107.

Seddeek, M.K., Badran, H.B., Sharshar, T., Elnimr, T. (2005), “Characteristics Spatial Distribution and Vertical Profile of Gamma-Ray Emitting Radionuclides in Coastal Environment of North Sinai”, *Journal of Environmental Radioactivity* 84, 21-25.

Strategic Environmental Assessment. (2010), “Central Namib Uranium Rush”, SEA. Geological Survey of Namibia, Ministry of Mines and Energy, Windhoek, Namibia.

Sham, M.H., Shaheen, N., Jaffar, M., Khalique, A., Tariq, S.R., Manzoor, S. (2006), “Spatial Variations in Selected Metal Contents and Particle Size Distribution in An Urban and

Rural Atmoshere of Islamabad Pakistan", *Journal of Environmental Management* 78, 128-137.

Shams, I., Uosif, M., Elsama, R. (2013), "Gamma Radioactivity Measurements in Nile River Sediment Samples", *Turkish Journal of Engineering and Environmental Science* 37, 109-122.

Shimboyo, S.A. (2013), "Natural Radioactivity in Soils of the Walvis Bay- Henties Bay Coastal Area, Namibia. An Msc Thesis, Department of Physics University of Namibia.

Singh, S., Rani, A., Mahajan, R.K. (2005), "^{226}Ra, ^{232}Th and ^{40}K Analysis in Soil Samples From Some Area of Punjab and Himachal Pradesh, India Using Gamma Ray Spectrometry", *Journal of Radiation Measurements* 39, 431-439.

Steinhausler, F., Lettner, H. (1992) "Radiometric Survey in Namibia", *Radiation Dosimetry* 1 4, 553-555.

Steinnes, E. (1995), Mercury: In Heavy metals in soil. (2nd edition), (B.J. Alloway, ed), New York: Blackie.

Sood, D.D., Manohar, S.B., Reddy, A.V.R. (1981), Experiments in Radiochemistry: India Association of Nuclear Chemists and Allied Scientists (IANCAS).

Taskin, H., Karavus, M., AY, P., Topuzoglu, A., Hindiroglu, S., karahan, G. (2009), "Radionuclide Concentrations in Soil and Lifeline Cancer Risk Due to the Gamma Radioactivity in Kirklareli", *Turkey Journal of Environment Radioactivity* 100, 49-53.

Tavendale, A.J., Ewan, G.T. (1963), "A High Resolution Lithium-Drift Germanium Gamma Ray Spectrometer", *Nuclear Instrument and Methods in Physics Research Section A* 25, 185-187.

Taylor, G. (1990), Quantity and Quality of Storm Water from Runoff from Western Daytona Beach, Florida, and Adjacent Areas. USGS Water-Resources Investigation Report 90-4002.

Tijani, M., Onodera, S. (2009), Hydrogeochemical Assessment of Metals Contamination in an Urban Drainage System: A case study of Osogbo Township, SW-Nigeria", *Journal of Water Resources and Protection* 1(3), 164-173.

Tippie, V. (1984), An Environmental Characterization of Chesa-Peak Bay and Framework For Action, In: V. Kennedy (ed.). The Estuary as a Filter, New York: Academic Press.

Tomlinson, D., Wilson, J., Harris, C., Jeffrey, D. (1980), "Problems in the Assessment of Heavy Metal levels in Esti-arie and the Formation of a Pollution Index", *Helgoland Marine Resources 33* (1-4), 566-575.

Tsabaris, C., Eleftueriou, G., Kapsimalis, V., Anagnostou, C., Vlastou, R., Durmishi, C., Kedhi, M., Kalfas, C.A. (2007), "Radioactivity Levels of Recent Sediments in the Butrint Lagoon and the Adjacent Coast of Albania", *Applied Radiation and Isotopes* 65, 445-453.

Turhan, S., Gundiz, L. (2008), “Determination of Specific Activity of ^{226}Ra, ^{232}Th and ^{40}K for Assessment of Radiation Hazards from Turkish Pumice Samples”, *Journal of Environmental Radioactivity* 99, 332-342.

Tyson, P.D., Lindesay, J.A. (1992), The Climate of the Last 2000 Years in Southern Africa”, *The Holocene* 2 (3), 271-278.

Tzortzis, M., Teetos, H., Christofides, S., Christodoulides, G. (2005) “Radiation Measurement and Dose Rate in Commercially Used Natural Tilling Rocks (Granites)”, *Journal of Environmental Radioactivity* 70, 223-235.

Ubwa, S.T., Abah, J., Ada, C.A., Alechen, E. (2013), Levels of some Heavy Metals Contamination of Street Dust in the Industrial and High Traffic Density Areas of Jos Metropolis, *Journal of Biodiversity and Environmental Science* 3 (7), 13-21.

United Nation Environment Programme. (2012), “Lead Pollution and Poisoning Crisis”, UNEP Report of Environmental emergency response mission in Zamfara State Nigeria.

United Nations Scientific Committee on Effects of Atomic Radiation. (1988), “Sources and Effects of Ionizing Radiation”, UNSCEAR Report to the General Assembly with Scientific Annexes, United Nations Publication, United Nation, New York.

United Nations Scientific Committee on Effects of Atomic Radiation. (1993), “Sources and Effects of Ionizing Radiation”, UNSCEAR Report to the General Assembly with Scientific Annexes, United Nations Publication, United Nation, New York.

United Nations Scientific Committee on Effects of Atomic Radiation. (1998), “Sources and Effects of Ionizing Radiation”, UNSCEAR Report to the General Assembly with Scientific Annexes, United Nations Publication, United Nation, New York.

United Nations Scientific Committee on Effects of Atomic Radiation. (2000), “Sources and Effects of Ionizing Radiation”, UNSCEAR Report to the General Assembly with Scientific Annexes, United Nations Publication, United Nation, New York.

United State Environmental Protection Agency. (1994), “Contaminated Sediment Management Strategy-Reinventing Government to Streamline Decision Making”, USEPA, Washington, DC 151. EPA/823/R-94/001.

Van Blerk, J., Kruger, I.D., Louw, I., Potgieter, N. (2010), Strategic Environmental Assessment (SEA) for the Central Namib Uranium Rush Radiation impact study, document reference number ASC-1012A-1, Aquisim Consulting (pty).

Von Oertzen, D. (2010), Cumulative Effects Analysis: Radiation; Chapter 7.12 of Main Report of Strategic Environmental Assessment for the Central Namib Uranium Rush, Geological Survey of Namibia, Ministry of Mines and Energy.

Wackerle, R. (2009), Natural Terrestrial Radiation of the Erongo Region, Central Western Namibia, Processing Report, Namibia: Geointrepid Consulting Services.

Ward, N.I., Dudding, A., Lyndon, M. (2004), “Platinum Emmissions and Levels in Motorway Dust Samples: Influence of Traffic Characteristics”, *Science of the Total Environment* 334-335, 457-463.

Ward, J.D., Seely, M.K., Lancaster, N. (1983), “On the Antiquity of the Namib”, *South African Journal of Science* 79. 175-183.

Watson, S.J., Jones, A.L., Oatway, W.B., Hughes, J.S. (2005) “Ionizing Radiation Exposure of the UK Population. Review”, Health Protection Agency, Center for Radiation, Chemical and Environmental Hazards, Radiation Protection Division, Chilton, Didcot, Oxfordshire, OXII ORQ, UK.

WHO/FAO. WHO/FAO Food Additives Data Systems. Evaluation by the Joint Committee on Food Additives, 1956-1984. FAO Food and Nutrition Paper 30/Rev. Rome.

World Nuclear Association. (2011), “Radiation and Nuclear Energy”, http://www.world nuclear.org/info/inf30.html [Updated August 2011].

Wilson, W.F. (1994), A Guide to Naturally Occurring Radioactive Material, Oklahoma: Pennwell Books.

Wu, Y.S., Fang, G.C., Lee, W.J., Lee, J.F., Chang, C.C., Lee, C.Z. (2007), A Review of Atmospheric Fine Particulate Matter and Its Associated Trace Metal Pollutants in Asian Countries during the Period 1995-2005. *Journal of Hazardous Material.* 143, 511–515.

Xinwei, L., Lingqing, W., Xiaodan, J., Leipeng, Y. (2006), “Specific Activity and Hazards of Archeozoic-Cambrian Rock Samples Collected from the Weibei area of Shaanxi, China”, *Radiation Protection Dosimetry* 118, 352-359.

Yalcin, M.G., Narin, I., Soylak, M. (2008), Multivariate Analysis of Heavy Metal Contents of Sediments from Gumusler Creek, Nigde, Turkey. *Environ. Geol.* 54(9), 1155-1163.

Young, H.D., Freedman, R.A. (2008), University Physics with Modern Physics (12 edition), San Francisco: Pearson Education, Pearson Addison-Wesley.

Zhang, W., Feng, H., Chang, J., Qu, J., Xie, H., Yu, L. (2009), Heavy Metal Concentration in Surface Sediments of Yangtze River Intertide Zone: An Assessment from Different indexes. *Environmental Pollution.* 157, 1533-1543.

APPENDIX A

Table A1: Location for collection of 26 sediment samples at Walvis Bay.

Sample No.	Sample Code	Position	
		Latitude (^{o}S)	Longitude (^{o}E)
1	WB-1	22^{o}55’20.0’’	014^{o}31’17.7’’
2	WB-2	22^{o}55’19.2’’	014^{o}31’18.9’’
3	WB-3	22^{o}55’18.4’’	014^{o}31’20.1’’
4	WB-4	22^{o}55’17.6’’	014^{o}31’21.2’’
5	WB-5	22^{o}55’16.8’’	014^{o}31’22.4’’
6	WB-6	22^{o}55’15.9’’	014^{o}31’23.8’’
7	WB-7	22^{o}55’15.0’’	014^{o}31’24.9’’
8	WB-8	22^{o}55’14.0’’	014^{o}31’26.0’’’
9	WB-9	22^{o}55’13.1’’	014^{o}31’27.1’’
10	WB-10	22^{o}55’12.4’’	014^{o}31’27.9’’
11	WB-11	22^{o}55’11.6’’	014^{o}31’29.0’’
12	WB-12	22^{o}55’10.8’’	014^{o}31’29.8’’
13	WB-13	22^{o}55’10.2’’	014^{o}31’30.5’’
14	WB-14	22^{o}55’09.2’’	014^{o}31’31.6’’
15	WB-15	22^{o}55’08.4’’	014^{o}31’32.6’’
16	WB-16	22^{o}55’07.7’’	014o31’33.4’’
17	WB-17	22^{o}55’07.3’’	014^{o}31’33.8’’
18	WB-18	22^{o}55’06.9’’	014^{o}31’34.5’’
19	WB-19	22^{o}55’06.3’’	014^{o}31’35.4’’
20	WB-20	22^{o}55’05.5’’	014^{o}31’36.1’’
21	WB-21	22^{o}55’04.7’’	014^{o}31’37.0’’
22	WB-22	22^{o}55’04.0’’	014^{o}31’37.9’’
23	WB-23	22^{o}55’03.3’’	014^{o}31’38.7’’
24	WB-24	22^{o}55’02.8’’	014^{o}31’39.2’’
25	WB-25	22^{o}55’02.3’’	014^{o}31’39.9’’
26	WB-26	22^{o}55’01.6’’	014^{o}31’40.6’’

Table A2: Location for collection of 26 sediment samples at Swakopmund.

Sample No.	Sample Code	Position	
		Latitude (^{o}S)	Longitude (^{o}E)
1	SWK-1	22^{o}40’26.3’’	014^{o}31’25.1’’
2	SWK-2	22^{o}40’25.4’’	014^{o}31’24.8’’
3	SWK-3	22^{o}40’24.8’’	014^{o}31’24.9’’
4	SWK-4	22^{o}40’24.5’’	014^{o}31’25.0’’
5	SWK-5	22^{o}40’23.9’’	014^{o}31’25.1’’
6	SWK-6	22^{o}40’22.9’’	014^{o}31’25.2’’
7	SWK-7	22^{o}40’21.8’’	014^{o}31’25.5’’
8	SWK-8	22^{o}40’21.2’’	014^{o}31’25.7’’’
9	SWK-9	22^{o}40’19.9’’	014^{o}31’25.7’’
10	SWK-10	22^{o}40’18.8’’	014^{o}31’26.1’’
11	SWK-11	22^{o}40’18.5’’	014^{o}31’26.2’’
12	SWK-12	22^{o}40’17.5’’	014^{o}31’26.2’’
13	SWK-13	22^{o}40’17.3’’	014^{o}31’26.2’’
14	SWK-14	22^{o}40’16.5’’	014^{o}31’26.2’’
15	SWK-15	22^{o}40’15.7’’	014^{o}31’26.0’’
16	SWK-16	22^{o}40’14.2’’	014^{o}31’25.8’’
17	SWK-17	22^{o}40’13.2’’	014^{o}31’25.4’’
18	SWK-18	22^{o}40’12.0’’	014^{o}31’25.0’’
19	SWK-19	22^{o}40’11.5’’	014^{o}31’25.1’’
20	SWK-20	22^{o}40’10.4’’	014^{o}31’24.7’’
21	SWK-21	22^{o}40’09.8’’	014^{o}31’24.2’’
22	SWK-22	22^{o}40’09.6’’	014^{o}31’24.2’’
23	SWK-23	22^{o}40’08.8’’	014^{o}31’24.0’’
24	SWK-24	22^{o}40’08.2’’	014^{o}31’23.7’’
25	SWK-25	22^{o}40’06.6’’	014^{o}31’23.6’’
26	SWK-26	22^{o}40’05.5’’	014^{o}31’24.2’’

Table A3: Location for collection of 26 sediment samples at Henties Bay.

Sample No.	Sample Code	Position	
		Latitude (^{o}S)	Longitude (^{o}E)
1	HB-1	22^{o}07’35.4’’	014^{o}17’00.2’’
2	HB-2	22^{o}07’34.5’’	014^{o}16’59.4’’
3	HB-3	22^{o}07’33.4’’	014^{o}16’58.4’’
4	HB-4	22^{o}07’32.6’’	014^{o}16’57.6’’
5	HB-5	22^{o}07’31.5’’	014^{o}16’53.0’’
6	HB-6	22^{o}07’30.4’’	014^{o}16’56.1’’
7	HB-7	22^{o}07’28.7’’	014^{o}16’54.1’’
8	HB-8	22^{o}07’27.6’’	014^{o}16’53.0’’
9	HB-9	22^{o}07’25.2’’	014^{o}16’50.8’’
10	HB-10	22^{o}07’24.1’’	014^{o}16’49.1’’
11	HB-11	22^{o}07’23.5’’	014^{o}16’48.1’’
12	HB-12	22^{o}07’21.9’’	014^{o}16’47.1’’
13	HB-13	22^{o}07’21.1’’	014^{o}16’45.9’’
14	HB-14	22^{o}07’19.6’’	014^{o}16’44.3’’
15	HB-15	22^{o}07’18.1’’	014^{o}16’42.9’’
16	HB-16	22^{o}07’16.0’’	014^{o}16’41.0’’
17	HB-17	22^{o}07’14.2’’	014^{o}16’39.7’’
18	HB-18	22^{o}07’13.0’’	014^{o}16’38.4’’
19	HB-19	22^{o}07’12.0’’	014^{o}16’37.1’’
20	HB-20	22^{o}07’10.5’’	014^{o}16’35.4’’
21	HB-21	22^{o}07’08.7’’	014^{o}16’34.0’’
22	HB-22	22^{o}07’07.1’’	014^{o}16’32.7’’
23	HB-23	22^{o}07’05.0’’	014^{o}16’30.4’’
24	HB-24	22^{o}07’03.4’’	014^{o}16’29.1’’
25	HB-25	22^{o}07’02.2’’	014^{o}16’28.0’’
26	HB-26	22^{o}07’01.2’’	014^{o}16’27.1’’

APPENDIX B

Table B1: Concentrations of Heavy Metals in Soils and Critical Concentrations in Soils (Alloway, 1995)

Metals	Normal soil concentrations (mg/kg)	Critical soil concentrations (mg/kg)
As	0.1 – 40	20 – 50
Cd	0.01 – 2.0	3 – 8
Cr	5 – 1500	75 – 100
Cu	2 – 250	60 – 125
Hg	0.01 – 0.5	0.3 – 5
Mn	20 – 10000	1500 – 3000
Ni	2 – 750	100
Pb	2 – 30	100 – 400
Sb	0.2 – 10	5 – 10
Se	0.1 – 5	5 – 10
Sn	1 – 200	50
V	3 – 500	50 – 100
Zn	1 – 900	70 – 400

Table B2: Critical Dose of some Heavy Metals that causes Toxicity in Humans (WHO/FAO, 1985)

Heavy Metal	Toxic level in humans
Fe	200.00mg/day
Cr	200.00mg/day
Pb	1.00mg/day
Zn	150 – 600.00mg/day

APPENDIX C

Table C1: Elemental concentrations of ^{238}U, ^{232}Th and ^{40}K from Walvis Bay Beach

Location	Element	Mass Fraction (mg/kg)	Uncertainty
WB-1	^{238}U	11.37	15.30
	^{232}Th	6.57	21.00
	^{40}K	1.02	5.00
WB-2	^{238}U	14.06	18.30
	^{232}Th	8.78	23.10
	^{40}K	1.15	3.40
WB-3	^{238}U	10.34	36.20
	^{232}Th	8.35	23.70
	^{40}K	1.36	3.50
WB-4	^{238}U	12.41	12.60
	^{232}Th	7.47	26.70
	^{40}K	1.24	3.10
WB-5	^{238}U	11.22	16.00
	^{232}Th	6.95	19.90
	^{40}K	1.27	3.70
WB-6	^{238}U	11.59	14.20
	^{232}Th	5.93	24.30
	^{40}K	1.08	3.50
WB-7	^{238}U	10.88	21.50
	^{232}Th	5.99	33.50
	^{40}K	1.10	3.70
WB-8	^{238}U	13.94	12.60
	^{232}Th	7.78	24.30
	^{40}K	1.05	3.50
WB-9	^{238}U	0.00	0.00
	^{232}Th	11.50	31.70
	^{40}K	1.08	5.70
WB-10	^{238}U	13.95	11.30
	^{232}Th	8.42	20.00
	^{40}K	1.06	3.40
WB-11	^{238}U	13.90	16.90
	^{232}Th	9.13	26.50
	^{40}K	1.08	4.20
WB-12	^{238}U	8.17	21.4
	^{232}Th	8.32	20.80
	^{40}K	1.08	4.20
WB-13	^{238}U	0.00	0.00
	^{232}Th	7.04	24.00
	^{40}K	1.18	3.90
WB-14	^{238}U	13.36	18.70
	^{232}Th	5.46	24.90
	^{40}K	1.21	4.30

Table C1: Elemental concentrations of ^{238}U, ^{232}Th and ^{40}K from Walvis Bay Beach (continued).

Location	Element	Mass Fraction (mg/kg)	Uncertainty
WB-15	^{238}U	6.86	16.73
	^{232}Th	9.94	22.00
	^{40}K	1.15	3.80
WB-16	^{238}U	8.61	17.50
	^{232}Th	9.87	21.00
	^{40}K	1.18	3.80
WB-17	^{238}U	7.95	21.00
	^{232}Th	7.83	27.10
	^{40}K	1.12	4.60
WB-18	^{238}U	16.61	18.60
	^{232}Th	7.70	25.60
	^{40}K	1.28	3.70
WB-19	^{238}U	18.32	13.40
	^{232}Th	10.05	25.43
	^{40}K	1.32	4.30
WB-20	^{238}U	16.11	16.10
	^{232}Th	8.29	26.90
	^{40}K	1.34	3.70
WB-21	^{238}U	12.32	20.70
	^{232}Th	8.81	21.50
	^{40}K	1.20	4.20
WB-22	^{238}U	9.45	29.60
	^{232}Th	5.63	27.80
	^{40}K	1.15	4.20
WB-23	^{238}U	12.07	19.9
	^{232}Th	6.53	26.5
	^{40}K	1.21	4.00
WB-24	^{238}U	10.89	18.30
	^{232}Th	0.00	0.00
	^{40}K	1.12	4.20
WB-25	^{238}U	13.85	15.90
	^{232}Th	7.81	17.10
	^{40}K	1.17	3.90
WB-26	^{238}U	22.38	19.60
	^{232}Th	0.00	0.00
	^{40}K	1.65	3.80

Table C2: Elemental concentrations of ^{238}U, ^{232}Th and ^{40}K from Swakopmund Beach

Location	Element	Mass Fraction (mg/kg)	Uncertainty
SWK-1	^{238}U	9.38	19.7
	^{232}Th	9.69	17.10
	^{40}K	1.12	3.70
SWK-2	^{238}U	10.70	19.40
	^{232}Th	8.37	20.30
	^{40}K	1.26	3.20
SWK-3	^{238}U	15.12	18.30
	^{232}Th	13.79	20.10
	^{40}K	1.30	4.80
SWK-4	^{238}U	8.16	27.00
	^{232}Th	0.00	0.00
	^{40}K	1.49	3.10
SWK-5	^{238}U	10.15	17.70
	^{232}Th	0.00	0.00
	^{40}K	1.11	4.00
SWK-6	^{238}U	13.76	13.30
	^{232}Th	9.59	19.70
	^{40}K	1.06	4.20
SWK-7	^{238}U	9.78	27.10
	^{232}Th	0.00	0.00
	^{40}K	1.14	3.40
SWK-8	^{238}U	15.02	17.00
	^{232}Th	6.99	22.70
	^{40}K	1.31	3.90
SWK-9	^{238}U	7.91	22.10
	^{232}Th	0.00	0.00
	^{40}K	1.20	3.20
SWK-10	^{238}U	11.21	20.70
	^{232}Th	10.14	17.20
	^{40}K	1.28	3.40
SWK-11	^{238}U	11.82	14.40
	^{232}Th	9.41	16.80
	^{40}K	1.07	3.60
SWK-12	^{238}U	9.05	25.80
	^{232}Th	8.98	26.50
	^{40}K	1.28	3.80
SWK-13	^{238}U	10.75	21.30
	^{232}Th	9.04	25.50
	^{40}K	1.34	3.30
SWK-14	^{238}U	7.16	31.90
	^{232}Th	7.26	22.60
	^{40}K	1.30	3.10

Table C2: Elemental concentrations of ^{238}U, ^{232}Th and ^{40}K from Swakopmund Beach (continued).

Location	Element	Mass Fraction (mg/kg)	Uncertainty
SWK-15	^{238}U	8.57	14.00
	^{232}Th	6.95	21.30
	^{40}K	1.18	3.70
SWK-16	^{238}U	15.29	14.10
	^{232}Th	6.94	22.60
	^{40}K	1.30	3.20
SWK-17	^{238}U	7.34	22.40
	^{232}Th	7.55	21.90
	^{40}K	1.44	2.80
SWK-18	^{238}U	123.46	19.00
	^{232}Th	111.19	23.60
	^{40}K	19.95	3.40
SWK-19	^{238}U	15.54	16.60
	^{232}Th	0.00	0.00
	^{40}K	1.68	3.80
SWK-20	^{238}U	14.92	16.10
	^{232}Th	0.00	0.00
	^{40}K	1.18	4.30
SWK-21	^{238}U	15.18	14.00
	^{232}Th	9.99	18.80
	^{40}K	1.22	4.60
SWK-22	^{238}U	14.60	18.80
	^{232}Th	11.30	23.20
	^{40}K	1.14	6.80
SWK-23	^{238}U	18.89	20.70
	^{232}Th	7.80	23.80
	^{40}K	1.40	4.70
SWK-24	^{238}U	10.45	19.80
	^{232}Th	8.13	21.80
	^{40}K	1.36	3.80
SWK-25	^{238}U	11.55	31.90
	^{232}Th	8.87	32.30
	^{40}K	1.45	3.50
SWK-26	^{238}U	14.73	19.60
	^{232}Th	0.00	0.00
	^{40}K	1.36	3.90

Table C3: Elemental concentrations of ^{238}U, ^{232}Th and ^{40}K from Henties Bay Beach

Location	Element	Mass Fraction (mg/kg)	Uncertainty
HB-1	^{238}U	9.12	17.60
	^{232}Th	11.28	21.27
	^{40}K	1.07	2.90
HB-2	^{238}U	18.58	12.10
	^{232}Th	19.21	14.60
	^{40}K	0.94	5.20
HB-3	^{238}U	17.10	10.60
	^{232}Th	12.99	13.00
	^{40}K	0.94	3.90
HB-4	^{238}U	14.18	11.70
	^{232}Th	9.96	18.50
	^{40}K	1.12	3.40
HB-5	^{238}U	16.16	10.40
	^{232}Th	8.82	15.50
	^{40}K	1.23	4.70
HB-6	^{238}U	16.75	11.90
	^{232}Th	17.13	13.70
	^{40}K	1.09	3.30
HB-7	^{238}U	14.96	12.70
	^{232}Th	5.60	41.00
	^{40}K	1.13	3.80
HB-8	^{238}U	13.75	10.40
	^{232}Th	6.70	21.40
	^{40}K	1.15	3.20
HB-9	^{238}U	11.93	27.40
	^{232}Th	6.22	28.60
	^{40}K	1.08	5.10
HB-10	^{238}U	2.05	10.80
	^{232}Th	7.37	39.70
	^{40}K	1.13	3.40
HB-11	^{238}U	15.99	13.30
	^{232}Th	13.07	19.37
	^{40}K	1.04	4.00
HB-12	^{238}U	18.83	11.00
	^{232}Th	13.97	13.50
	^{40}K	1.10	4.10
HB-13	^{238}U	9.99	19.80
	^{232}Th	0.00	0.00
	^{40}K	1.25	3.90
HB-14	^{238}U	11.62	16.50
	^{232}Th	8.34	24.90
	^{40}K	1.28	3.40

Table C3: Elemental concentrations of ^{238}U, ^{232}Th and ^{40}K from Henties Bay Beach (continued).

Location	Element	Mass Fraction (mg/kg)	Uncertainty
HB-15	^{238}U	17.34	10.20
	^{232}Th	16.39	11.40
	^{40}K	0.79	4.00
HB-16	^{238}U	12.22	16.10
	^{232}Th	9.64	13.53
	^{40}K	1.07	3.70
HB-17	^{238}U	18.82	11.60
	^{232}Th	15.62	9.30
	^{40}K	1.03	4.00
HB-18	^{238}U	12.49	16.20
	^{232}Th	8.40	20.20
	^{40}K	1.36	3.10
HB-19	^{238}U	17.66	14.70
	^{232}Th	0.00	0.00
	^{40}K	1.54	3.40
HB-20	^{238}U	14.82	20.00
	^{232}Th	7.16	28.40
	^{40}K	1.32	3.60
HB-21	^{238}U	15.98	9.60
	^{232}Th	13.96	19.00
	^{40}K	1.03	3.90
HB-22	^{238}U	9.35	24.60
	^{232}Th	7.37	26.10
	^{40}K	1.16	4.30
HB-23	^{238}U	12.32	26.60
	^{232}Th	8.85	21.34
	^{40}K	1.15	3.90
HB-24	^{238}U	18.03	12.80
	^{232}Th	12.54	15.30
	^{40}K	1.06	4.80
HB-25	^{238}U	16.69	23.50
	^{232}Th	14.75	21.70
	^{40}K	1.16	4.20
HB-26	^{238}U	12.62	32.80
	^{232}Th	8.23	27.80
	^{40}K	1.22	4.20

Table C4: Standard sources used in the study

Nuclide	Reg. No.	Half-life	Activity (kBq)
^{152}Eu	S313.PH	13.33	3.02
^{232}Th	S314.PH	1.405×10^{10}	1.08
^{226}Ra	S315.PH	1600	3.1
Matrix NG3	S312.PH	*	42

Table C5: The minimum detectable activity

Nuclide	MDA (Bq.kg $^{-1}$)
^{238}U	0.11
^{232}Th	0.10
^{40}K	0.14

APPENDIX D

QUESTIONNAIRE

SECTION 1 – ABOUT YOU

Tick as applicable

Sex: Male [ ] Female [ ]

Level of Education

(a) No formal Education [ ] (b) Primary Level [ ]

(c) Secondary Level [ ] (c) Tertiary [ ]

Age range

(a) 15 – 20 years [ ] (b) 21 – 30 years [ ]

(c) 31 – 40 years [ ] (d) 41 – 50 years [ ]

(e) 51 and above [ ]

SECTION 2 – ACTIVITY AT THE BEACH

Swakopmund [ ] Walvis Bay [ ] Henties Bay [ ]

LEISURE ACTIVITY:

(a) Leisure {fishing} [ ] (b) Leisure {diving} [ ] (c) Leisure {walking} [ ]

(d) Leisure {picnic at the shore} [ ] (e) Leisure {horse riding} [ ]

(f) Leisure {sun bathing} [ ] (g) Leisure {relaxation at beach house} [ ]

OCCUPATIONAL ACTIVITY:

(a) Vendors [ ] (b) Shop retailers [ ] (c) Sanitation workers [ ]

Others [ ]

SECTION 3 – TIME BUDGET AT THE BEACH

1. Destination before visiting the beach was:

(a) My home [ ] (b) Beach house [ ]

(c) My hotel [ ] (d) Other (specify)……

2. What is your next destination after leaving the beach?

(a) My home [ ] (b) Beach house [ ]

(c) My hotel [ ] (d) other (specify)……..

3. My visit to the beach is seasonal (tick all appropriate options)

(a) Winter [ ] (b) Summer [ ]

(c) Spring [ ] (d) Autumn [ ]

4. How often do you visit the beach?

(a) Once or twice a year [ ] (b) Three to four times a year [ ]

(c) Five times and more [ ] (e) Other (specify) ……

5. During your visit, how many days do you spend in leisure at the beach?

(a) One to three days [ ] (b) Four to seven days [ ]

(c) Eight to ten days [ ] (d) Other (specify) ……...

LEISURE ACTIVITY:

6. How many hours per day do you spend in leisure activity at the beach? [ ]

Specify activity……..

OCCUPATIONAL ACTIVITY

7. My visit is work related and I spend this number of hours at the beach in leisure;

Specify ……. Time [ ]

8. My visit is work related and I spend this number of hours in occupational activity

Specify ……... Time [ ]

OTHERS

9. I spend this number of hours in other activity

Leisure [ ] Occupation [ ]

END

APPENDIX E

List of presentations & publications

➢ Presentations

Title: Heavy metal seasonal distribution in shore sediment samples along the coastline of Erongo region, Western Namibia. Oral presentation at the Research Week of the Faculty of Health and Applied Sciences, Namibia University of Science and Technology (FHAS Research week) 11th – 13th May 2016, Windhoek, Namibia.

➢ Peer reviewed paper publications

1. **Sylvanus A. Onjefu**, Nnenesi A. Kgabi, Simeon H.Taole, Owen P.L. Mtambo, Charles Grant, Johann Antoine. (2016), Occupancy Factor Model for Exposure to Natural Radionuclides along the Coastline of Erongo Region, Namibia, *Journal of Geoscience and Environmental Protection* 4, 117-126
http://www.scirp.org/journal/gep
http://dx.doi.org/10.4236/gep.2016.45012

2. **Onjefu Sylvanus Ameh**, Kgabi Nnenesi Anna, Taole Simeon Halahala, (2016), Heavy Metal Seasonal Distribution in Shore Sediment samples along the Coastline of Erongo Region, Western Namibia, *European Journal of Scientific Research* 139 (1), 49-63. http://www.europeanjournalofscientificresearch.com